A Study of Crustal Uplift along the Kapuskasing Zone Using 2.45 Ga Matachewan Dykes

Baoxing Zhang

Ph.D. Thesis. Department of Geology, University of Toronto
June, 1999

Abstract

The Kapuskasing Zone (KZ) diagonally cuts across the regional structural trend of the Archean Superior Province on the Canadian Shield and disrupts the 2.45 Ga Matachewan dyke swarm. Studies using different approaches revealed that the KZ is a huge SE-verging thrust with vertical uplift of 20~30 km at about 1.9 Ga. This major structure appears to end at about 100 km east of Lake Superior. Until now, the southwestward extension of the KZ into the Wawa Gneiss Domain (WGD) has remained obscure, due to weak geophysical anomalies and poor geological exposure. Regional variations in paleomagnetic polarity and feldspar clouding intensity are two physical properties of the Matachewan dykes related to their intrusion depth. This thesis aims to explore these two important features of the dykes and to use them as tools to reveal the structural framework of the KZ extension in the WGD.

Feldspar clouding in Matachewan dykes is caused by a distribution of pseudo-single domain stoichiometric magnetite grains. The magnetite was formed by exsolution of iron from the feldspar structure. The exsolution occurred in the deeper section of the dykes during slow cooling with the crust. The degree of clouding, having a positive correlation with depth of dyke emplacement, can be quantified by both image analysis and magnetic measurement on feldspar separates, providing a new parameter for the study of relative crustal uplift.

The change of paleomagnetic polarity of the Matachewan dykes is shown to be an effective method for mapping major faults. Five major faults in the study area were revealed or confirmed, defining two new uplifted blocks (Gould Lake Block, GB, and Pineal Lake Block, PB) of the Kapuskasing Zone in its extension. GB is a second order uplift thrusted along the Budd Lake fault (BLF). The discovery of the PB extends the KZ southwestward for about 60km. It is sinistrally offset from the Chapleau Block (CB) by about 15 km. Paleomagnetic data and measurement of the country rock foliation indicates that the blocks have been rotated clockwise around steeply dipping axes related to the southeast of the KZ after the dyke intrusion. This rotation is part of the regional deformation related to the formation of the KZ.

The reversely magnetized (R) and normally magnetized (N) dykes outside the KZ are virtually the same age and both of them have primary magnetizations. N dykes within the KZ are

probably formed at the same time as those outside the KZ since they have a similar paleomagnetic direction. However, a negative baked contact test from N dykes in the KZ suggests that the N remanence in the lower sections of the dykes is not primary, unlike the N remanence outside the KZ. A plausible explanation is that the acquisition of the N remanence in lower sections of the dykes was delayed because of high ambient temperature. The slow cooling allowed Fe to precipitate from the feldspar structure to form fine-grained magnetite. During this time, a reversal of the Earth's magnetic field occurred, and the new magnetic direction was preserved in the deeper parts of the dykes.

A series of ARM experiments demonstrates that the cloudy feldspars are capable of carrying a high coercivity magnetization and in the NRM spectrum of N polarity dykes, the cloudy feldspars are the carriers of up to 70% of the total high-coercivity remanence. This indicates that the cloudiness, having an age similar to that of the N remanence, is an original feature rather than a product of later unrelated metamorphic events.

Analysis of small-scale brittle structures in dyke outcrops revealed a local paleostress field characterized by horizontal E-W compression and N-S extension. This is consistent with the regional stress field at about 1.9 Ga when the KZ was formed. The formation of the KZ is probably due to the reactivation of the Ivanhoe Lake Fault (ILF, started in Archean) triggered by the collision of the American Midcontinent from the south with the Superior Province during the Penokean orogeny at about 1.85 Ga.

Acknowledgment

I want to thank my supervisor Professor Henry Halls for the opportunity to carry out my thesis project on this exciting and challenging topic. The whole process of the research has been benefited from his enthusiastic guidance and help. His worldwide experience of geological activities always made the fieldwork very enjoyable. Discussions with him on the tennis and squash courts at Erindale College often inspired my work.

I also want to thank the professors of my supervisory committee at the University of Toronto, Professor Pierre Robin, Professor David Dunlop, Professor John Rucklidge, and Professor Alexander Cruden, for sharing their professional expertise, giving guidance to my studies at different stages.

The study got much benefit from Professor Pierre Robin's "walk-in and discussion" office on many prompt problems. Professor David Dunlop and Dr. Özden Özdemir gave many suggestions and stimulation in rock magnetic studies. Professor Currie Palmer at the University of Western Ontario kindly instructed me on the feldspar separation technique that made the central part of the study possible. Chris Hunt and other scientists at the Institute of Rock Magnetism, Minnesota, provided instruction and financial support to finish the rock magnetic studies. Dr. Claudio Cermignani and Dr. Neil Coombs at the University of Toronto helped to do the scanning electron microscope work.

During many years of study Erindale, I enjoyed discussions and social gatherings with other professors and fellow students, Professor Sandy Cruden, Professor Dan Schultze, Professor Barbara Murk, Dr. Monika Bailey, Dr. Yongjian Zai, John Dehls, Dragan Andjelkovic, James Siddorn, Doug Ciceri and Chris Fratton. Dr. Monika Bailey assisted with the proofreading of the manuscript of the thesis. I also want to thank Jake Wiktorek, Mark Smethurst, and Jon Mound for field assistance.

I appreciate the help from Adam Sosin and Jennifer Wiszniewski in the Earth Science department, Erindale College. The research was supported by NSERC awarded to H. C. Halls.

Table of Content

List of Tables

List of Figures

Chapter I

Chapter II

Chapter III

Chapter IV

Chapter V

Appendix

Introduction

1. Problem Definition and Principal Objectives of the Study

The Kapuskasing zone (KZ), a 500 km long Archean to early Proterozoic crustal uplift, extends across the Archean Superior Province from James Bay in the north to Lake Superior in the south (Fig. 1.1). It forms a complex zone of deformation along which deep crustal Archean gneisses, in upper amphibolite to granulite facies, have been raised in a series of fault-bounded blocks. This structure is marked by gravity and magnetic anomalies for most of its distance until south of Chapleau. As part of Lithoprobe, Canada's national earth science research program, the KZ has been extensively studied. The structural frame of the KZ north of Chapleau has been well constructed. However, the nature of its extension southwestward into the Wawa Gneiss Domain (WGD) remains unknown due to the lack of geophysical expression and poor exposure. The study area (Fig. 1.2) is therefore a critical location to understand the regional geology, the pattern of the KZ continuation and its relation to major faults in the area.

One outstanding geological feature of the area is a large Proterozoic mafic dyke swarm, the Matachewan dyke swarm (2.45 Ga), which cuts across and exhibits deformation associated with development of the KZ (Fig.1-2). Dykes intruded into the KZ (1) have opposite paleomagnetic polarity to the majority population of the swarm and (2) their plagioclase feldspars show patches of brownish discoloration (clouding). Not only is the dyke swarm distorted by the KZ, but these two important properties of the dykes were discovered to vary across the KZ as a result of the deformation (Halls & Palmer 1990). Since the KZ exposed rocks of deeper crustal levels, this phenomenon indicates an important fact that the properties of the dykes are related to dyke intrusion depth. If it is true then dykes can be used directly to study the KZ. However, detailed investigation is required to test the constancy, to determine the cause of the phenomenon, and to develop suitable methods for further study. The Matachewan dykes in the center of the WGD, at the possible extension of the KZ, are ideal subjects for this investigation.

Proterozoic dyke swarms are common features of almost all Archean cratons around the world. Dual paleomagnetic polarity and variable levels of cloudy feldspars are found in many other Proterozoic dyke swarms worldwide (Chapter I). Therefore, understanding the variation of these properties related to regional geological deformation, provides a general method of using the dykes for regional structural study.

The thesis is then concerned with the concept of testing and using these observations as an exploration tool for new segment of the KZ in the southwest of the Chapleau block. The research is of broad significance in two ways: (1) to explore the southwestward extension of the KZ, a major structural feature of the Canadian Shield and (2) to develop a new means of using Proterozoic dykes to study large scale crustal warping in Archean terranes where lithological markers are subtle or lacking.

2. Outline of Work

Six field trips were made to an area of about 10,000 km^2 within five summers (1991~1996). The study area is part of the centre of Wawa Gneiss Domain (WGD) (Fig. 1-2), composed of variably deformed plutonic and supracrustal rocks. Over 200 sites were visited and oriented samples were collected from 188 dykes along five traverses across the study area (Fig. 1-3). Host rock samples at most sites were also obtained. Country rock foliation was measured along some traverses and detailed post-dyke structures on over 20 dyke sites were documented.

At least one thin section from each site was made and examined. Scanning Electronic Microscopy (SEM) was applied to examine chemical elements within feldspar crystals of different clouding intensity to discuss the formation of the cloudiness. To determine the nature of the clouding material of the feldspars, hysteresis properties, Curie temperature, and Verwey transition were measured on feldspar separates of different cloudiness. To quantify the clouding intensity, both optical (image analysis) and magnetic methods were applied.

Paleomagnetically, about 1500 cores were demagnetized in detail to collect information about remanent magnetization. Distribution of paleomagnetic polarities along with feldspar cloudiness of the Matachewan dykes is used to detect major faults and uplifted blocks. Variation of the directions of remanent magnetization is discussed to understand the relative movement among the blocks. Measurement of host rock foliation within different blocks is analyzed and compared with the result of paleomagnetic study on the dykes.

For further insight into the correlation between feldspar clouding and remanent magnetization of the dykes, a series of ARM (Anhysteretic Remanent Magnetization) experiments were carried out on whole rock, feldspar and magnetite separates, A detailed baked contact test was also done on two dykes within the KZ to explore the formation of normal remanent magnetization related to delayed cooling of the dykes.

Finally, structural data collected from brittly deformed dykes were processed. Reconstructing the maximum principal compression direction at each site, helps to understand an important post dyke deformation, which may relate to the formation of the Kapuskasing Zone.

1. Outline of Thesis

The thesis is composed of five Chapters and one appendix.

Chapter I introduces the geological background of the study area. Starting from the regional geological setting of the Superior Province, the introduction goes into the structural framework and the evolution of the Kapuskasing Zone. Thereafter it introduces the Matachewan dyke swarm and its appearance in relation to the Kapuskasing Zone.

Chapter II focuses on an investigation of feldspar clouding in the Matachewan dykes. This study includes observation of the cloudy feldspars using optical and electron microscopes and magnetic treatment of feldspar separates. This chapter tries to provide answers to (1) nature the clouding particles;(2) possible origin of the cloudiness; and (3) quantification of the clouding intensity and its application to geological study.

Chapter III presents results of a paleomagnetic study of the Matachewan dykes in the area. It first introduces general demagnetization characters of the Matachewan dykes, then comes to the distribution of oppositely magnetized dykes in the study area and how the distribution reveals the faulting structures of the KZ extension.

Chapter IV discusses the relation between the two important properties of the Matachewan dykes, their feldspar clouding and Normal remanent magnetization, as well as the relationship of these properties with depth of dyke intrusion. ARM experiments on feldspar separates, magnetite separates, as well as whole rock are introduced. Result of a baked contact test of dykes in the KZ are presented.

Chapter V gives a summary of results and discussion, especially concerning the possible age of formation of the feldspar clouding. A probable model for the deformation of Matachewan dykes and formation of the KZ is proposed.

The **Appendix** documents the structural measurement on dyke outcrops in the vicinity of two major faults. Different structural criteria are measured and analyzed to determine the state of crustal stress existing at the time of faulting activity.

Chapter I. Geological Background

1 Geology of the Kapuskasing Zone

1.1 Geological setting: structural frame work of southern Superior Province

The Superior Province of the Canadian Shield is the largest Archean province on the Earth. It is thought to have formed as the result of repeated interaction of tectonic plates mainly between 3.1 and 2.7 Ga (Card, 1990). The age of metamorphism is constrained by the age of the youngest deformed, metamorphosed rocks (<2.68 Ga, detrital zircon age), and by the age of crosscutting massive plutons, 2.67 Ga (Corfu and Sage, 1992). The most common metamorphic zircon age is 2.66 Ma (Krogh and Moser, 1994) indicating the age of the main metamorphic phase. The Superior Province was finally stabilized by ca. 2.5 Ga (Percival and West, 1994).

Bounded by orogens of Paleo- and Meso-Proterozoic age around the margins (Fig.1-1), the southern part of the Superior province is composed of sub-parallel east-northeast-trending belts of alternating volcanic-plutonic terranes and meta-sedimentary belts, which resemble island arcs and accretionary prisms respectively at modern plate margins (Williams et al., 1992). Recent interpretations of the evolution of the southern Superior Province involve successive accretion of island arcs onto a northern cratonic nucleus (Percival et al., 1992). Thus the evolution may record the oldest example of large-scale plate interaction and marginal accretion to form continental crust. After the stabilization, uplift and erosion have removed up to 10 km of the crust (Percival and West, 1994).

To the south of the Quetico-Opatica meta-sedimentary belt lies an 800 km long belt of volcano-plutonic complexes, the Wawa-Abitibi orogen (Moser, 1994) (Fig.1-4). It is interpreted as a zone of convergence between oceanic lithosphere and the developing Superior craton (Williams et al., 1992) beginning at ca. 2.7 Ga (Corfu and Davis, 1992; Corfu, 1993). The Wawa-Abitibi orogen is separated into the Wawa and Abitibi subprovinces by the Kapuskasing Zone (KZ), a 150 km wide, 500 km long, NE trending uplift zone. The northern Wawa Gneiss Domain (WGD) is also referred to as the Val Rita Block (Percival and McGrath 1986) and the southern WGD as the Agawa migmatite terrain (Sims et al. 1980) (Fig.1-4). The area of study is in the center-east part of WGD, at the present end of the KZ (Fig. 1-2 and 1-4). Here the rocks are tonalitic gneiss (~65% of the exposed area), mafic gneiss (~10% of the exposed area), with less amounts of paragneiss and pegmatite (Moser 1994).

1.2 Structural features of the Kapuskasing Zone

The Kapuskasing Uplift (KU) is a region containing a west-to-east greenschist to granulite facies metamorphic transition interpreted as an oblique cross section through Archean crust (Percival and McGrath 1986). According to metamorphic grades, it can be assigned to three crustal levels from west to east, upper-crust: Michipicoten greenstone belt (MGB), mid-crust: Wawa Gneiss Domain (WGD), and lower-crust: Kapuskasing Zone (KZ) (Percival and West, 1994). An illustration can be given by a crustal cross section simplified from seismic data (Fig.1-5). The KZ is a curvilinear NNE trending, predominantly fault bounded Archean gneiss terrane transecting the E-W trending Quetico-Opatica meta-sedimentary-plutonic and Wawa-Abitibi volcanic-plutonic subprovinces. It is composed of three fault-bounded blocks of uplifted crust (Percival and McGrath 1986) (Fig.1-4). Each block is characterized by distinctive lithology, structure, and metamorphic grade. Metamorphic assemblages indicate variable paleopressure on different blocks implying differential uplift between the blocks and juxtaposition of different crustal levels (Percival 1985, Percival and McGrath 1986, Leclair 1989, 1990).

The northernmost **Fraserdale-Moosonee block (FMB)** is contained between Foxville and Bad River thrust faults (Fig.1-4) and was interpreted as a pop-up (Percival and McGrath 1986), or flower structure (Goodings and Brookfield 1992). The block consists mainly of granulite-facies paragneiss with some mafic gneiss and minor diorite, tonalite, pyroxenite, and anorthosite (Bursnall et al. 1994). Garnet-orthopyroxene-plagioclase-quartz assemblages yield paleopressures of 0.83-0.94 Gpa, equivalent to at least 13 km of uplift relative to rocks west of the block (Percival and McGrath 1986).

The second block is the **Groundhog River block (GRB)** which contains upper amphibolite- to granulite-facies assemblages in mafic, tonalitic gneiss and paragneiss. It is bounded to the west by the Saganash Lake fault (SLF), accommodating approximately 10 km of listric normal displacement to the west (Percival and McGrath 1986). To the east, it is bounded by the Ivanhoe Lake fault (ILF) which dips about 20° northwest according to seismic reflection data. It is interpreted as a thrust zone and the Groundhog River block as a perched thrust tip (Percival and McGrath 1986). Paleopressure estimates from this block are in the range of 0.7-1.0 GPa (Percival and McGrath 1986, Leclair 1992) implying at least 15 km of uplift along the ILF.

A 65 km gap without granulite or aeromagnetic anomalies, between FMB and GRB has been interpreted as a down-faulted section against the Kineras normal fault (Percival and McGrath 1986) or as a strike-slip basin formed during sinistral transpression (Goodings and Brookfield 1992).

The third block, the **Chapleau block (CB)**, contained between the southern continuation of the SLF and the ILF, is the largest high-grade block in the uplift. It is separated from the Groundhog River block by the Wakusimi River fault (WRF). The deepest levels immediately west of the ILF consist of planar mylonitic para- and orthogneisses, including stratiform anorthosite-gabbro-ultramafic intrusions, metamorphosed to upper amphibolite or granulite grade at 0.7 to 0.9 GPa (Card 1990). To the southwest, the KZ broadens to the southwest and merges with the WGD.

Existence of relatively high-grade rocks along the Lake Superior shoreline north of the Montreal River fault (MRF) (Card 1979, Corfu 1987) indicates the possible continuation of the KZ through WGD southwest of Chapleau block. The Montreal River fault juxtaposes greenschist-amphibolite grade Archean rocks to the south against higher amphibolite grade gneiss to the north and is thought to be a southwesterly continuation of the ILF (Grunsky, 1981).

1.3 Evolution of the Kapuskasing Zone

A. Structural Models of the KZ

The KZ was first revealed by its gravitational (Garland 1950; Innes et al. 1967) and aeromagnetic (Canadian federal-provincial aeromagnetic surveys, ~1967) anomalies caused by high grade metamorphic rocks cross-cutting the regional structural grain of adjacent lower grade subprovinces. Within about half century, several interpretations and models for the KZ have been proposed. These include: upper crustal thinning (Garland 1950), mafic intrusions along a Proterozoic rift system (Innes 1960, Innes et al. 1967), a zone of faulting involving rotations between crustal blocks and uplift of the high-grade metamorphic rocks (Bennett et al. 1967; Thurston et al. 1977), a failed arm of a triple junction associated with the Lake Superior Keweenawan structure (Burke and Dewey 1973), a sinistral transcurrent fault system (Watson 1980), and an intra-cratonic basement uplift (Fountain and Salisbury 1981).

The Lithoprobe project, a national program of co-operative study on the Canadian Landmass, promoted an increased study of the Kapuskasing region in the 1980s~1990s. Geochronology, geobarometry, seismic reflection as well as gravity data collected around the KZ provided another interpretation, which concludes that the KZ is a Proterozoic thrust fault system, the base of which crops out along the SE margin of the KZ in the Ivanhoe Lake fault zone (Percival and Card 1983, Percival and McGrath 1986, Cook 1985; Percival et al. 1989; Geis et al. 1990) (Fig. 1-5). In this model, the crust on the NW side has overridden the crust to the SE by at least 15 km vertically along the ~35° NW dipping ILF (Percival and West 1994). Approximately 27 km of shortening is implied which was consumed by homogeneous thickening of the lower crust. The NE-SW trending normal faults on the west side of the KZ are interpreted as collapse structures formed in response to crustal thickening (Percival and McGrath 1986).

Evidence of significant transcurrent movement along the KZ was found by West and Ernst (1991) and Goodings and Brookfield (1992) on the basis of aeromagnetic data. West and Ernst (1991) proposed a modification of the simple thrust-generated geometry based on the configuration of the Matachewan dyke swarm. They inferred a 70 km dextral Proterozoic movement along the KZ.

B. Chronology of the KZ Development

Isotopic systems with a range of closure temperatures provide constraints on the cooling and uplift history of the KZ. Summarized from isotopic age data in the area, Percival and West (1994) constructed a one-dimensional thermal model for the regional cooling history. Another constraint is provided by post-Archean igneous units intruded into the KZ at different times. At least 10 swarms of post-metamorphic dykes cut the southern Superior Province (Halls et al. 1994) (Fig. 1-6a) and two sets of alkalic rock-carbonatite complexes occur in spatial association with the KZ (Percival and West 1994). Three of the dyke swarms provide constraints on the uplift history of the KZ: the NNW trending Matachewan (2473~2445 Ma, U-Pb age, Heaman 1997), the NE trending Biscotasing (2167±1.5 Ma, U-Pb age, Buchan et al. 1993), and the ENE trending

Kapuskasing (2043 ± 14 Ma, Ar-Ar age, Hanes et al. 1988) dyke swarms. Based on granulite geobarometry, total uplift involved in the KZ is about 33 km and the uplift history of the Kapuskasing region can be divided into three intervals: 1). Modest pre-Matachewan dyke events (0-8 km); 2). Modest Matachewan - Kapuskasing events (4-7 km); 3). Major thrust (10-17 km) (Percival et al. 1994). Below is a detailed discussion on age of the events.

Both U-Pb and K-Ar geochronology and differences between crystallization pressures of Matachewan dykes and their country rock suggests a minor event involving some uplift in northern parts and burial in the southern parts of the Chapleau block at ~2630 Ma. (West and Ernst 1991, Percival and West 1994, Percival et al. 1994). However, the final juxtaposition of the granulites in the KZ against the Abitibi greenstone belt along the ILF must be no earlier than 2500 Ma (Hanes et al. 1994). With reference from U-Pb chronology and paleomagnetic studies (Symons and Vandall 1990, Symons et al. 1994), the first significant uplift occurred between ca. 2500 and 2454 Ma before the intrusion of Matachewan dykes.

At 2300-2250 Ma, reactivation of major faults (ILF and BLF) resulted in hydrothermal alteration along the faults, which reset the Ar-Ar age of micas (Hanes et al. 1994).

Barometric data on closely spaced Matachewan-Kapuskasing dyke pairs indicates a modest uplift of 4~7 km (Percival et al. 1994) between the emplacement of the two dyke swarms (about 2445~2040 Ma).

The main uplift of the KZ happened between 1950-1850 Ma (Percival and West 1994) as a SE-directed upthrusting along the ILF. The Matachewan and the Kapuskasing dykes were deformed by the movement (Card et al. 1981, Ernst and Halls 1984, Bates and Halls 1991, West and Ernst 1991,Buchan and Earnst, 1994). The 2040 Ma Kapuskasing dykes have been offset by discrete faults of the ILF but the 1885 Ma Cargill complex in the KZ and 1850 Ma Sudbury

Igneous Complex have undergone only minor offset by Kapuskasing-related structures (Percival and West 1994, Buchan and Ernst 1994). These structural evidences indicate that the KZ major activity must have finished before 1885 Ma. Geochronological study supports a significant activity around 1950 Ma. These studies include a whole-rock Ar-Ar date from the ILF zone of 1947 Ma (Hanes et al. 1994), a Pb isochron on plagioclase from Matachewan dykes of 1960 Ma (Smith et al. 1992), and a whole-rock Rb-Sr age on pseudotachylite in the western Superior province of 1950 Ma (Peterman and Day 1989).

Deformation at 1950 Ma could be related to Early Proterozoic orogenesis at the margins of the Superior Province (Gibb 1983) such as the Trans-Hudson orogen at 1820-1750 Ma (Hoffman 1989, Bleeker 1990, Halls et al. 1994), and the Penokean orogen at about1860 Ma (Sims et al. 1989, Percival and Peterman 1994).

After the major uplift, the KZ became relatively stable. There was only minor hydrothermal activity (1900-1700 Ma) (Hanes et al. 1994), intrusion of alkalic complexes and lamprophyre dykes between 1145-1015 Ma (Sage 1991), and some late shearing (1100 Ma, Hanes et al. 1994).

2. Matachewan Dykes

2.1 Distribution of the Matachewan dyke swarm

The Archean shield in the vicinity of the KZ is cut by swarms of mafic dykes of at least 10 different ages that range over the whole Proterozoic (Fahrig and West 1986, Fahrig 1987, Osmani 1991, Fig.1- 6a). The most prominent and oldest is the NNW trending Matachewan swarm that is shown clearly in the shaded relief aeromagnetic map (Fig.1-6b). Aeromagnetic data define the full extent of the swarm (West and Ernst 1991). Extending about 700 km and occupying an area of more than 250,000 km^2, the swarm appears to radiate approximately from a central point in the present Huronian basin under the north shore of Lake Huron. With different azimuths and separated by relatively dyke-free terranes, the dykes are concentrated into three subswarms (M_1, M_2 and M_3 from east to west, Fig.1-6c). M1 strikes north to northwest and is mainly restricted to the Abitibi and Opatica subprovinces, immediately east of the KZ. Only the northern extremities are impinged upon and disturbed by the KZ. Subswarms M_2 and M_3, however, have been obviously distorted by the KZ. Particularly in M_3, dykes strike northwest through the Abitibi Subprovince, traverse the KZ with a northerly strike, and gently curve into a west-northwest trend in the western subprovince, describing a broad Z-pattern. Paleomagnetic study indicates that this is a secondary feature caused by tectonic deformation related to the formation of the KZ (Bates and Halls 1991). The average width of the dykes is generally about 15-20 m outside the KZ but 10-15 m within. Average dip is within 5° of the vertical (Halls and Bates 1990) except along the east shore region of Lake Superior and within the Chapleau block where they dip eastwards as a result of westward tilting and uplift (Card et al. 1981, Halls and Shaw 1988).

The age of the Matachewan dykes dated using the U-Pb baddeleyite and zircon method by Heaman (1989) is $2452^{+3}/_{-2}$ Ma. More recent data are $2473^{+16}/_{-9}$ Ma for M_2 and $2445.8^{+2.9}/_{-2.6}$ Ma for M_3 (Heaman 1997).

2.2 Petrology of the Matachewan dykes

Matachewan dykes are iron-rich tholeiites (Nelson et al. 1990, Halls and Palmer 1990) often characterized by green to white calcic plagioclase phenocrysts up to 15 cm across. The phenocrysts generally have an equant, subhedral shape and concentrate into zones that parallel the sides of the dyke. The matrix is subophitic, comprising subequal amounts of plagioclase and clinopyroxene. Additional primary minerals, in accessory amounts, are magnetite, biotite, and apatite. Green amphibole usually mantles and/or replaces clinopyroxene but may also occur as discrete crystals. Although the dykes do not appear to have suffered regional metamorphism, they have experienced a widespread hydrous alteration involving saussuritization of the feldspar and consumption of pyroxene to produce actinolitic amphibole and chlorite. Generally, the alteration is more conspicuous in dykes that intrude those areas of the Superior Province which have the lowest grade of regional metamorphism (amphibolite to greenschist) (Halls et al. 1994). Paleomagnetic data indicate that Matachewan dykes from hydrously altered populations preserve a primary magnetization that was formed at the time of initial cooling (Irving and Naldrett 1977; Buchan et al. 1990; Halls 1991). The alteration is therefore likely to be deuteric or autometamorphic in origin, i.e., caused by primary volatiles or by hydrothermal solutions or groundwater mixing with the magma near the site of final crystallization (Halls et al. 1994).

In the dykes that intruded into the KZ where the country rock has been metamorphosed at amphibolite to granulite degrees, feldspar crystals exhibit grayish to brownish discoloration (Halls and Palmer 1990). The distribution of dykes with these "cloudy feldspars" is so closely related to the uplifted KZ that it was thought to be related with the depth of dyke intrusion (Halls and Palmer 1990).

2.3 Paleomagnetism of the Matachewan dykes

Paleomagnetic studies on Matachewan dykes began in the 1960s (Strangway 1961, 1964; Fahrig et al. 1965). Those studies revealed two high coercivity, high unblocking temperature, dual-polarity remanences with approximately antipodal directions (near 30/+20 and 210/-20), hereafter referred to as N (normal) and R (reversed) respectively. Further studies demonstrated that this dual polarity remanence could be found across the entire swarm (Irving & Naldrett 1977; Ernst

& Halls 1984; Halls & Shaw 1988; Halls & Palmer 1990; Bates & Halls 1990; Buchan et. al. 1990; Bates & Halls 1991, Halls 1991). All dykes carry one of the two remanences with R in the majority. Outside of the KZ, both N and R dykes give positive baked contact tests, in which the baked country rocks carry the same remanence direction as the dykes, but farther from the dyke margin an older remanence is recovered (Everett & Clegg 1962). This indicates that both remanences are primary formed during the initial cooling of the magma (Irving & Naldrett 1977, Buchan et al, 1990). This discovery suggested that the Earth's magnetic field was capable of reversing in Early Proterozoic time (Schutts & Dunlop 1981; Buchan et. al. 1990). Crosscutting relations and reheating effects on adjacent dykes suggest that only a single field reversal, from R to N, occurred during the time period of Matachewan igneous activity (Halls, 1991). U-Pb dating by Heaman (1977) on zircon and beddeleyite in dykes of both N and R polarity of subswarm M3 outside of the KZ gives a collective age of $2445.8^{+2.9/-2.6}$ Ma and indicates no discernible age difference between the dykes supporting a single field reversal. A second date of $2473^{+16/-9}$, obtained from subswarm M2, suggests that Matachewan igneous activity lasted about 30 Myr.

Dykes of N polarity form about one fifth of the total population (Halls & Bates 1990). This ratio increases slightly from south to north along the swarm, which indicates possible growth of the swarm to the NW because the Earth's magnetic field changed direction from R to N at the waning stage of the Matachewan dyke intrusion (Halls & Bates 1990). Regional study near the KZ discovered that the relative abundance of N and R dykes changes locally. This occurs most prominently in the Chapleau block where the highest grade metamorphic rock appears and the dyke population is entirely of N polarity (Halls & Palmer 1990). Since the KZ is a consequence of uplift along the margin faults, dykes within the zone have their deeper sections exposed. The unique spatial relation between N and R polarities indicates that at deeper crustal levels the dykes were normally magnetized compared to the R on the upper section of dykes, which makes the polarity change a possible marker for differential uplift. Paleomagnetic directions in different polarity domains around the KZ were systematically studied and compared (Bates & Halls 1991). The results suggested a post- dyke rotation around vertical axes, which distorted the radiating shape of the swarm into a big Z-shape pattern (Bates & Halls 1991).

3. A Second Thrust Block

At about 50 km west of Chapleau along Hwy 101 (Fig.1-5), Matachewan dykes demonstrate properties to those within the KZ: they are petrologically fresh, contain cloudy feldspars and have N magnetic polarity. They occur within amphibolite facies gneisses with retrograded clinopyroxene (Moser, 1994) and where Ar-Ar biotite ages of 2.3 Ga, similar to those within the KZ, are found (Hanes et al. 1994). This evidence, together with slightly higher paleopressures for both gneisses and dykes compared to those farther east (Percival et al. 1994) and the presence of a positive 10 mGal gravity anomaly (Percival and McGrath, 1986), suggests a major fault (the Budd Lake fault zone, Moser, 1988) that may be similar in nature, age, and trend to the Ivanhoe Lake fault (Halls and Palmer, 1990), but with a smaller vertical displacement of about 12 km (Percival et al. 1994). The first project of this thesis was to use the Matachewan dykes in a more extended study of the Budd Lake fault zone, particularly with respect to its longitudinal extent.

Chapter II. Cloudy Feldspars in the Matachewan Dykes

1. Introduction

Plagioclase feldspars, the most common rock forming minerals, are solid solutions of albite (Ab, $NaAlSi_3O_8$) and anorthite (An, $CaAl_2Si_2O_8$) in composition with complex structures. A pure plagioclase, free of inclusion, is colourless. However, in many kinds of igneous rocks ranging from anorthosites to mafic intrusion rocks, feldspar lathes exhibit, in thin sections under plane polarized light, locally gray to brown patchy discoloration due to ultramicroscopic dust-like inclusions (Fig. 2-1). Occasionally the colour can be uniform and much darker to almost opaque.

This phenomenon has been studied for more than a century in different kinds of igneous rocks. Recent observation revealed that cloudy feldspar occurs widely in mafic dykes that transect early Proterozoic age shield areas, particularly where they cut high grade (upper amphibolite to granulite) terranes, such as satellite dykes of the Great Dyke in Zimbabwe (Robertson & van Breemen 1970), Matachewan dykes on Canadian Shield (Halls & Palmer 1990), Vestfold Hills in Antarctica (e.g. Halls & Zhang 1995b), northeastern Baltic Shield (e.g. Halls & Zhang 1995b), dykes on Wyoming Shield, USA (Armbrustmacher & Banks 1974), Scourie dykes in Scotland (e.g. MacGregor 1931), Dharwar craton in India (Pichamuthu, 1959), and the North China Craton (Zhang 1988). Less often, middle Proterozoic dykes show a similar phenomenon when they have been uplifted adjacent to major thrust faults, for example, 1.28 Ga Sudbury dykes along the Grenville Front (Palmer et al. 1977), 0.93 Ga Blekinge dykes within the Proterozoic zone of southern Sweden (Johansson 1992), and 1.1 Ga Kulgera dykes (Zhao & McCulloch 1993) near the Woodroffe thrust fault in central Australia. A most important observation is that the degree of clouding increases with the regional metamorphic grade of the country rocks, which indicates that the clouding may relate to the depth of dyke intrusion. Since dyke swarms are widely distributed across Precambrian shields worldwide, feldspar clouding could become an important tool for regional studies of crustal warping.

The Matachewan dyke swarm in the vicinity of the KZ is an ideal subject for cloudy feldspar studies related to the depth because the uplift of the Kapuskasing Zone exposed different vertical levels of the dykes. The study will not only help to understand the local geology and the evolution of an important structure of the Canadian shield, the Kapuskasing Zone, but also will be a significant contribution to regional geological study on the other cratons by developing a new method, a new monitor for the study of relative uplift.

1. Previous Studies

2.1. Primary observation

Törnebohm (1877) was the first one who noticed the abnormal appearance of dusty brownish pigment in fresh plagioclase in Swedish diabase-gabbro rocks. Special "brown tint" coloured laths of feldspars in a peridotite from Scotland "due to the existence of nebulous masses of foreign materials distributed irregularly through them" was also observed by Judd (1885). In particular, Judd noticed that the discoloration was "clearly related to the depth from the surface at which the rocks were originally situated" and "Although it is impossible to trace the structure to which this peculiarity is due by means of the microscope, yet the circumstance of its being exhibited only in the feldspar of deep-seated rocks is of great significance...". Williams (1886) gave the first clear description of the "dust" in Baltimore gabbros: "When viewed with a low magnifying power the plagioclase appears to be covered with a fine black or brown dust, which, under the highest magnifying power, is resolved into a mass of very minute opaque dots and lines."

Two years later, Teall used the word "cloudy" to describe this appearance of feldspar in his book "British Petrology" (Teall, 1888) and connected the peculiar character with contact-metamorphism.

Kynaston (1905) and Bailey (1916) supported Teall's suggestion of a contact metamorphic origin on the basis of studies of phenocrysts from andesite lavas influenced by later intrusions in Glen Etive, Glen Nevis, and Glen Coe districts, England. Knopf and Jonas (1929) considered the inclusions to be ilmenite or magnetite.

2.2 Detailed Studies

The first systematic summary of cloudy feldspar studies was done by MacGregor (1931) based on his own study in contact-metamorphosed minor intrusions in Aberdeenshire, Ayrshire and Sutherland, Scotland (MacGregor, 1929, 1930). He reviewed the earlier knowledge about cloudy feldspars and made the following conclusions:

a. The clouding is caused by the appearance of iron oxide, concentrated to some extent by migration. The preferential clouding of basic plagioclase is due to its having an original iron content higher than that of albitic or potassium feldspars.

b. The cloudiness is not an original feature of feldspars. It is a product of thermal metamorphism caused either by regional heating connected with depth or by the heat of neighboring igneous magma. The re-heating can be very late in terms of age, but not so severe as to recrystallize the feldspars.

MacGregor's interpretation was accepted by many petrologists; so much so that the occurrence of cloudy feldspar in a wide variety of rocks was cited as an indication for the rock having been subjected to thermal metamorphism. In particular, the phenomenon was observed to be most developed in hypabyssal intrusions such as dykes and sills.

Grout (1933) found clouded plagioclase in hornfels xenoliths in gabbros of Minnesota. The feldspars were generated from clay minerals, so that the cloudiness was caused by inclusions of the parent minerals. Williamson (1936) and Shand (1945) stated that the boundary between clouded and unclouded areas did not always show a change of composition.

Poldervaart and Gilkey (1954) reviewed the literature that appeared after MacGregor's (1931) summary and suggested that the requisites for plagioclase clouding are (1) elevated temperature for a prolonged period, (2) presence of an aqueous pore fluid, and (3) supply of iron from the original rock. They concluded that clouding is produced by diffusion of material into the plagioclase through channels produced by unmixed plagioclases of intermediate composition. Concentration gradient is the dominant driving force for the ionic diffusion.

Pichamuthu (1959) was the first one who made a statistical study on the distribution of dykes with cloudy feldspars related to regional metamorphic zones. He noticed that in Mysore State (India) about 500 basic dykes of different ages and petrographic types exhibit cloudy feldspars in the southern end of the State where the deeper sections of the Earth's crust (suggested by amphibolite and granulite metamorphism) are exposed. About 190 km away to the north where the host rock was in greenschist grade, feldspars in the dykes are clear. He concluded that regional thermal metamorphism was the only reason for the characteristic distribution of the clouded dykes.

2.3 Studies with Modern Techniques

Burns (1966) investigated the chemical and mineralogical changes associated with metamorphosed dolerite dykes in the Scourie-Loch Laxford area, Sutherland, Scotland. He also suggested that clouding is associated with introduction of water from outside the feldspar. When heated above 800°C, both clear and cloudy feldspars increase slightly in weight during heating, which was thought to be caused by oxidation of the iron present. However, the increase in weight found in clear feldspar is three times as large as that found in the cloudy, the author concluded that in cloudy feldspars, more of the Fe is in the state of Fe^{3+} compared to clear feldspars. Therefore the conclusion was reached that oxidation state of iron in the feldspar is the main controlling factor in the abnormal properties of the cloudy feldspar.

Anderson (1966), Philpotts (1966), and Bridgwater and Harry (1968) studied cloudy feldspars from anorthosite rocks at Libreville, Quebec, in the Morin series of Quebec, and in Precambrian intrusions of southern Greenland. Despite the complex geological environments, all the studies agreed that the clouded plagioclase was annealed for a long time during the cooling of the rock.

Transmission Electron Microscopy (TEM) together with microanalysis and electron diffraction was introduced to observe the clouding particles in plagioclase (Smith, 1979; Morgan and Smith 1981) from the Scourie dykes in Scotland. The clouding particles with grain size from 0.5 to 0.01 μm were identified as magnetite with only trace Ti content. (Ti/Fe = 0~0.052, corresponding to ülvospinel contents between 0 and 14.8%). Most of the particles are equidimensional or ellipsoidal in shape with minor to major axial ratios from 1 to 0.3.

Hargraves and Young (1969), Davis (1981), as well as Morgan and Smith (1981) discussed the magnetic properties of the clouding particles. Those authors came to the same conclusion for mafic rocks from different places, that at least part, if not all, of the clouding particles are submicroscopic magnetite grains which can carry a stable Natural Remanent Magnetization (NRM).

After an intensive study of cloudy and clear feldspars in metadolerite and quartz dolerite dykes in the Bighorn Mountains, Wyoming, Armbrustmacher and Banks (1974) stated that exsolution of intra-crystal iron incorporated in the plagioclase accounts for the clouding. The exsolution occurred because of slow subsolidus cooling of the dykes intruded into a terrain heated by metamorphic processes.

In metamorphosed mafic intrusive rocks from the Grenville Province, feldspars are cloudy where olivine shows coronitic rims of spinel. This phenomenon was observed by Whitney (1972) in the Adirondacks intrusions and by Bethune and Davidson (1988) in the 1.28 Ga Sudbury dykes' deep equivalents in the Grenville Front. The generation of the feldspar cloudiness was ascribed to a metamorphic reaction associated with corona formation. However, Emmet (1982) reported that in diabase from a Caledonian Nappe in Norway, feldspar clouding preceded corona formation. According to Johansson (1992) cloudy feldspars developed in mafic intrusions along the Protogine Zone in southern Sweden regardless of whether or not olivine or coronas around olivine are present.

3. Current Study

Feldspar clouding in the Matachewan dykes was first reported by Halls and Palmer (1990). They noticed that cloudy feldspar occurs in normal polarity Matachewan dykes as well as NE trending Kapuskasing dykes within the KZ where the host rocks are at upper amphibolite to granulite grades of metamorphism. However, feldspars in Matachewan and Kapuskasing dykes within lower metamorphic grades outside of the KZ are clear. By comparison with other similar cases elsewhere in the world, they proposed that cloudy feldspars in fresh, undeformed Matachewan and Kapuskasing dykes (both iron rich tholeiites) are a reflection of the dykes having been emplaced in relatively deep crust, and that the intensity of the clouding increased with emplacement depth.

Palmer and Barnett (1992) performed a Curie temperature test on cloudy feldspars separated from a Kapuskasing dyke. The experiment indicated that the opaque particles within the plagioclase have Curie temperature in the range 570°C ~ 590°C corresponding to pure magnetite.

Based on the foregoing studies, more detailed examinations were performed on cloudy feldspars of Matachewan dykes in this thesis. The study focuses on three aspects: (1) determination of the nature of the clouding materials by direct observation (using optical and electron microscopes) and magnetic examination, (2) discussion of a possible origin model for the cloudiness, and (3) development of a method of applying the feldspar clouding to geological study.

3.1. Nature of feldspar cloudiness

3.1.1. Direct observations

Approximately 200 thin sections from the Matachewan dykes were examined during the study. Dykes that exhibit cloudy feldspars are petrologically fresh with preserved chilled margins. Under the petrographic microscope, the Matachewan dyke is subophitic, comprising similar amount of plagioclase feldspars and clinopyroxene (about 90% in total). The subordinate minerals are magnetite (~5%), amphibole, biotite and apatite (~5% together). Olivine is absent in all thin sections including the most clouded ones. In accordance with Johansson (1992), it seems that the appearance of olivine and its corona development is not necessary for the formation of clouded feldspar, indicating that feldspar clouding is an original magmatic feature rather than a later metamorphic product.

The original mineral assemblage and texture imply that the Matachewan dykes did not suffer a regional metamorphism. However some of them have experienced a widespread hydrous alteration which involves saussuritization of feldspars and the production of an actinolitic amphibole and chlorite at the expense of clinopyroxene. Green amphiboles usually grow around the pyroxene but may also occur as discrete crystals. Although the degree of alteration is variable within any given dyke population, alteration is generally heavier in the area farther away from the KZ (Fig.2-2) where dykes intruded into shallower crustal levels. This distribution indicates that the alteration is an inverse function of the depth of dyke intrusion.

The plagioclase in the dykes is generally labradorite (An_{50} ~ An_{70}) (Halls and Palmer 1990) in composition. No compositional zoning is observed but polysynthetic twins are well developed. The degree of the cloudiness varies from grain to grain (Fig. 2-3a). In uniformly developed cloudy feldspars, the cloudiness usually has a clear mantle (Fig.2-1d, Fig.2-3b). At high magnification (x300), the cloudiness shows as smaller opaque particles tending to lie along albite twin lamellae (Fig.2-4 a,b). However, under an electron microscope, most of the inclusions appear as short rods and long needles of various sizes randomly distributed within the feldspar matrix (Fig.2-4 c,d). The appearance thus suggests that at least two different phases may have precipitated.

The cloudiness seems to be an original feature. It occurs in fresh feldspar laths that exhibit sharp twinning lamellae under polarized light. Cloudiness does not affect optical features of feldspars. Twinning and cleavages continue smoothly through cloudy parts of a crystal. Cloudiness is obviously distinct from saussuritization, which involves crystallization of new minerals at the expense of feldspars. The newly crystallized minerals, mostly sericite, chlorite and other minerals, have independent optical features that totally replace that of the feldspar (Fig. 2-5 a, b).

Close examination under optical microscope can distinguish some other large inclusions (>1/10 mm) that show independent optical properties. They can be different minerals such as biotite, hornblende, as well as magnetite. They seem likely incorporated by feldspar crystals accidentally during crystal growth. These inclusions also occur in clear feldspars and are not the particles that contribute to the cloudiness.

Although the cloudiness varies among grains in a thin section, the overall clouding degree is independent of locations across a dyke outcrop. In two cloudy dykes (Site 183 and 189, Fig.1-3) of medium width (12 m and 20 m respectively), a profile of samples was taken across each of them with about 1 meter spacing (15 samples for site 180, 22 samples for site 189). For both dykes, from the chilled margins to the centres, the feldspar grain size changes from <1/10mm to 2~3 mm. However the clouding degree, from visual inspection of thin sections, remains similar. It suggests that clouding intensity is not a function of either grain size nor crystallisation rate across an individual dyke at the same crustal level.

Halls and Palmer (1990) had originally reported feldspar clouding in the Matachewan dykes along Highway 101 in the Chapleau region and western side of the Budd lake fault (BLF). The present work in the southern end of the KZ revealed a regional distribution of cloudy dykes. Combined with the distribution of magnetic polarity of the dykes (discussed in Chapter III), this discovery confirmed the existence and extension of the Budd Lake fault (BLF), Montreal River fault (MRF), McEwan Lake fault (MLF), Saganash Lake fault (SLF), and Nagasin Lake fault (NLF). These faults (detailed descriptions in Chapter III) outline the structural framework of the area (Fig.2-6). Another obvious feature presented in Fig.2-6 is that generally cloudy dykes occur in regions of normal (N) magnetic polarity whereas the clear dykes characterize the reversely (R) magnetized domains. The change of paleomagnetic polarity and feldspar cloudiness of the Matachewan dykes coincide with the locations of the faults, which make the feldspar clouding an important parameter to map the major faults. The correlation between feldspar clouding and normal polarity magnetization will be discussed in Chapter IV.

3.1.2. Magnetic study on cloudy feldspars

The presence and composition of ferrimagnetic oxides in rocks can usually be determined by either direct microscopic observation or measurement of magnetic properties on whole rock or mineral separates. Due to small size (<1 μm), the clouding particles in the feldspar could not be identified microscopically. Their magnetic properties therefore became targets to explore (Hargraves and Young 1969, Davis, 1981, Morgan and Smith, 1981). However, most of the previous work was on samples from a discrete plutonic intrusion or a single dyke. In this thesis, a comprehensive series of experiments has been carried out on feldspars of different cloudy degree from a series of dykes that were intruded at different depths.

Experiments, done at the Institute of Rock Magnetization (IRM), University of Minnesota, included measurement of Curie temperature, hysteresis properties, and low-temperature remanence acquisition. They were designed to study the nature of the clouding particles.

A. Sample preparation

Twenty-three dykes with feldspars of different clouding degrees (determined by thin section inspection) across the BLF were selected. The samples were crushed and ground into grain size of 74~104 μm (mesh #200~#150). Coarse magnetite particles were first separated by a hand magnet. The rest were then separated into dark and light group of grains by a Frantz magnetic separator. The dark coloured grains are mainly pyroxene, amphibole, and coarse magnetite while the light are mainly feldspars. This step was repeated several times with a different electric current to remove the small fraction of composite plagioclase + dark grains until over 90~95 percent of the light coloured grains were pure feldspars. Within the feldspar separates, grains that have dark mineral(s) attached to them were removed by hand under a binocular microscope. Fig.2-7 shows the process of sample preparation.

B. Curie temperature test

Each specific composition of magnetic mineral has a unique Curie temperature. Therefore, the determination of this temperature is diagnostic of such minerals as well as composition within the titanomagnetites (Özdemir and O'Reilly, 1981; Keefer and Shive, 1981) and ilmenohaematites (Duff, 1979). The procedure is to heat and cool a specimen in a strong magnetic field and monitor the variation of magnetization (susceptibility) with the temperature. The experiment was done on a Curie balance (Kappa Bridge). The samples used are typical cloudy feldspars separated from a Matachewan dyke (TK49, Fig.1-3). A plot of susceptibility as a function of temperature (Fig.2-8, D. J. Dunlop and B. Zhang, unpublished data) shows a clear Curie temperature of 575°~580°C from both heating and cooling curves indicating that the clouding particles are pure magnetite. Although the experiment was conducted in inert gas, chemical change(s) occurred during heating since the specimen contains air. The chemical reactions, causing the heating and cooling curves to be dissimilar, are unknown. Between 600°C and 700°C, the susceptibility signals are almost reduced to the noise level, indicating that hematite, if it exists, is only in trace amount. This result is consistent with that obtained by Palmer and Barnett (1992) on the cloudy feldspar separates from a Kapuskasing dyke.

The susceptibility shows an obvious thermal enhancement from about 200°C to 550°C (Hopkinson effect). The enhancement factor is about 3 with a broad Hopkinson peak, which is similar to what Dunlop (1974) found in single domain magnetite particles with a broad blocking temperature spectra.

C. Hysteresis properties

Hysteresis of a magnetic particle is due to its ability to preserve the isothermal remanence acquired by the application of a magnetic field at a constant temperature. For a multi-domain size grain, this property is explained by domain wall migration over some energy barriers followed by failure to return to the original position when the applied field is cancelled, while for a single domain particle the property is caused by domain rotation to the applied field direction. Fig.2-9a and Fig.2-9b give the idealized hysteresis loop for large multidomain and randomly oriented uniaxial single domain grains of magnetite respectively. The shape and coercive force (H_c) of the hysteresis loop are closely dependent on grain size (Dunlop and Özdemir 1997).

Hysteresis loops of feldspar separates from 23 dykes were obtained on a "Princeton Measurements Micromag 2900" alternating gradient force magnetometer at the IRM. The results are shown in Table 1 and Fig.2-9c gives some examples of the results. All samples produce loops similar to that of single domain-superparamagnetic grain size magnetite (Dunlop and Özdemir 1997). Although there are differences at saturation magnetization (M_s), all samples have similar coercive force values indicating that magnetite particles in all the feldspars have similar grain size. Using the method of Day et al. (1977), it was determined to be pseudo single domain (PSD) grain size, approximately from 0.1 to a few μm (Fig.2-10).

Table 1. Hysteresis Properties of Feldspar Separates

Sample	D. (km)	Mass(mg)	Hcr(mT)	Hc(mT)	Ms(nAm^2)	Mr(nAm^2)	Cloudiness	
TK4-9	10.00	11.86	75.70	42.10	8.89	3.39		
TK30-3	9.60	11.97	59.80	30.10	24.40	7.54	4.2	
TK10-4	7.60	8.43	83.80	44.30	12.40	4.63		
TK11-7	6.60	12.48	81.20	41.70	34.40	12.50	7.7	
TK14-2	5.60	9.42	59.30	31.60	34.30	11.60		
TK16-5	5.00	11.57	68.10	26.10	26.40	8.26		
TK18-2	4.50	13.05	68.60	35.20	47.80	17.60		
TK1-8	4.30	14.90	74.70	40.10	54.50	20.40		
TK19-4	4.00	12.10	59.00	21.30	43.90	12.10	13.39	
TK21-3	3.50	13.20	73.20	37.90	64.00	23.40		
TK24-5	2.50	8.01	68.50	34.80	43.00	14.90	19.8	
TK49-5	1.00	12.95	98.20	52.20	92.80	36.10		
TK51-1	0.50	12.59	70.40	35.20	91.20	27.10	27.48	BLF
TK34-2	1.50	13.66	60.60	32.30	34.50	10.80		
TK54-4	2.00	9.70	50.90	19.20	22.90	4.53		
TK55-3	2.50	11.00	53.30	28.10	14.20	3.09	1.7	
TK43-5	5.00	8.27	44.00	24.80	12.00	3.15	0	
TK38-1	6.50	10.19	66.90	37.70	82.70	30.60		
TK37-5	7.00	11.04	94.90	52.40	33.80	14.20		
TK36-7	10.00	9.48	66.60	34.00	39.10	13.50		

Note:
1. D. Distance from the BLF on the ground
2. Cloudiness is from image analysis of thin sections. Relative to site TK43

D. Low-Temperature properties

Another way to test single to pseudo-single domain magnetites is by looking at their magnetic behaviour at a low temperature between 110 K and 120 K, where a step-like drop of remanent magnetization is expected due to the change of crystal structure of magnetite at the Verwey transition. The Verwey transition is an abrupt change in coercivity, remanence, susceptibility (Aragòn et al., 1985; Aragòn, 1992), and electrical conductivity of magnetite (Verwey, 1939, 1947) because of a change in the crystal structure of magnetite from orthorhombic (below) to cubic (above) at 118 K (T_v). Magnetically, a sudden drop in remanent magnetization occurs because of the disappearance of crystalline anisotropy (O'Reilly 1976). Single crystal studies indicate that T_v = 118 K is a maximum temperature for pure stoichiometric magnetite. Small degrees of nonstoichiometry (effect of Ti, for example) or impurities in magnetite depress T_v below 100 K and reduce the amplitude of the transition (Kuipers and Brabers, 1976, Aragòn, et al., 1985; Özdemir and Dunlop, 1993).

Low temperature treatment was performed on a Quantum Design Magnetic Property Measurement System (MPMS) at the IRM, a system designed to observe the behaviour of remanent magnetization of magnetic materials at low temperatures. The samples were magnetized in a high magnetic field (2.5 T) at a temperature of 5 K, then slowly warmed up to room temperature (300 K) in a field free space. The saturation isothermal remanent magnetization (SIRM) was measured at intervals of every 5 K up to room temperature. After a rapid decay of SIRM from 5 K to 20 K, the magnetization remained at a stable plateau until 110K (Fig.2-11). A step-like drop occurs in the temperature range 110 -120K for all the feldspar specimens, corresponding to the Verwey transition (T_v) of magnetite. It confirms the presence of virtually stoichiometric and Ti-free magnetite in the feldspars, in agreement with the Curie point test. Given the spontaneous magnetization of pure magnetite (M = 92.36 Am^2/kg) and density of magnetite (5.19 g/cm^3), using the remanent magnetization of the feldspar separates at 50 K, weight percentages of magnetite, from relatively clear to most cloudy feldspars, are estimated to range from 0.06% to 0.44% (Table 2).

Table 2. Low Temperature Remanent Magnetization

Samples	Weight	Wt%Fe_3O_4	M_{50k}	M_{300k}	$(M_{50k}-M_{300k})/W$	D. from BLF
TK4-9	241.81	0.171	3.79	1.69	8.68	10
TK30-3	194.28	0.095	1.69	0.87	4.23	9.6
TK10-4	226.12	0.221	4.60	2.20	10.61	7.6
TK11-7	249.61	0.143	3.29	1.53	7.08	6.6
TK14-2	261.65	0.188	4.53	1.98	9.74	5.6
TK16-5	256.31	0.113	2.65	1.16	5.83	5
TK18-2	254.74	0.199	4.66	1.90	10.81	4.5
TK1-8	233.95	0.184	3.96	1.95	8.60	4.3
TK19-4	241.91	0.150	3.33	1.49	7.63	4
TK21-3	234.60	0.208	4.49	2.49	8.53	3.5
TK24-5	211.71	0.220	4.29	1.74	12.04	2.5
TK49-5	230.81	0.352	7.47	3.80	15.91	1
TK51-1	216.25	0.295	5.87	2.18	17.05	0 BLF
TK34-2	262.47	0.124	2.99	1.03	7.48	1.5
TK54-4	251.83	0.066	1.54	0.68	3.40	2
TK55-3	268.47	0.059	1.47	0.65	3.04	2.5
TK43-5	263.27	0.050	1.21	0.55	2.49	5
TK38-1	261.38	0.435	10.45	4.38	23.23	6.5
TK37-6	268.81	0.184	4.56	2.35	8.24	7
TK36-7	259.21	0.216	5.16	2.22	11.32	10
Unit	(mg)		($\times 10^{-4}$emu)	($\times 10^{-4}$emu)	($\times 10^{-4}$emu/g)	(km)

3.2 Origin of the cloudiness

Regarding the origin of the cloudiness, although many hypotheses were advanced (see Section 2, Previous Study, in this chapter), only three of them have been commonly recognized:

1. An original feature of some feldspar crystals, caused by the tiny inclusions that the feldspar incorporated at the time of crystallisation (Törnebohm 1877, Tilly 1921).

2. A consequence of diffusion of Fe from outside of feldspar. Unmixing of plagioclase between albite and anorthite produced the channels for the diffusion (Poldervaart and Gilkey 1954).

3. A result of precipitation of structural iron caused by (a) metamorphic heating, either contact or regional metamorphism, at some time unrelated to the intrusion itself (MacGregor, 1931), or

(b) slow cooling of the dykes and of their host crust following their emplacement (Armbrustmacher and Banks 1974).

In the Matachewan dyke swarm, geochemical data indicate no obvious compositional differences across the swarm (Nelson et. al., 1990; Phinney and Nelson, 1991). Fe concentration (in the form of Fe_2O_3) from eight different regions in the swarm shows similar contents of 15% on average with less than 1% variation (Table 3, Fig.2-12a). X-ray fluorescence analysis on 11 dykes across the BLF demonstrates that despite the great variation in feldspar clouding degree, the Fe concentration (in form of Fe_2O_3) is only slightly different (Table 4, Fig.2-12b). These data mean that the difference in cloudiness is not a measure of different bulk iron contents. Therefore, the cause must be related to iron distribution within the rocks, particularly, the feldspar crystals. To detect the element concentration, Scanning Electron Microscopy (SEM) was applied to feldspar crystals with different clouding intensity in the SEM labs of Department of Geology and Metallurgy and Materials Sciences, University of Toronto.

Eight dykes with fresh feldspars of different clouding degrees were chosen for the experiment. Two representative grains from each thin section were examined. For each grain, four or five squares of 30~50 μm side were scanned across so that the reading from each square is a total element concentration including elements inside and outside the feldspar structure. Besides O, six major elements Si, Al, Ca, Fe, K, and Na were detected. Concentrations of Mg, Ti, Cr, and S are below detection levels even in the most clouded area, which suggests that the particles are iron oxides (magnetite) alone and not ilmenite, chromite, rutile, spinel, or sulfide minerals. This result is consistent with that from the metadolerite dykes, Southeastern Bighorn Mountain, Wyoming (Armbustmacher and Banks, 1974).

Table 3. Fe_2O_3(Wt%) Concentration across the Matachewan Dyke Swarm

Region	Polarity	N	Fe_2O_3(Wt%)	δ
Rocky Island Lake	R	21	15.2	1.5
Ranger Lake	R	10	15.1	1.1
Timmins	R	11	14.7	1.2
Hwy 101	R	7	14.9	1.2
Budd Lake-Tik Road	N	8	15.5	1.2
Missinaibi Lake	R,N	13	15.2	1
Hornepayne	R	27	15.4	1.5
Hearst	R,N	6	15.6	1.6

Note:
N: number of dykes analyzed;
δ: Standard deviation of average Fe_2O_3 concentration
Data are from W. M. Phinney (unpublished) except Budd Lake-Tik road;
For location of the areas see Fig.3-13

Table 4. X-Ray Fluorescence Whole Rock Analysis

Dykes	SiO_2	Al_2O_3	CaO	MgO	Na_2O	K_2O	Fe_2O_3	MnO	TiO_2	P_2O_5	Cr_2O_3	LoI	Sum	D.T.(m)	Location
TK12-1-2	50.10	13.30	8.93	5.65	2.03	1.28	14.60	0.21	1.94	0.23	<0.01	0.70	99.1	>3.5	on WCM
TK1-6-10	50.90	13.10	9.23	5.94	2.30	0.61	14.60	0.20	1.13	0.12	<0.1	0.25	99.1	17~25	20cm ECM
186-6-1	50.60	13.80	9.08	5.85	2.43	0.78	14.90	0.21	1.23	0.14	0.03	0.40	99.5	30	4cm ECM
188-1-1	51.30	13.50	9.50	5.65	2.30	0.57	15.00	0.21	1.24	0.14	<0.01	0.03	99.2	21	10cm WCM
189-1-1	52.10	12.90	8.39	4.40	2.56	0.91	16.90	0.22	1.71	0.23	<0.01	0.20	100.2	23	5cm WCM
190-4-1	51.50	12.80	7.96	4.27	2.53	0.92	16.60	0.21	1.68	0.23	<0.01	0.20	99.0	7	1m ECM
191-6-1	51.30	12.60	8.22	4.04	2.52	0.79	17.40	0.24	1.81	0.25	<0.01	0.10	99.3	3.7	12cm ECM
SL11-1-1	53.60	12.60	6.41	3.43	3.74	0.93	16.00	0.19	1.87	0.25	<0.01	0.75	99.9	8.1	Interior
TK43-3-4	50.10	15.50	8.89	4.70	2.68	0.65	14.40	0.19	1.25	0.14	<0.01	0.05	99.1	13	70cm ECM
TK34-2-1	50.10	13.50	8.69	5.69	2.64	0.78	15.00	0.22	1.84	0.23	<0.01	1.10	99.9	>6.2	Interior
TK40-2-2	49.00	13.50	9.24	6.47	2.05	0.93	15.30	0.21	1.83	0.25	0.02	0.20	99.1	5.5	4cm ECM

Note:
D.T.: Dyke thickness
Element weight percentage and sum are calculated as oxides;
WCM, ECM = west chilled margin, east chilled margin

Across cloudy parts into relatively clearer zones in a crystal, Fe content does not show significant variation (Fig.2-13), except at the clear mantle where the Fe content drops dramatically. This indicates that the differences in feldspar cloudiness are not caused by the relative concentration of iron. The average of ten scanning areas from two feldspars in each thin section gives the Fe content estimation of the sample. The results show that all the feldspars from dykes with different clouding, have similar average iron content of about 1% atomic percentage (equivalent to about 1.5% by weight with an uncertainty <0.45%) (Fig.2-14), which suggests that the concentration of Fe_3O_4, not total Fe, causes the difference of the clouding intensity. Calculated from saturation magnetization at low temperature (6K), the Fe_3O_4 concentration in feldspars ranges from 0.72% (clear) to 1.89% (cloudy) with equivalent Fe percentage from 0.52% to 1.37% wt. These results imply that for the relatively clear and cloudy feldspars in Matachewan dykes, about 35% to 91% of the available iron respectively has exsolved to form the cloudiness.

Therefore, the result of the SEM work on Matachewan dykes is not in favour of the first two hypotheses about the origin of the cloudiness. In all these cases, "original extra inclusion", "Fe inward diffusion" would cause the cloudier grains and cloudier parts of a grain to yield relatively higher Fe concentration. Although the first two causes may be applicable to feldspar clouding in other cases, the phenomenon in Matachewan dykes can be best explained by the third hypothesis, the exsolution model: all feldspars captured a similar amount of Fe in their structure when they crystallized. However, in certain favourable conditions, Fe in some crystals exsolved from the structural sites and formed magnetite (see Chapter V for a possible process). In relative clear crystals and less cloudy part of a cloudy crystal, most of the iron is still in the crystal as substitution atoms of the structure. The exsolved Fe hardly migrated in the feldspar so that the SEM measures total Fe, which is similar across a crystal. Furthermore, lacking of metamorphic features in the dykes as well as magnetic property of the cloudy feldspar (Chapter IV) indicates that the model 3(b) is probably the best explanation of the "Matachewan clouding", that is the Fe exsolution occurred during slow cooling of the dykes intruded into deeper crustal levels.

3.3 Models for clear and cloudy feldspars

Decrease in solubilities of Fe^{2+} and Fe^{3+} in the feldspar appears to be the cause of cloudiness. When the feldspar originally crystallises from the mafic magma, Fe^{2+} (ionic radius = 0.74 Å) substitutes for Ca^{2+} (0.99 Å) and Fe^{3+} (0.64 Å) for Al (0.51 Å) in significant proportions in the feldspar structure. Solubilities of the ferrous anorthite ($Fe^{2+}Al_2Si_2O_8$) and ferric anorthite ($CaF_2{}^{3+}Si_2O_8$) components into the plagioclase may be enhanced, not only by higher temperatures, but also by higher pressures. Driven by a decrease of these solubilities with lowering temperature, and perhaps pressure, clouding of feldspar thus corresponds to expulsion of the Fe^{2+} and Fe^{3+} ions from the feldspar structure.

It is important to recognise that this expulsion of ions from the feldspar must be accompanied by precipitation of at least one silicate other than plagioclase in addition to magnetite. Examples of possible precipitation reactions, expressed in terms of end-member components, include:

$Fe^{2+}Al_2Si_2O_8 + CaFe^{3+}Si_2O_8 = Fe^{2+}Fe_2{}^{3+}O_4 + CaAl_2Si_2O_8 + 2SiO_2$ (1)

ferrous anorthite ferric anorthite magnetite anorthite quartz

but also:

$Fe^{2+}Al_2Si_2O_8 + CaAl_2Si_2O_8 = CaFe^{2+}Si_2O_3 + 2Al_2SiO_5$ (2)

ferrous anorthite anorthite hedenbergite (cpx) alumino-silicate

$Fe^{2+}Al_2Si_2O_8 = Fe^{2+}SiO_3 + Al_2SiO_5$ (3)

ferrous anorthite ferrosilite (opx/cpx) alumino-silicates

$NaFe^{3+}Si_3O_8 = NaFe^{3+}Si_2O_3 + SiO_2$ (4)

ferric albite ferric jadeite (cpx)

Other reactions can be obtained by combining 2 or more reactions above. For example, Reactions (1) + (2) add to:

$2\,Fe^{2+}Al_2Si_2O_8 + CaFe^{3+}Si_2O_8 = Fe^{2+}Fe_2{}^{3+}O_4 + CaFe^{2+}Si_2O_3 + 2SiO_2 + 2Al_2SiO_5$

ferrous anorthite ferric anorthite magnetite hedenbergite (cpx) quartz alumino-silicate

Iron reported from feldspar analyses (Deer *et al.*, 1992) is dominantly Fe^{3+}. Smith (1974) suggests a ratio of $Fe^{2+}:Fe^{3+} = 1:10$. If solubilities were in the same proportion at the high temperature at which cloudy feldspar originally crystallised, precipitation of magnetite (Fe^{2+}:Fe^{3+} = 1:2) could only relieve the feldspar of at most 3/11 of its total iron, and only if all of its Fe^{2+} were taken up in magnetite. However, as reported above, magnetic measurements suggest that in some grains, as much as 91% of the total iron in the feldspar precipitated as magnetite. For that to be possible, the high temperature plagioclase would need to have accepted a ratio of Fe^{2+}:Fe^{3+} = 3:10.

Kinetics of these reactions may be controlled, or at least affected, by nucleation and growth of the product phases, as well as by diffusion of the ions involved. It is essential to note that precipitation of the new phases, although driven by the decrease in solubility of Fe, should require a sufficiently long 'time-temperature' history to allow it to proceed.

The clear margins of many feldspar grains testify that Fe ions have been able to diffuse out of the grains over the width of these margins. That outward diffusion of Fe must be accompanied by outward diffusion of Si and/or Al, or by inward diffusion of Ca and/or Na. These metasomatic transfers across the clear margin may be driven by the higher surface energy of the precipitates, compared to the surface energy in larger grains outside of the feldspar. But the transfers may also have been driven by the reactions of the precipitates with phases located outside of the feldspar grains.

It follows from the above considerations that a clear feldspar grain could come about in several ways:

(1) The feldspar crystallised under conditions where the solubilities of Fe^{2+} and/or of Fe^{3+} were low. If for example, one or both of these solubilities were greatly enhanced by pressure, feldspar crystallised at shallow depth may not contain sufficient Fe for it to precipitate.

(2) The feldspar has not had a sufficient time-temperature history that allowed precipitation to proceed.

(3) The feldspar has, on the contrary, had sufficient time at the right temperature not only to precipitate its iron, but also to expel the resulting products outside of its margin.

In the dykes studied here, clear feldspar have been found to have iron content similar to cloudy ones, eliminating Model (1). Clear feldspars are found in dykes emplaced at relatively shallow depths and cooled relatively rapidly (Halls & Palmer, 1990; this study); Model (3) can therefore also be excluded. The observation of MacGregor (1931), discussed above, that feldspar clouding in minor intrusions can also be activated by contact metamorphism, points to Model (2) as the most likely explanation.

3.4 Geological Application of Cloudy Feldspar Study

A general observation (Halls and Palmer 1990) is that feldspar clouding in the dykes appears to increase with the depth of dyke emplacement. This observation was directly proved by the discovery that the clouding intensity gradually increases when the Budd Lake fault is approached from the NW on its upthrown side (Fig. 2-6). A similar phenomenon was observed at the newly discovered McEwan Lake fault (MLF) on its eastern side. Therefore, the clouding level in principle could be used as a measure of the depth of the dyke intrusion, providing other factors such as overall composition, cooling rate, etc. are constant. Regardless of how complex the exact relation is, the positive correlation between clouding level and the emplacement depth suggests the need to work towards some empirical relation between the two. This would require a quantification of the clouding intensity. Here we explore both optical and magnetic methods to achieve this result.

3.4.1. Quantification of Feldspar Clouding Intensity

A. Optical Quantification

A computerized image analysis technique, employing the software package DIDACTIM, was first used to measure clouding intensity. Optical observation shows that among dykes in the same swarm, a deeper clouding usually has larger cloudy area in the feldspar crystals. Therefore clouding intensity can be expressed as a percentage of clouding area of the feldspars. In brief, an image of a thin section is taken into the computer by video camera or high-resolution scanner. After calibration by about 10 feldspar grains, the computer can recognize more than 95% of the feldspar image and all other mineral images can be eliminated. Then a gray scale standard is set up for cloudy feldspars. According to the standard the percentage of the cloudy area can be calculated.

This method gives a relative cloudiness when using the same clouding standard for all the samples. However, some limitations exist:

1. The result represents the volume percentage of the cloudiness over the whole feldspar mineral, but could not tell the actual clouding intensity (darkness) of the feldspars.
2. Partial alteration affects the result dramatically since the computer reads it as cloudiness in the image.
3. A reliable result is strongly dependent on uniformity of thickness of the thin sections being used.

The cloudiness of feldspars from seven dykes was evaluated using this method. Five of them were from the NW side of the BLF and two from the SE side. Each result is the average of two thin sections from the same dyke.

B. Magnetic Quantification

Saturation magnetization values of feldspar separates directly represent the concentration of magnetite in the feldspar, so that they can be used directly to quantify the clouding intensity. Another magnetic parameter is the amplitude of Verwey transition of the feldspar separates. The amount of remanence lost at the Verwey transition (T_v) should be a function of magnetite grain size (Özdemir and Dunlop, 1997) and amount of magnetite. Because of the similarity of grain size, the Verwey transition amplitude is thus mainly a function of magnetite content in the feldspars studied here. The experimental result proved this argument. If the difference of remanent magnetization at 50 K and 300 K, taken as the amplitude of the transition, is plotted against the magnetite concentration derived from the magnetization at the temperature of 50 K, a linear relationship occurs (Fig.2-15). It is noticed that the saturation magnetization of the feldspar separates is not a function of the amplitude of Verwey transition. It is probably because the existence of magnetite of superparamagnetic grain size.

For the seven sites that have been tested by computer image analysis, optical clouding intensity shows positive linear relations to the saturation magnetization as well as to the amplitude of the Verwey transition (Fig. 2-16). This correlation suggests that the magnetite content in the feldspar accounts for the clouding, thus strongly supporting the argument about the origin of the cloudiness. Therefore, the clouding intensity can be precisely quantified by either of the magnetic measurements.

3.4.2. Feldspar clouding and the depth of dyke intrusion

The experiment results were applied to a local thrust fault, the Budd Lake fault (BLF), to directly test correlation between feldspar clouding intensity and dyke intrusion depth. Geobarometry data on both dykes and country rocks (Palmer and Barnett, 1992; Percival et.al.,1994) indicate that there was a crustal uplift on the NW side of the BLF after dyke intrusion. The BLF could be a listric thrust comparable with the ILF (Zhang and Halls, 1992), with the up-thrown side tilted to the NW causing deeper sections of the dykes to be exposed closer to the fault.

Saturation magnetization (M_s) of feldspar separates from different dykes is plotted with respect to the position of dykes along the traverse across the BLF (Fig.2-17). A progressive increase in M_s occurs towards the fault on its northwestern (up-thrown) side, followed by a sudden drop on the downthrown side once the fault is crossed. Feldspar clouding intensity derived from image analysis on seven dykes is also plotted according to the distance of the dykes from the fault. It demonstrates a linear function with the M_s and the distance to the fault. The profile starts about 10 km away from the fault, and the M_s shows an almost linear relationship with distance, which indicates that if the angle of crustal tilting is about constant, the degree of feldspar cloudiness is linearly related to the depth of dyke intrusion.

4. Conclusions

From the study of cloudy feldspars in the Matachewan dykes, the following conclusions can be made:

1. Almost pure magnetite particles cause the feldspar clouding.

2. The size of the particles is within the pseudo-single domain range.

3. The magnetite was formed by exsolution of iron from the feldspar structure during slow cooling.

4. The degree of clouding in feldspars can be quantified by both image analysis and magnetic measurements on feldspar separates. The magnetic methods give more precise determinations.

5. A test on the BLF demonstrates a positive relationship between the clouding intensity and the dyke intrusion depth.

Chapter III. Paleomagnetic Study on Matachewan Dykes

1. Introduction

Mafic dyke swarms have been found on Precambrian cratons around the world. Strong, stable magnetism and large areal extension make mafic dyke swarms important targets of paleomagnetic study. Besides the usage in defining the apparent polar wander paths (APWP) and demonstrating polarity reversals, research has been directed to using paleomagnetism to study geological structure and tectonics at different scales. For example, detailed paleomagnetic analysis of individual dykes and their contact zones has been used to estimate the uplift and erosion that has taken place since dyke emplacement (Schwarz 1977, Buchan and Schwarz 1981), and the variation of magnetic declination and inclination of dykes that cover a large area has defined regional deformation (Bates and Halls, 1991).

In the giant Matachewan dyke swarm, previous paleomagnetic study has revealed two antipodal remanences, N and R, with a ratio about 1:4. This ratio changes locally in the vicinity of the KZ (See Chapter I, section 2). The change is so intimately related to the major faults, such as the ILF, BLF, and MRF (Fig.3-1), that it seems to be a good marker to map the traces of major faults in the area.

A detailed paleomagnetic study was conducted on the Matachewan dykes in an area of about 2500 km^2 between Wawa and Chapleau (Fig.1-1, Fig.1-2), that covers a possible extension of the KZ in the Wawa gneiss domain. The principal objective of this paleomagnetic study is to use the magnetic polarity method to explore for any hitherto unknown uplifted crustal blocks that might represent a further segment of the KZ, similar to the Chapleau block. At the same time, based on the paleomagnetic study of Bates and Halls (1991) on a broader scale, the data can be used to test for any block rotations within the study area that might further define the tectonic development of the KZ.

2. Sampling and Demagnetizing Procedures

In total, 188 dykes were sampled in the study area (see Fig.1-3 for locations). Among them, 112 dykes gave a stable Matachewan direction (76 N, 36 R) and 17 are non-Matachewan dykes distinct by their trend, petrology and magnetic direction. The others are either strongly altered or struck by lightning, which destroyed the primary remanence. The strike directions of the dykes were better known than their dips because most of the sites are exposed in flat outcrops. Typically, six to eight oriented samples were collected from each site, depending on the quality of the outcrop. Samples were mostly drilled in the field and were oriented using both a sun and a magnetic compass. A minority of oriented block samples was also collected and drilled in the laboratory. Based on earlier experience (Halls 1992, personal communication) samples from unaltered chilled margins tend to give more stable directions. Therefore, an effort was made to get samples from fresh margins wherever possible. The attitude of each sampled site was recorded with a detailed sketch. This information generally included trend, dip, thickness, sample locations, degree of alteration, secondary veining as well as country rock structure. In the laboratory, all cores were cut into 2.4 x 2.4 cm cylindrical specimens.

At those sites which offered the possibility of a baked contact test (Everett and Clegg, 1962) up to 20 oriented samples were obtained. These sites either involved cross-cutting dykes or offered single dykes with potentially suitable host rocks.

All specimens (at least one per sample) were subjected to detailed stepwise alternating-field (AF) demagnetization in the Rock Magnetic Laboratory, Erindale College, using a Schonstedt

GSD-1 instrument with a peak field intensity of 100 mT. A limited amount of thermal demagnetization was carried out with a Schonstedt TSD-1 furnace. Remanence was measured on a modified DIGICO spinner magnetometer. At higher fields, an averaging procedure (Halls, 1986) was carried out, whenever needed, to reduce scatter of magnetic directions. Data were analyzed using principal-component analysis (Kirschvink 1980, with maximum angular deviation of 10°), remagnetization circles (Bailey & Halls, 1984) and orthogonal vector plots (Zijderveld, 1967). Sample remanence directions were then averaged for each dyke to produce a site mean (Table 5).

3. Characteristics of the remanence

The natural remanent magnetization (NRM) of samples has intensities that vary from less than 0.1A/m to over 10 A/m. It is composed mostly of two (sometimes three) components. Thermal demagnetization analysis shows that the high-coercivity component has a narrow blocking-temperature range for both N and R dykes. The component begins to be resolved as the Curie point of magnetite (585°C) is approached, then the intensity of the magnetization falls rapidly (within less than 10°C) and the specimen becomes unstable magnetically (Fig.3-2). The NRM demagnetization properties indicate that the remanence is a thermal and/or chemical magnetization carried by fine-grained magnetite (Pullaiah et al. 1975).

Because of the narrow range of blocking temperatures, it is difficult to define a stable endpoint by thermal demagnetization. However, since in AF demagnetization, removal of a low-coercivity component describes a great-circle path on a stereographic net, convergence of the paths define the potential site mean direction (Fig.3-3), AF is therefore the preferred technique for the demagnetization of dyke samples.

Typically, after removal of a weak viscous magnetization, two linear segments are resolved during AF demagnetization. The first component removed has a low coercivity range (<20 mT) and poorly defined directions. Site means are scattered around the present Earth's field (PEF) direction (~352°/77°, Garland 1979) (Fig.3-4) indicating a recent viscous origin (viscous remanent magnetization, VRM). The low-coercivity spectrum overlaps that of the higher coercivity components, so that the vector plots of remanence directions are initially curved. The stable component is often isolated after the intensity falls to below 10% of the initial NRM value.

Generally, R dykes have a weaker high coercivity component than that of N dykes and the R component is often defined with less precision than the N. This property indicates that the R remanence is mainly carried by coarser grain size magnetite compared with the N.

4. Distribution of R and N dykes marks major faults in Study Area

The pattern of distribution of N and R polarities within the study area divided into distinct polarity domains. Combined with other geophysical and geological evidence, these polarity domains represent fault-bounded tectonic blocks (A, B, C, D, E, and F). Among them A is an uplifted wedge (Gould Lake block GB), F is part of the RA region in Bates and Halls (1991), E is southern part of the Chapleau block (CB). Fig.3-5 shows the detailed distribution of these blocks, which for the first time, reveals that the KZ extends southwestward as a sinistrally offset segment (block D) of the Chapleau block. The resulting discovery of two previously unrecognized uplifted blocks (A and D in Fig.3-5) establishes the strength of this new technique in which the magnetic properties of dykes are used to map major faults in an Archean terrane having uniform or subtly varying lithology.

4.1 Extension of Budd Lake Fault:

Study of the Budd Lake Fault (BLF) was initiated by the discovery of a one meter wide NE trending dyke cut off by a fault trending 020° and dipping 24° W (Site TK65) beside Budd Lake, about 50 km west of ILF along Highway 101 (Moser 1988). All previous geological and geophysical observations (Chapter I, section 3) supporting the existence of the fault were all made along the single profile of Highway 101 and therefore, the nature of the strike extent of the fault to north and south was not clear. More traverses in the south and north are needed to give a better control and understanding of the fault.

NE of the intersection of highway 101 and Highway 651, north of the Budd Lake (Fig.1-3 and Fig.3-5), dykes along an approximately 10 km road to Spencer Lake as well as on the lake (SL1 ~ SL9) are heavily veined and fractured (see Appendix for structural analysis) and failed to give stable remanent magnetization. This may indicate that the BLF or its satellite faults cut through in the area. On Highway 101, discovery of a new R dyke (TK60) at the intersection of Highway 651 and Highway 101 located the fault more precisely at 5 km west of Budd Lake. The fault seems to be dextrally offset for a few kilometers by a N-S fault (the McEwan Lake fault, see discussion below).

To the south of Highway 101, dykes on Gould Lake (Fig.1-3, SL10 ~SL12) gave a stable N remanent magnetization (Fig.3-5). A traverse along the Tik Road revealed another polarity change across the Agawa River canyon. Approaching the fault along the Tik road from northwest, the magnetic polarity of Matachewan dykes changes from mixed R-N to entirely N, then becomes completely R after crossing the Agawa River (Fig.3-5). This change coincides closely with the variation of the feldspar clouding: clear-increasingly cloudy-clear (Chapter II). This discovery extended the BLF about 20 km SW to the Agawa Canyon Fault (ACF), and also suggested that domain A, NW of the BLF, is probably a new uplifted block (Gould Lake Block, GB, Fig.3-5).

4.2 Discovery of a new fault, McEwan Lake fault (MLF)

On the 1:50000 topographic map, a lineament formed by a chain of lakes is apparent, of which McEwan Lake is the largest one (the fault was named after it, MLF). A distinct series of NNW-trending topographic depressions, which geologically might represent compositional belts, ancient faults, or dyke related structures, appear on the eastern side but cannot be followed across the supposed trajectory of the fault (Fig.3-6). Rocks on the western side have steeper foliation on average and are more fractured, contain more amphibolitised volcanics, pink granites, and epidote and quartz veins.

Two sampling traverses, along the Tik road and the Powerline road (Fig.3-5), were made across this feature. As both traverses cross the N-S chain of lakes, dykes change polarity from R to N (Fig.3-5) to the SE and feldspars become accordingly cloudy. These changes strongly suggest a N-S trending fault (MLF) which is up thrown on its eastern side.

The fault has clear aeromagnetic and gravity expression (Gupta. 1991a, 1991b). The sense of displacement is consistent with the aeromagnetic data. A sharp gradient, coincident with the topographic lineament is obvious on the total field aeromagnetic map and Bouguer gravity map of the region (Fig.3-7, Fig.3-8). Higher magnetic values are found in the east and lower ones in the west. The aeromagnetic anomaly is consistent with deeper crust gneissic rocks in the east tending (on average) to be more magnetic than their shallower crustal equivalents of lower metamorphic grade in the west (Grant 1985).

A detailed gravity survey was then conducted (Halls and Mound, 1998) across the fault. The gravity data were modeled and the resultant profile suggests a thrust fault dipping 20- 25°E that has a total vertical displacement of at least 5 km (Fig.3-8). Tonalite gneisses on the western side of the fault have about 5% modal amphibolite and biotite, but on the eastern uplift side they have about 10% plus rare garnet, a compositional change that is not obvious in the field but which leads, together with a lower hydrous alteration, to a slightly higher mean density (by about 0.1g/cm^3) (Halls and Zhang, 1998).

4.3. Second N-S fault, Nagasin Lake fault (NLF):

This fault is also marked by a linear chain of lakes (Nagasin Lake is one of them) but neither gravity nor aeromagnetic anomalies are obvious. It is constrained by a change of magnetic polarity and feldspar cloudiness of dykes at three locations. The first traverse was discovered by Halls and Palmer (1990) along Highway 101 and a nearly N-S fault was suggested (Fig.3-5). A traverse on Windermere Lake (Fig.1-3) extended the fault in a NNW direction for about 15 km. Due to extensive drift cover, the polarity change in the southern part of the fault is not as well constrained as that along profiles on the Windermere Lake in the north and highway 101 in the middle. However, undoubted R sites KS15 and TA14 help to control the location of the NLF and ILF (Fig.3-9 a, b). The lack of a pronounced change in metamorphic grade of the Archean rocks across the fault within the uplifted zone suggests that the dominant motion is sinistral transcurrent.

4.4. Extension of Montreal River fault (MRF):

Although MRF was thought to be probably an extension of the ILF (Grunsky 1981), the nature of its connection with the ILF was unclear. Along the power line traverse, the N polarity of the dykes changes into R across the Montreal River (Fig.3-5). Normal dyke sites, TK66, TK67, and TK 68 constrain the northern limit of the fault. The new paleomagnetic results then extend the Montreal River fault about 30 km in the ENE direction to the NLF, forming the southern margin of the PB. However, N dykes TK73 & TK 74 have clear feldspars suggesting that the uplift on the northern side of the MRF was small (probably <5 km compared with the McEwan Lake fault. During the E-W shortening to form the KZ, movement along the MRF was probably dominantly dextral.

4.5 A possible extension of Saganash Lake fault (SLF):

Along the section of Highway 101 between MLF and SLF, most dykes have R polarity. At about 10 km south along Mank Lake road, Matachewan dykes show an along-strike polarity change (Fig.3-5), defined by a definite R dyke TK85 (Fig.3-9c) and a series of N dykes to the south (beginning with TK86). Dyke outcrops also show brittle deformation. Referring to the polarity change on Highway 101 to the northeast, an ENE-WSW trending fault downthrown to the north, is suggested. Although it does not show an obvious aeromagnetic anomaly, it has an expression in gravity. However, the gravity gradient is much less than that on other faults in the vicinity (Fig.3-8) suggesting it may have a smaller dip. From the map, it seems to represent a westerly continuation of the Saganash Lake fault (SLF) which was interpreted by Percival and McGrath (1986) as a normal fault dipping NW in the Groundhog River block. In the Chapleau block, however, Manson and Halls (1997) interpreted it as a NW verging thrust fault from the Lithoprobe seismic data of Percival and West (1994). A gravity survey across the fault also suggests a reverse nature (B.Nitescu, 1998 personal communication).

4.6 New KZ Block: Pineal Lake Block

The discovery and confirmation of the major faults above demonstrated that the lateral variation in magnetic polarity and feldspar cloudiness of the Matachewan dykes are useful fault-mapping tools. The newly detected faults provide a structural framework for the area. From that a completely new and unsuspected segment of the Kapuskasing zone is revealed (Fig.3-5). This result shows that the KZ continues to the SW for another 60 km as a fault-bounded block, sinistrally offset from the Chapleau block by about 20 km. This new block of the KZ is named the Pineal Lake Block (PB, Block D in Fig.3-5) after the largest settlement contained therein (Halls and Zhang 1998). A gravity survey across the MLF and the increasing cloudy intensity of feldspars towards MLF on PB suggest the block has been tilted eastward. This tilting also has an expression in paleomagnetic direction of the dykes, which is discussed in the next section. In Block C, both polarity and feldspar in Matachewan dykes are similar to relatively low-grade upper crustal domains south of the KZ. Thus, the KZ as a series of upfaulted crustal blocks, does not appear to continue west of the McEwan Lake fault. Limited dyke sites in the centre and at the margin of the MRF indicate a probably northward tilting of Block C. About 30-km west of the MLF, lies the parallel trending Agawa Canyon fault (ACF). Dykes on the west of the ACF have exclusively R polarity suggesting a down-to-the-west sense of displacement (Halls & Shaw1988)(Fig.3-10). Geological compilations (Ontario Geological Survey, 1991) suggest a possible sinistral component of displacement similar to that of the NLF.

Fig.3-10 gives the polarity distribution of all Matachewan dykes sampled in the study area (detailed demagnetization data for each site is in appendix). A comparison of Fig.3-10 with Fig.3-1 demonstrates the importance of these results in clarifying and improving our understanding of the fault distribution at the southern end of the Kapuskasing zone.

5. Variation in paleomagnetic Directions

Previous regional paleomagnetic work by Bates & Halls (1991) has found significant variations in the directions of the remanence. Their study covered all three subswarms with the most on M_3 (Table 7). The study area of this thesis is located in their C region (Fig.3-11). Their two important discoveries about magnetic directions of the Matachewan dykes are:

(1) R inclination increases regionally northward whereas N inclination remains relatively uniform. In the regions where N and R dykes occur together, the N inclination is larger than the corresponding R. These differences are unlikely to be caused by deformation because the N polarity data have virtually uniform inclination, and the R data would require too large an amount of crustal tilting. Instead, the inclination difference was attributed to apparent polar wander (Bates and Halls 1991). Dykes at greater distances from the focal region intruded at a later date than those that are more proximal. Cross cutting relations indicate that N dykes are relatively younger than R dykes (Halls 1991), thus the inclination increase implies that during the main phase of the swarm evolution, either Laurasia drifted to higher latitude or the magnetic pole moved southward relative to the dykes.

(2) For both R and N, there is a positive correlation between the average trend of dykes and the declination. This correlation is more obvious in the M_3 subswarm where dykes describe a broad Z-shape. This observation proved, that within and north of the KZ, the dykes had been rotated about steeply dipping axes to produce a distorted version of a once linearly radiating swarm.

Paleomagnetic data in the thesis reinforce the results of the regional study. The characteristic Matachewan paleomagnetic signature is clearly recovered from almost every stable N and R dyke in different parts of the swarm. At individual sites the feature of either N or R is obvious. In a local area, the direction of the remanent magnetization is quite uniform. However, a close examination on block mean directions revealed a systematic variation in both declination and inclination (Table 6).

Table 6. Paleomagnetic Directions of Different Blocks

Block	Dyke Trend(°)	σ(°)	Polarity	N	D(°)	I(°)	K	α_{95}(°)	Φ_{63}(°)
A	339	8.6	N	21	27.2	24.8	60.5	4.1	7.4
D	348	12.1	N	40	23.3	28	52.2	3.2	7.9
E	352	10.2	N	39	28.3	20.6	84.7	2.5	6.2
B	355	9.9	R	23	221.5	-20.1	25.6	6.1	11.3
C	331	18.5	R	12	204.7	-19.4	36.9	7.2	9.4
F	331	4.3	R	6	196.3	-16.7	64.5	8.4	7.1

Note:
σ: Standard deviation of dyke trend
N: Number of dykes in the block
D: Block mean declination
I: Block mean inclination
K: Estimate of precision parameter
α_{95}(°): Semiangle of the cone of 95% confidence
Φ_{63}(°): Angular standard deviation of paleomagnetic data

5.1 Test of the paleomagnetic data

Before any tectonic interpretation of the variation can be valid, paleomagnetic data need to be examined to ensure that the regional variations in direction are not the product of other unrelated effects such as contamination of the data by secondary components and anisotropy of the remanence.

a. Contamination by secondary components

Variation in magnetic direction and particularly polarity asymmetry could indicate an unremoved component, most likely a viscous one due to the present Earth's field (PEF) (Tarling, 1983). Tests of existence of this possibility were done on site mean level. The result is that the distribution of stable end-points of site-mean directions has no preferred trend approaching the PEF direction (352°/77°, Garland 1979), or other particular directions (Fig.3-12). This test indicates a lack of contamination attributed to the incomplete removal of a PEF or other component. Therefore the asymmetry in directions is real.

b. Magnetic anisotropy

The other possible cause of paleomagnetic variation is the effect of magnetic anisotropy. The magnetization of a dyke could be deflected either as a result of anisotropy of magnetic susceptibility of the diabase due to magma flow (Stacey 1960), or from shape anisotropy related to the tabular nature of the dyke body (Abrahamsen 1986). According to the calculation of Bates and Halls (1991), both effects are insufficient to cause a distinguishable systematic change in the declination to explain the observed spread.

In my study, a further empirical test was done by plotting paleomagnetic declination against dyke trend for each site in all blocks. If the effect of the anisotropy is large enough to be detectable, dyke declinations should show a positive relationship with dyke trend. The mean dyke trend and mean declination in each of the six blocks were plotted in Fig.3-13 (a: N blocks and b: R blocks). The absence of any positive correlation indicates that neither flow-induced nor shape anisotropy is significant.

5.2 Variation in Paleomagnetic Inclination

In accordance with the regional study (Bates and Halls 1991), the results in this thesis confirm the trend of inclination variation. For R dykes, the inclination increases with latitude of the sampling region. Note that block F is part of the RA area in the regional map (Fig.3-11), whose magnetic direction is 204.1° declination and −11.6° inclination. This direction is used as a reference to test relative rotation for other blocks. North of the MRF, within block C and block B (Fig.3-5) geographically located further north, average inclination is −19.4° and −20.1° respectively. The block-mean inclinations of N are steeper (~5.7°) than those of R (Table 7).

These two comparisons, in a smaller scale but more detailed level, indicate that there has been a steepening of the inclination with time during the Matachewan igneous activity. This variation fits well with the regional picture in both trend and amplitude (Fig.3-14).

Table 7. Regional Block Mean of Paleomagnetic Data from Matachewan Dykes

Location	Polarity	No. of Sites	D(°)	I(°)	K	α_{95}(°)	Φ_{63}(°)	δ(°)	σ(°)
MT	N	---	---	---	---	---	---	360	---
	R	10	207	-16	54	7	---	---	---
OS	N	---	---	---	---	---	---	360	---
	R	16	210	-14.8	39	6	---	---	---
RA	N	3	23.2	17.9	49	17.9	8	326	90
	R	17	204	-11.6	52	5.4	10		---
RL	N	3	19.2	20.7	45	18.6	9	325	16
	R	19	209	-6	42	5.2	9	---	---
WL	N	1	15.7	24.9	---	---	---	350	13
	R	3	217	-9.7	190	9.1	4	---	---
C & ML	N	37	30.1	22.4	66	2.9	---	---	---
	R	19	224	-23.4	41	5.3	---	---	---
OL	R	4	185	-23.1	110	8.9	6	310	3
HP	N	3	10.3	24	220	8.4	4	326	10
	R	11	191	-25.6	100	4.5	6	---	---
HT	N	6	14.3	31.6	89	7.1	6	337	10
	R	10	199	-17.8	66	6	7		---
MK	N	15	38.9	32.3	40	6.1	9	344	10
	R	14	223	-23.8	24	8.2	12		
TM	N	5	21.4	28.2	430	3.7	3	347	12
	R	15	209	-14.8	87	4.1	6	---	---
C1	N	14	26.4	23.8	87	4.3	6	353	10
C2	N	1	32	31	---	---	---	353	10
	R	5	229	-28.4	47	11.3	8	---	---
C3	N	5	30.5	24.5	94	7.9	6	339	10
Block A	N	21	27.2	24.8	61	4.1	7.4	339	9
Block D	N	40	23.3	28	52	3.2	7.9	348	12
Block E	N	39	28.3	20.6	85	2.5	6.2	352	10
Block B	R	23	222	-20.1	26	6.1	11.3	355	10
Block C	R	13	205	-19.4	37	7.2	9.4	331	18
Block F	R	6	196	-16.7	65	8.4	7.1	331	4

Note:
N: Normal
R:
Reverse
K: Estimate of precision parameter
α_{95}(°): Semiangle of the cone of 95% confidence
Φ_{63}(°): Angular standard deviation of paleomagnetic data
δ(°): Mean dyke trend
σ(°): Standard deviation of dyke trend

5.3 Variation in Paleomagnetic Declination:

The spread of paleomagnetic declinations is greater than that of inclinations, especially for the R dykes (Fig.3-12). Variation of the inclination is ascribed to a relative movement between the geomagnetic pole and Laurasia, either the pole excursion or tectonic drift. In either scenario, any relative movement not parallel to dyke strike would result in an accompanying change in declination, so that the change of declination should have a smooth correlation with the change of the inclination. However, neither regional (Bates & Halls 1991) nor local (this thesis) observations show this type of related variation. This indicates that the change of declination could be a consequence of post dyke deformation. Regional study revealed a positive relation between mean paleomagnetic declination and mean dyke strike for different regions (Bates and Halls 1991). Blocks studied in this thesis fit well into this relation (Fig.3-15), which suggests that, as part of the regional deformation, the variation of the paleomagnetic declination of dykes in different blocks is caused by relative rotation of the blocks about steeply inclined axes.

Southeast of the KZ, in the Abitibi subprovince, all data sets from M_1, M_2, and M_3 have virtually identical mean site directions despite variation in dyke strike from 360° in the east to 325° in the west (Bates and Halls 1991). This observation clearly indicates that the dyke swarm has not been significantly disturbed, so that the average magnetic declinations, 208° and 21°, were suggested to be the respective R and N values for Matachewan swarm (Bates and Halls 1991). Fig.3-16 shows block-mean directions of the newly studied blocks at 95% confidence level. Compared with the reference declinations, their distribution suggests that:

(1) Among the 3 N blocks A, E and D within the KZ, the declinations are very close to each other indicating that within the KZ the relative deformation was dominated by vertical motion (uplift). Dykes in each block give bigger declination compared to the reference (21°) suggesting

that all blocks have undergone small clockwise rotations around steeply inclined axes. The mean directions in block E and D are significantly different at the 95% confidence level (Fig.3-16) despite their close proximity. This difference suggests some horizontal tilting. After about 10° westward rotation around a N-S horizontal axis, the direction of block D perfectly overlaps with that of block E. This operation suggests that compared to block E, block D has tilted about 10° eastward around a N-S horizontal axis. This result is in accordance with that derived from the feldspar clouding and gravity studies on block D, which show that Block D had been upthrown westward along MLF and tilted to the east.

(2). The R blocks have similar inclination but different declination, which indicates that at shallower crust levels outside the KZ, there was a greater component of rotation about steeply inclined axes than that in the KZ. These differences may be because outside the KZ, the remanence is primary and therefore has seen more deformation (rotation). But inside the KZ, the N magnetization of dykes is relatively late. Compared to the original declination (208°), block C (204.7°, -19.4°) and block F (using the direction 204.1°, -11.6° of RA region that includes block F, Fig. 3-12) remain almostly unchanged, but block B (221.5°, -20.1°) has been rotated clockwise by about 14°. This rotation is expressed by the marked change in the trend of the dykes between the blocks (Fig.3-5). Across the MRF, dykes continuously extend from block F into block C with similar strikes (in both blocks strikes are close to 331°, Table 5,6). However, in block B the mean trend of dykes is about 355° (Table 6).

6. Study of Country Rock Foliation

The study area is located in the centre of the Wawa Gneiss Domain. The relatively homogeneous mid-crust metamorphic rocks are mainly composed of tonalitic gneiss and mafic gneiss (Chapter I). Variation in metamorphic grade is not obvious. Moser (1988, 1994) has studied the structure of the country rock regionally. In this thesis, measurement of host rock foliation (compositional layering) across the major faults was done to examine the direct evidence of block rotation observed from paleomagnetic data of the dykes.

More than a hundred sites were measured in the field along traverses across the BLF and MLF. The reading for each station is the result of averaging several measurements at a site. The average strike and dip of foliation in the host rock for each block are shown in Fig.3-17.

The change of average strike in different blocks suggests that blocks A and B underwent some clockwise rotation around vertical axes relative to the blocks C and D. The amounts are 20° and 35° respectively. This result is in accordance with both dyke configuration and paleomagnetic data, which suggest that all blocks have undergone clockwise rotation especially block B. Relative to block C, for example, block B rotated 17° and 15° according to magnetic data and the trend of the dykes respectively (Table 7). However, 32° rotation between the two blocks is suggested by the country rock foliation measurement (Fig.3-17). This difference may imply that the dextral rotation started before the emplacement of the Matachewan dykes and it had reached about half of the total amount before the dyke intrusion.

A systematic variation of dips was also noticed along each profile. Analysis of structural evolution of the central Wawa gneiss domain was done by Moser (1994), who found that in the deeper structural levels, the rocks tend to develop planar fabrics with generally shallower dips. This may be caused by late Archean subhorizontal ductile shearing (Bursnall et. al 1994). My field measurements of host rock foliation give support to Moser (1994)'s observation. In block A and D, which tilts NW and SE respectively due to thrusting, host rock foliation becomes flatter when the fault is approached (Fig.3-17). Although not as clear as block A, a similar phenomenon can be seen for block D which is up-thrust to the NW wards on the MLF.

7. Conclusions

1. The Change of paleomagnetic polarity of Matachewan dykes in the study area has lead to the discovery or confirmation of five major faults. It proved that the polarity change of dykes is a very applicable tool to map major faults. This result revealed two new uplifted blocks (GB and PB). GB was uplifted by a second thrust along the BLF which is comparable with the ILF in structural style; PB seems to be the SW wards continuity of the KZ from the Chapleau block but it was sinistrally offset about 15 km.
2. Variation of paleomagnetic direction was caused by apparent polar wander as well as regional structural deformation. The inclination difference among the R dykes from different blocks and between N and R dykes indicated that the area moved towards higher latitude during Matachewan igneous activity. The declination change revealed clockwise rotation for all the blocks north of the KZ. A difference in mean paleomagnetic directions between blocks D and E may represent an eastward tilting of the PB, in agreement with the feldspar clouding observation and gravity survey data.
3. Measurement of host rock foliation directly supports the relative rotation and tilting of blocks suggested by paleomagnetic study and average strikes of Matachewan dykes. The dextral rotation started before the dykes' intrusion.

Chapter IV. Feldspar Clouding and the Normal Remanent Magnetization

1. Introduction

Observation on the Matachewan dykes in the study area combined with data from other parts of the swarm revealed a correlation between feldspar clouding and paleomagnetic polarity. In summary, outside of the Kapuskasing Zone, both R and N dykes have clear (if not altered) feldspars; dykes emplaced in the uplifted KZ have N polarity and most of them have cloudy feldspars. The almost corresponding appearance of cloudy feldspars and N polarity within the KZ strongly indicates a close relation of the two phenomena. More than 250 individually AF demagnetized samples from about 100 N dykes were examined in terms of the relation between feldspar clouding and coerçivity of the natural remanent magnetization. The result is that, statistically, feldspar clouding increases dykes' remanence intensity in the higher coercivity ranges (Zhang and Halls 1995). The histogram (Fig.4-1) offers a direct demonstration for this relation.

2. Cloudy Feldspars Carry Normal Remanent Magnetization

In order to further understand the function that cloudy feldspars play in the Natural Remanent Magnetization (NRM), a series of rock magnetic experiments were performed on samples from dykes that have stable remanent magnetization but varying clouding intensity of the feldspars.

The first was Anhysteretic remanent magnetization (ARM) treatment on samples from three dykes:

TK37: Trend: 10°; Dip: unavailable; Width: >29.1m; Polarity: N; Feldspar clouding degree: 12

TK19: Trend: 346°; Dip: 80°E; Width: ~28.5m; Polarity: N; Feldspar clouding degree: 3.6

TK34: Trend: 338~346°; Dip: unavailable; Width: >6.2m; Polarity: R; Clear feldspar

(The clouding level is measured by the saturation magnetization of the feldspar separates)

ARM is an artificial room temperature remanence that most closely resembles the naturally occurring thermal remanent magnetization (TRM)(Dunlop & West 1969). It allows the study of the properties of TRM without chemical changes induced by heating the samples. In the laboratory, it is produced in a sample by applying a constant external magnetic field during application of a decaying alternating field. The direct field serves to bias the final orientation of magnetic moment while the alternating field is being reduced to zero. In the experiment, the ARM was produced by demagnetizing the samples in an AF field of 100 mT in the presence of a DC field of 0.25 mT. Cylindrical specimens of feldspar separates from the dyke samples were prepared by tightly sealing the grains into plastic holders. A feldspar specimen and an intact rock core were selected from each dyke. The samples were previously demagnetized by an alternating field (AF) of 100 mT before the ARM was applied. After the ARM was put in, all samples were then AF demagnetized in steps up to 100mT.

Feldspar separates used for the experiment weighed about 5 g for each dyke. From the known density (2.62 g/cm^3), the ARM per unit volume of feldspar at each demagnetizing step was obtained. Given the volume percent of feldspar content in the whole rock from image analysis of the thin sections, the percentage of remanence carried by feldspar in the whole rock samples was calculated after each demagnetization step. Results of the experiment showed that the percentage of remanence carried by the feldspars in different dykes has a positive correlation with their feldspar clouding intensity. The maximum percentage of ARM contributed by feldspars in dykes TK37, TK19, and TK34 is 78%, 20%, and 6.5% respectively (Fig.4-2). The positive relations of clouding degree and the ARM percentage suggests convincingly that cloudy feldspars must play an important role in the NRM of the dykes.

In NRM AF demagnetization of N dykes, a stable magnetization was usually isolated after a demagnetization field of 60 mT, which is in accordance with the results of the ARM experiment. This coincidence implies that cloudy feldspars are at least partly the carriers of the stable N component.

To further explore the relative roles played by cloudy feldspar and coarse magnetite in the NRM, another experiment was performed using a typical medium cloudy feldspar dyke (TK49). The NRM of TK49 (Fig.4-3A) is composed of two components that can be separated into high (H_c>40 mT) and low coercivity parts (H_c<40 mT) (Fig.4-3B). A weighed rock core, feldspar separate specimen and coarse magnetite separate specimen of TK49 were given ARM under identical conditions described in the first experiment. The results show that the coarse-grained magnetite in the rock carries a big percentage (as high as 70%) of the ARM as low coercivity magnetization. However, it drops quickly to less than 5% after 60 mT. The percentage held by feldspar grains is about 10% at the beginning, but it increases almost linearly and reaches the highest, about 50% after, 80 mT (Fig.4-4).

This study established a direct relation between cloudy feldspar and the high coercivity component of NRM in a dyke. Fig.4-5 shows a comparison of the NRM and ARM components. Three remanence pairs are plotted: whole rock ARM with NRM, feldspar ARM with the high H_c component, and coarse magnetite ARM with the low H_c component. Each pair exhibits a strong similarity in shape. This indicates that the low coercivity component of NRM of the Matachewan dykes is carried by the coarse grained magnetite, while the sub-microscopic magnetites in cloudy feldspars are the main carriers of the higher coercivity component.

3. Formation of N Remanence within the Kapuskasing Zone

The phenomenon that the Matachewan dykes have N magnetization at deeper crustal levels but R magnetization at the shallower can be explained by two possible hypotheses (Fig.4-6):

1. The N dykes were intruded after the R epoch. Both N and R dykes represent separate episodes of magma intrusion, between which the Earth's magnetic field reversed from R to N. However, the N dyke intrusion was largely confined to deeper crustal levels as blade-like dykes (Fig.4-6a).

2. Most of the dykes intruded during the R epoch but their lower parts did not acquire a remanence until after the R to N reversal of the Earth's magnetic field had occurred (Fig.4-6b).

Both of the models can form the present pattern provided post-dyke exposes the dyke roots. However, a magnetic study can offer a test of the hypotheses. First of all, a baked contact test was carried out.

Although positive baked contact tests had been previously obtained for dykes outside the KZ (Irving and Naldrett 1977; Buchan et al. 1990; Halls 1991), no comparable data were available on N dykes within the zone nor had a search been made for a possible underlying R signature of these dykes. Two N Matachewan dykes (sites 161 and 223 of Halls and Palmer 1990) were chosen for this experiment because of the availability of extensive outcrops of fine-grained tonalite host rock. This type of host rock is known from previous paleomagnetic measurements as a carrier of stable remanence (Halls 1992, personal communication). The two sites are about 150 meters apart. Twenty-seven country rock samples and 17 dyke samples (7 from dyke 161 and 10 from dyke 223) were obtained. All samples were subjected to either AF or thermal demagnetization and the results are given in Fig.4-7.

1. At both dyke sites, baked contact tests appear to be negative: the tonalites carry an N magnetization out to several dyke widths. It indicates that the N remanence is a secondary magnetization: both dyke and host rock gained a thermo-chemical N magnetization together during slow cooling.

2.Regardless of polarity, tonalites closer to the dykes give high coercivity (H_c) end points and square-shouldered decay curves in thermal demagnetization. In contrast, tonalites farther from the dykes yield remanences with lower coercivity spectra and thermal demagnetization curves with distributed unblocking temperatures (T_{ub}) up to 585°C, the magnetite Curie temperature (Fig.4-7 A,B,C). This phenomenon indicates that heat from the dykes played some role in the process of magnetization of the host rock. Probably heat at closer distance from the dyke helped to produce more fine grained magnetite. Also fine magnetite particles caused the feldspar clouding in the dykes and gained the N magnetization (a chemical remanence magnetization or CRM) when they grew larger than the critical blocking volume.

3.Although the majority of the tonalite samples (24 out of 27) are N, three (samples 23, 26 and 27) gave a clear R signature (Fig.4-7D). However, these R samples have higher coercivity and T_{ub} spectra. In seven samples where both N and R magnetization can be detected, the R always has higher coercivity and T_{ub} (Fig.4-7E). This result suggests that the host rock and dykes were R magnetized originally and later overprinted by N as the dykes cooled sufficiently to acquire a final N magnetization (TRM and CRM). Only those R remanences carried by high T_{ub} grains survived.

This result indicates that the N magnetization is not a product of regional metamorphism that happened after the dyke intrusion. AF demagnetization of the N dykes has documented several cases in which one dyke carries both R and N signatures. During the demagnetization, after removal of the Viscous Remanent Magnetization (VRM), R components were isolated, and after the intensity dropped to less than 10% of the NRM, stable N components were resolved (Fig.4-8). This phenomenon probably indicates that the R is carried by coarse magnetite that had been magnetized in the R epoch, whereas the N is carried by fine grain magnetite (probably mainly in cloudy feldspars) that was magnetized in the followed N epoch. It also suggested that many, if not the majority, of the dykes within the KZ may, like their counterpart outside, have been intruded during the R epoch. Since only one reversal (R to N) occurred during Matachewan activity (Halls 1991), the N dykes intruded after the Earth's magnetic field reversal (model one) should not have the R signature. The paleomagnetic results therefore support the second hypothesis. Geochronologic study (Heaman 1997) suggested that R and N dykes have the same age (Chapter V), which also supports the second model. That is, the Matachewan dykes have reversely magnetized tops and normally magnetized roots. Geobarometric studies across the BLF give a relative uplift of about 12 km (Palmer & Barnett 1992, Percival et al. 1994). However, the gravity survey across the MLF suggests a vertical displacement of about 5 km (Halls and Mound, in press). Therefore the separation depth between an R dyke and its remagnetized root is at least 5 km.

Chapter V. Conclusions and Discussions

1. Conclusions

The thesis focused on two important properties, feldspar clouding and paleomagnetic polarity change, of 2.45 Ga Matachewan dykes intruded into the area immediately southwest of the Kapuskasing Zone. The correlation between both phenomena and the depth of dyke intrusion was discussed. The result was tested as a mapping method, which revealed the southwestward extension of the Kapuskasing Zone in the Wawa Gneiss Domain. Three aspects of its result are summarized here:

1.1 New Observation and Application of Feldspar Clouding

On the subject of feldspar clouding, the study tried to give answers to the problem of its cause and furthermore to convert the phenomenon into a novel monitoring method for the study of relative crustal uplift. Curie temperature and Verwey transition tests indicate that the cloudiness is caused by submicroscopic magnetite with mainly pseudo-single domain grain size. Scanning Electron Microscope data suggest that the magnetite was formed from exsolution of Fe from the feldspar structure during slow cooling of the rocks. ARM experiments imply that cloudy feldspars are capable of carrying high coercivity remanent magnetization. In the Natural Remanent Magnetization, the cloudy feldspars play an important role in the high coercivity N component. Saturation magnetization and amplitude of Verwey transition of feldspar separates can precisely quantify the clouding intensity. Application of the quantification of cloudy feldspars across the Budd Lake fault demonstrated that the clouding intensity is a positive function of dyke intrusion depth.

1.2 Southwestward Extension of the Kapuskasing Zone revealed by Matachewan dykes

The study of this thesis on the Matachewan dykes in the Wawa gneiss domain has led to several new discoveries about the nature and evolution of the KZ in its southwest extension. The research successfully defined two previously unknown faults (MLF, NLF) and extended three faults (BLF, MRF, and SLF) in the Kapuskasing Zone. For the first time, these discoveries outline the structural framework of the Kapuskasing zone in its southwest extension in the Wawa Gneiss Domain. The new faults define two uplifted blocks, Gould Lake block (GB) and Pineal Lake block (PB). The Gould Lake block may represent a higher thrust slice in a series of imbricate thrusts of which the Ivanhoe Lake fault forms the basal member. The Pineal Lake block forms the fourth block in a series that defines the Kapuskasing Zone and is sinistrally offset about 20km from the Chapleau block. It comprises a fault-bounded region of amphibolite facies tonalite gneiss and migmatite that extends about 100 km southwest of the southernmost occurrence of granulite facies rock within the Chapleau block. A major east dipping thrust, the McEwan Lake fault, forms its western margin.

The direction of paleomagnetic remanent magnetization of dykes from different blocks shows systematic variation caused by apparent polar wander and regional deformation. This study strengthened the conclusions from the large-scale study of Bates and Halls (1991). The variation of inclination indicates the combined effect of northward development of the swarm and northward drift of the continent relative to the Earth's magnetic pole during Matachewan igneous activity. Variation of declination represents relative rotation among the blocks. The generally dextral rotation can be proved by the change in dyke trends and host rock foliation from different blocks.

1.3 Correlation of Feldspar Clouding, N Remanent Magnetization, and the Depth of Dyke Intrusion

The concentration of normally magnetized dykes within the KZ in a mainly reversed magnetized swarm is a consequence of delayed cooling of the dykes in deeper crustal levels followed by uplift. Matachewan dykes were emplaced in the R epoch and the upper section gained its reversed magnetization when they cooled through the magnetite Curie temperature. Cooling of the deeper parts (at least 5 km below), however, was delayed due to higher ambient temperature until the Earth's magnetic field changed direction from R to N. The slow cooling provided a suitable condition for feldspars to release the iron from their structure to form the magnetite which then acquired N remanent magnetization during growing and/or during subsequent cooling.

An important consequence of this study is a novel method that identifies differential uplift in the Canadian Superior Province, using paleomagnetic polarity and feldspar clouding in a Proterozoic dyke swarm. The method complements more conventional geobarometric and geochronological techniques applied to the host rocks and provides an independent means for tectonic study.

Proterozoic dykes are abundantly distributed in almost every Archean craton on the Earth (Halls and Fahrig; 1987). Those that exhibit cloudy feldspar are generally paleoproterozoic in age or have been uplifted along major faults (Halls and Zhang 1995). Fortunately, many of those dykes, intruded into relatively dry deeper crust, tend to be petrologically fresh, thus facilitating the observation of the clouding phenomenon. Many Proterozoic swarms also have dual magnetic polarity (although not antipodal) (Buchan and Halls 1990), making them ideal structural elements for study using the methods developed in this thesis. Therefore, in general, this thesis provides an important means for the study of differential crustal uplift in cratons.

2. Discussion

2.1 Age of the Feldspar Clouding and N Remanent Magnetization

Geobarometry indicates that the N dykes in the Chapeau block were emplaced at a crustal depth of about 20 km (Percival et al. 1994), where the ambient temperature was close to 550°C at 2.45 Ga (Percival and West 1994). Elevated thermal gradients might be expected due to the presence of an underlying mantle plume, conductive heat from the dyke swarm, and possible advected heat if the region was undergoing uplift and erosion at the time of dyke injection.

A dyke cools quickly after intrusion. According to Delaney's (1981) one-dimensional heat transfer model, the cooling time has a relation with the temperature of a dyke:

$$t = \tau/4 * T^2/K_h$$

Where t is cooling time in seconds, T is thickness of the dyke in meters, K_h is the diffusivity of the host rock at ambient temperature and τ is defined as a non-dimensional time parameter varying between 1 and 10. When $\tau=1$, about as much heat has been lost to the host rocks as remains in the dyke, then t measures the time for a dyke to lose half of its heat; when $\tau = 10$, temperatures are everywhere small in comparison to the initial temperature difference between the magma and host rocks, in this case, t represents the time for a dyke to cool to its ambient rock temperature.

According to the calculation, cooling of a dyke to its ambient temperature is almost instantaneous. For example, a 20m-wide, 1150°C dyke intruded in granite will cool down to host rock ambient temperature of 25°C (at ground surface, $K_h=1.5\times10^{-6}$ m^2/s) in no more than 22 years. At a depth where the ambient temperature is about 500°C ($K_h=0.6\times10^{-6}$ m^2/s), it will take the dyke

53 years to cool down to the same temperature as that of the host rock. After that, the dyke will cool at a rate similar to that of host rock. U-Pb dates on sphene from the country rocks give values of 2.5~2.6 Ga within about 30 km of the ILF (Percival et al. 1988), suggesting that the mid-crust had cooled through temperature of about 600~700°C (U-Pb closure temperature of sphene) at this time. Rb-Sr biotite data from tonalite near sites 161 and 223 (Chapter IV) give an age of 2.34 Ga (Percival and Peterman 1994). Since the Rb-Sr closure temperature for biotite is about 250°C (Percival and Peterman 1994), it indicates that the crust cooled down about 400°C in about 200 million years. Therefore the average cooling rate of the crust, and of the dykes at the same depth, is about 2°C/Myr. A similar result can be seen from the Percival and West (1994) summary of temperature-time-depth relations for the Kapuskasing uplift (Fig.5-1). According to U-Pb dating, the time-span represented by the Matachewan swarm is about 30 million years (2473~2446 Ma, Heaman 1997). During this time period, since the deeper parts (~20 km deep) of dykes cooled down about 60°C (from 550°C to 490°C), both the cooling rate and temperature were suitable for the plagioclase to develop cloudiness and to acquire a substantial TRM/CRM component.

Two opposite polarity dykes from the R region (block B in Fig.2-11) give U-Pb ages that are indistinguishable at about $2445.8^{+2.9}/_{-2.6}$ Ma (Heaman, 1997) indicating that the R to N change occurred at about this time. Variation of paleomagnetic inclination also provides an approximate time limit on the occurrence of the secondary N remanence in depth.

U-Pb dating of two R dykes in Timmins area (M_1) gave $2473^{+16}/_{-9}$ Ma but $2445.8^{+2.9}/_{-2.6}$ Ma for an R dyke in block B (site 208)(Heaman 1997). The NRM results for the two sites are about 25° apart on the apparent polar wander path (APWP). Therefore the average apparent polar wander rate at the time was about 1°/m.y.. The N direction of magnetisation from a dated dyke in R region (site 214 in Fig.3-5) is within 10° of the average for all N dykes in the adjoining N polarity regions

(Halls and Palmer 1990; Bates and Halls 1991). Assuming a uniform rate of polar wander, this number suggests that the acquisition of the TRM/CRM N magnetization at depth occurred no more than 10 million years after the R epoch.

According to my study, the N remanence is 5.7° steeper than the R on average, corresponding to a change in paleolatitude of 2.9° (tan Inc. = 2 tan Lat.). If the 1°/m.y. drift rate is correct, then the N dykes started to get their magnetization about 2.9 Ma after the R. It indicates again that the acquisition of the secondary N remanence of the dykes in the KZ occurred right after the R. Since cloudy feldspars carry this remanence, it means that the cloudiness was also formed at about the same time as the N remanence. It is therefore a crustal cooling feature and not the product of a later re-heating such as a metamorphic event.

2.2 A Possible Tectonic Model of the Kapuskasing Zone

According to regional paleomagnetic studies on the Matachewan dyke swarm and aeromagnetic image reprocessing (Bates and Halls 1991,West and Ernst 1991, Chapter III), the formation of the KZ involved a horizontal dextral rotation within the KZ but sinistral rotation NW of the KZ around a vertical axis. By the time of the last important uplift of KZ at about 1900~1850 Ma (Percival and West 1994), the maximum principal compression was about E-W in the area of study (Halls et.al, 1994). This compression may also have caused brittle deformation of the dykes at outcrop scale, measurement of which at about twenty sites gives a paleostress field of approximately E-W to NW-SE horizontal compression (see Appendix). Westward thrusting along the MLF as well as distortion of the original fan shape of the Matachewan dyke swarm may also be consequences of the compression. This compression may be in direct response to Early Proterozoic collision at the southwestern margin of the Superior province during the Penokean orogeny (1.9~1.8 Ga, Sims et al. 1989, Percival and Peterman 1994, Riller et al. 1999).

The regional geometry and kinematics of major structures formed during the Penokean orogeny in the Great Lakes region suggest a rigid-body horizontal indentation origin (Riller et al. 1999). An indentation structure includes thrusts within and in front of the indentor as well as "mass escape" to both sides (Molnar and Tapponnier, 1977, Tapponnier et al.,1982) (Fig.5-2A). The site of indentation and the severity of the resulting deformation may have been determined in part by a SSW movement of the Western Superior Terrane due to the opening of James Bay. The first stage of the opening at about 1930 Ma (Goodings and Brookfield, 1992) caused sinistral strike-slip movement along the KZ, changing into transpressive motion at the southern end of the KZ where it turns to the WSW (Fig.5-2B). The main phase of this movement was at about 1830~1900 Ma (Goodings and Brookfield, 1992), more or less coincident with the Penokean orogeny. The Penokean indentation probably caused the main phase of the KZ thrust, dextral rotation of the Chapleau and Pineal Lake blocks, and the distortion of the Matachewan dykes (Fig.5-2C). The Penokean structures consist of dominantly upright, second-order fold trains transected by steeply south-dipping reverse and late-orogenic, dextral strike-slip faults which formed the giant Great lakes Tectonic Zone (GLTZ) and the Niagara Fault Zone (NFZ) (Fig.5-3) (Riller et al. 1999). This indentation probably also accounts for distributed, heterogeneous deformation in the southern Superior Province, such as the sinistral strike-slip Gravel River fault (GRF), the Quetico fault (QF) that has components of dextral shear and thrusting to the south (Williams, 1991), and the dextral strike-slip Murray fault (MF)(Riller et al., 1999).

This indentation may be comparable with the on-going collision between India and Eurasia (Fig.5-3) (Molnar and Tappennier, 1977). The similar structural pattern suggests a similar structural mechanics of the formation in spite of the different scales. Notice that the Kapuskasing structures located at the eastern edge of the Penokean indentation, and therefore maybe directly comparable only to the Assam/Bangladesh/India part of the Indian indentor (Fig.5-3). In spite of the complicated active structures in the latter, similar structural components were developed in the similar tectonic locations as that of the KZ to the Penokean orogen. In the two maps, the major structures not only resemble in manner but also develop at similar structural locations. For example, the Lung MenShan thrusts with the KZ; the Kang Ting faults with the Nagasin Lake fault and N-S sinistral faults farther east in Abitibi subprovince; The Kansu and Kunlun faults, Pamir thrust and Talasso Fergana fault with the Gravel River fault (GRF) and the Quetico fault (QF); the Himalyan front thrust with the GLTZ and NFZ; and the Red River fault with the Murray fault.

From spatial distribution, the KZ seems continuous into the 1.1 Ga Mid-continent Rift (MCR) in eastern Lake Superior (Fig.5-4). The two bounding faults of the KZ (ILF and SLF) are almost continuous with two faults of similar dip and sense of displacement, Montreal River fault (MRF) and Michipicoten Island fault (MIF) (Fig.5-4), which define the inversion of the Mid-continent rift in the centre and western part of the lake. The latest larger activity for the Lake Superior faults was during the Grenville Orogen (~1.1Ga), which is also the final stage of KZ activity (Hanes et al. 1994). The coincidence may suggest that the Lake Superior faults may be inherited from earlier basement faults that were part of an extended Kapuskasing structure (Manson & Halls 1997).

Appendix

Study of Outcrop Scale Structures Preserved in Matachewan Dykes

1. Introduction:

Matachewan dykes are emplaced in three subswarms, named M_1, M_2, and M_3 from east to west. Aeromagnetic maps show that M_1 and M_2 are clearly truncated by the KZ's eastern boundary faults. M_3 develops an open Z-shape bend as it crosses the KZ (Fig.A-1). On the plausible assumption, supported by paleomagnetic data (Bates and Halls 1991), that the dyke swarm as a whole was originally intruded radially from the present Lake Huron area, the present distribution pattern of M_3 is a product of distortion by post-dyke KZ deformation. The reprocessed digital aeromagnetic survey data from the centre-south Superior Province revealed the overall pattern of the swarm, which makes the dyke swarm an excellent marker for study of post-dyke regional deformation. By digitizing the aeromagnetic data on a grid map (Fig.A-2), West and Ernst (1991) concluded that the horizontal strain suffered by the KZ since emplacement of the dykes is mainly a northeast-southwest-trending band of dextral transcurrent deformation, which in the northeast is discontinuous and concentrated in a fault (SLF) (horizontal offset 60-80 km) and in the southwest widens through a series of horsetail splays into a ~80 km wide zone of distributed strain. The regional stress field in the BLF area, has a maximum principal compression oriented about E-W (Halls et al. 1994). Here, field structural measurement on dyke outcrops was done around the BLF and MLF region, in order to constrain the trajectory of the paleostress field at the time of their formation.

2. Post Dyke Deformation of the Kapuskasing Zone

Away from the Kapuskasing Zone (KZ) (such as in Hornepayne, Hearst, Timmins, Ranger Lake, and Rocky Lake areas), Matachewan dyke show few signs of deformation at the outcrop scale (Halls, personal communication). However, in the vicinity of the KZ, the dykes display small deformation features such as sheared dykelets, microfaults, offset phenocrysts and veins, slickenside lineations etc. All the features observed are of brittle character, suggesting they were formed by structural event(s) after dyke crystallization rather than by magma flow. Dykes that preserve deformational structures usually failed to give stable paleomagnetic data, indicating accompanying alteration. Most of the deformed dykes have close spatial relations with major fault zones. For example, on islands in Spencer Lake, all dyke outcrops (SL1~SL5, Fig. 3-7) are heavily faulted and veined indicating that the BLF or its satellite faults cut through them. On Hwy 101 near the Budd Lake where the BLF supposedly crosses, a 68° NE trending dyke (TK65) was cut off by a reverse fault with NE trend and dip 24°W. Many microfaults and slickensides are also exposed in the vicinity. At sites TK122 and TK124 on the Power line road, and TK103 on the TK road (Fig.3-5), severely fractured, veined, and micro-faulted dyke outcrops suggest the proximity of the MLF. In some case such as at sites TK85 and TK86 on the Mank Lake road (Fig.3-5), severe microfaulting becomes an indication of a nearby major fault (SLF).

In this study, structural criteria in the vicinity of the Budd lake fault (BLF) and McEwen Lake fault (MLF) were systematically documented. In most cases, although heavily veined and severely fractured, dyke outcrops indicate the proximity of major faults, they failed to give indication of the maximum stress field direction because of either a complicated pattern or limited exposure. At 21 of the locations in the field, structural criteria yield estimates of the horizontal maximum compressive stress direction. Almost all the measurements were done on flat outcrops.

After geometrical analysis, an approximately E-W to NE-SW direction of maximum compressive stress was estimated at the sites (Fig.A-3).

Four sites of conjugate micro-faults gave a precise estimate of the local stress field. Five to ten measurements were obtained on each site. Final directions were averages of the field measurements with standard deviation $\delta < 2°$. Wulff net projection gives the direction of local stress field at each site (Fig.A-4). The maximum compression direction derived from all four sites is about E-W and more or less horizontal.

In the field, the most reliable method to determine principal compression directions is by using sense of slip indicators on both conjugate planes. The actual projecting operation in Fig.A-4 is:

(1) project the two conjugate planes, their intersection is the direction of σ_2; Mark the slip directions on the observation surface;

(2) Find the direction of maximum compressive stress σ_1 on the bisector of the conjugate angle (usually, but not necessarily, the acute angle, see site TK48) facing the compression direction, and which is at 90° to σ_2 ;

(3) Find the minimum compression direction σ_3 , which is the pole of the plane determined by σ_1 and σ_2.

At some dyke sites, more than one phase of deformation was recognized. Chronological change of the local stress field direction (on the observation surfaces) can be seen, although the absolute age for each phase is unknown. Site B6 and KP9 are examples of these sites.

At site B6, an approximately 10m x 5m flat outcrop is exposed about 2 km south of the suspected trace of the BLF (Fig.A-5). A set of joints, oriented about 070° dip 50° N was preserved

(A), as well as a set of micro-faults, trending 300~320° vertical, and filled with quartz (B). First of all, a dextral movement along some joints of the A set was observed, which pulled the joints open and the cracks were filled with dark green chlorite(C). Joint **A** was offset by joint **B**. The offset and pull-open pattern of the joints on the surface indicates probably two phases of compression: an E-W maximum compression first that was responsible for the strike movement along joint **A**, followed by a NW-SE compression which caused offset of **A** by **B**.

On a NE trending dyke (Site KP9), at least four phases of deformation can be deduced from veins, extension joints, and micro-faults (Fig.A-6). The chronological sequence is: Chlorite vein **A**, an extension fracture indicating E-W tension or N-S compression; short quartz vein opening **B**, representing a NW-SE tension or NE-SW compression; long quartz vein **C**, indicating another phase of E-W tension or N-S compression; microfault **D**, with sinistral shearing from possible N-S compression.

A similar analysis was done on the other 15 sites. Fig.A-7 gives the distribution of all the structural sites and their estimated maximum compression directions on horizontal surface. For those having multi-phases deformation, the direction of the last phase is put on the map. The directions in general are quite uniform indicating that the southwestern end of the KZ suffered a regional horizontal compression along an E-W direction after the dyke intrusion. Beyond the map of Fig.A-7, there is abundant evidence at many other sites of post dyke compression along E-W to NW-SE directions (Halls et al. 1994, Halls personal communication). This result agrees with the regional stress field derived from digital image processing of aeromagnetic anomalies (West and Ernst 1991).

Multi-phase deformation can be observed from structures preserved in dykes. The absolute age of each phase is hard to determine. However, since the last phase of systematic E-W compression affected NE trending dykes that are thought emplaced at about 2.0 Ga (Percival, 1994), the structural event(s) that caused the deformation was at or after this time. This may be the same compression responsible for the E-W shortening that caused the reactivation of the Ivanhoe Lake fault and formed the Kapuskasing Zone.

References

Abrahamsen,N. 1986. On Shape Anisotropy. *In* Twenty-five years of geology in Aarhus. *Edited* by J. T. Moller. Geoskrifter, **24**: 11-21.

Leclair, A. D., Percival, J.A., Green, A.G., Wu, J., West,G.W., and Wang, W., 1994. Seismic reflection profiles across the central Kapuskasing uplift. Canadian Journal of Earth Sciences, **31**: pp. 1016-1026.

Anderson, A. T., Jr. 1966. Mineralogy of the Labrieville anorthosite, Quebec. American Mineralogy. **51**: pp. 1671-1711.

Aragón, R., et.al. 1985. Influence of nonstoichiometry on the Verwey transition, Phys. Rev., **31**: 430-436.

Aragón, R. 1992. Magnetization and exchange in nonstoichiometric magnetite. Phys. Rev., **46**: 5328-5333.

Armbrustmacher, T.J. & N.G. Banks 1974. Clouded plagioclase in metadolerite dykes, southeastern Bighorn Mountains, Wyoming. The American Mineralogist, **59**: 656-665.

Bailey, E. B., 1916, In the geology of Ben Nevis and Glen Coe. Mem. Geol. Survey, Scotland. pp. 204-209.

Bailey, R. C. and Halls, H. C. 1984. Estimate of confidence in paleomagnetic directions derived from mixed remagnetization circle and direct observational data. Journal of Geophysics, **54**: 174-182.

Bates, M. P. and Halls, H. C. 1990. Regional variation in paleomagnetic polarity of the Matachewan dyke swarm related to the Kapuskasing Structural Zone, Ontario. Canadian Journal of Earth Science, **27**: 200-211.

Bates, M. P. and Halls, H. C. 1991. Broad-scale Proterozoic deformation of the central Superior Province revealed by paleomagnetism of the 2.45 Ga Matachewan dyke swarm. Canadian Journal of Earth Science, **28**: 1780-1796.

Bennett, G., Brown, D. D., George, P.T., and Leahy, E. J. 1967. Operation Kapuskasing. Ontario Department of Mines, Miscellaneous Paper 10.

Bethune, K. and Davidson,A. 1988. Diabase dykes and the Grenville Front southwest of Sudbury, Ontario. In: Current Research, Part C, Geological Survey of Canada. Paper 88-1C, pp.151-159.

Bleeker, W. 1990. New structural-metamorphic constrains on early Proterozoic oblique collision along the Thompson Nickel Belt, Manitoba, In: The Early Proterozoic Trans-Hudson Orogen of North America. Edited by J.F. Lewry and M.R. Stauffer, Geological Association of Canada, special paper 37, pp. 57-73.

Bridgwater, D. and Harry, W.T. 1968. Anonthosite xenoliths and plagioclase megacrysts in Precambrian intrusions of south Greenland: Grönlands Geologiske Undersögelse Bulliton **77**: pp. 109-121.

Buchan, K.L. and Ernst, R.E. 1994. Onaping fault system: age constraints on deformation of the Kapuskasing structural zone and units underlying the Sudbury Structure. Canadian Journal of Earth Sciences, **31**: 1197-1205.

Buchan, K. L. and Halls, H. C. 1990. Paleomagnetism of Proterozoic mafic dyke swarms of the Canadian Shield. *In* Mafic dykes and emplacement mechanisms. *Edited* by A. J. Parker, P. C. Rickwood, and D. H. Tucker. A.A. Balkema, Rotterdam, The Netherlands, pp. 209-230.

Buchan, K.L., Neilson, D., and Hale, C. J. 1990 Relative age of Otto stock and Matachewan dykes from paleomagnetism and implications for the Precambrian polar wander path. Canadian Journal of Earth Sciences, **27**: 915-922.

Buchen, K. L. and Schwarz, E. J. 1981. Uplift estimated from remanent magnetization: Munro area of Superior Province since 2150 Ma ago. Canadian Journal of Earth Science, **18**: 1164-1173.

Burke, K. and Dewey, J. F. 1973. Plume-generated triple junctions: key indicators in applying plate tectonics to old rocks. Journal of Geology, **81**: 406-433.

Bursnall, J. T., Leclair, A. D., Moser, D. E., and Percival, J. A. 1994. Structural correlation within the Kapuskasing uplift. Canadian Journal of Earth Sciences, **31**: 1081-1095.

Burns, D. J., 1966. Chemical and mineralogical changes associated with the Laxfordian metamorphism of dolerite dykes in the Scourie-Loch Laxford area, Sutherland, Scotland. Geological Magazine, London, **103**: pp. 19-35.

Card, K.D. 1979. Regional geological synthesis, central Superior Province. In: Current Research, Part A. Geological Survey of Canada, Paper 79-1A, pp. 87-90.

Card, K.D. 1990. A review of the Superior Province of the Canadian shield, a product of Archean accretion. Precambrian Research, **48**: 99-156.

Card, K. D., Percival, J. A., Lafleur, J., and Hogarth, D. D. 1981. Progress report on geological synthesis, central Superior Province. *In* Current research, Part A. Geological Survey of Canada, Paper 81-1A, pp. 77-93.

Cook, F. A. 1985. Geometry of the Kapuskasing structure from a Lithoprobe pilot reflection survey, Geology, **13**: 368-371.

Corfu, F. 1987. Inverse age stratification in the Archean crust of the Superior Province: evidence for infra- and subcrustal accretion from high resolution U-Pb zircon and monazite ages. Precambrian Research, **36**: 259-275.

Corfu, F. 1993. The evolution of the southern Abitibi green stone belt in light of precise U-Pb geochronology. Economic Geology, **88**: 1323-1340.

Corfu, F. and Davis, D. W. 1992. A U-Pb geochronological framework for the western Superior Province of the Canadian Shield. *In* The Geology of Ontario. *Edited* by P. C. Thurston, H. R. Williams, R. H. Sutcliffe, and G. M. Stott. Ontario Geological Survey, Special Volume 4, Part 2, pp. 1335-1348.

Corfu, F. and Sage, R.P. 1992. U-Pb age constrains for deposition of clastic metasedimentary rocks and late-tectonic plutonism, Michipicoten belt, Superior Province. Canadian Journal of Earth Sciences, **29**: 1640-1651.

Davis, K.E. 1981. Magnetite rods in plagioclase as the primary carrier of stable NRM in ocean floor gabbros, Earth and Planetary Science Letters, **55**: 190-198.

Day, R., M. Fuller & V.A. Schmidt, 1977. Hysteresis properties of titanomagnetites: grain-size and compositional dependence. Physics of the Earth and Planetary Interiors, **13**: 260-267.

Deer, W. A., Howie, R. A., Zussman, J., 1992, An Introduction to the Rook-Forming Minerals. 2nd ed. Longman Group (FE) Limited.

Delaney, P. T. 1981. Heat transfer during emplacement and cooling of mafic dykes. *In* Mafic dyke swarms, *Edited by* Halls, H. C. and Fahrig, W. F., Geological Association of Canada Special Paper **34**: pp. 31-46.

Duff, B.A. 1979, Peaked curves for haematite-bearing rocks and concentrates. Phys. Earth Planet. Ints. **19**: 1-4.

Dunlop, D.J. 1974. Thermal enhancement of magnetic susceptibility. J. Geophys. Res. **78**: 7602-7613.

Dunlop, D.J. 1981. The rock magnetism of fine particles. Phys. Earth Planet. Inter. **26**: 1-26.

Dunlop, D.J. 1990. Developments in rock magnetism. Rep. Prog. Phys. **53**: 707-792.

Dunlop, D. J., Hanes, J. A., and Buchan, K. L. 1973. Indices of multidomain magnetite behavior in basic igneous rocks: alternating-field demagnetization, hysteresis, and oxide petrology. Journal of Geophysics Research, **78**: pp. 1387-1393.

Dunlop, D.J. and Özdemir3, Ö. 1997. Rock Magnetism, Fundamentals and Frontiers. Cambridge University Press.

Dunlop, D.J. and West, G. F. 1969. An experimental evaluation of single domain theories. Rev. Geophys. **7**: 709-757.

Eggleton, R.A., 1979. The ordering path for igneous K-feldspar megacrysts. Am. Mineral., **64**: 906-911.

Emmet, T.F. 1982. The petrography and geochemistry of corona-bearing dolerites from the Jutun Nappe, Central southern Norway. Mineralogical Magazine, **46**: pp.43-48.

Ernst, R. E. and Halls, H. C. 1984. Paleomagnetism of Hearst dike swarm and implications for the tectonic history of the Kapuskasing Zone, northern Ontario. Canadian Journal of Earth Sciences, **21**: 1499-1506.

Everett, C.W.F. and Clegg, G.A. 1962. A field test of paleomagnetic stability. Geophys. J. R. astr.Soc., **6**: 312-319.

Fahrig, W. F. 1987. The tectonic setting of continental mafic dyke swarms: failed arm and early passive margin. *In* Mafic dyke swarms. *Edited* by H. C. Halls and W. F. Fahrig. Geological Association of Canada, Special Paper 34, pp. 331-348.

Fahrig, W. F., Gaucher, E. H., and Larochelle, A. 1965. Paleomagnetism of diabase dykes of the Canadian shield. Canadian Journal of Earth Sciences, **2**: 278-298.

Fahrig, W. F. and Wanless, R. K. 1963. Age and significance of diabase dyke swarms of the Canadian Shield. Nature (London), **200**: 934-937.

Fahrig, W. F. and West, T. D. 1986. Diabase dyke swarm of the Canadian Shield. Geological Survey of Canada, Map 1627A.

Fountain, D. M. and Salisbury, M. H. 1981. Exposed cross sections through the continental crust: Implications for crustal structure, petrology and evolution. Earth and Planetary Science Letter, **56**: 263-277.

Garland, G. D. 1950, Interpretation of gravimetric and magnetic anomalies on traverses in the Canadian Shield in Northern Ontario. Publications of the Dominion Observatory (Ottawa), **16**: 5-58.

Garland, G. D. 1979. Introduction to Geophysics. W. B. Saunders Company, Philadelphia, PA.

Gates, T. M. and Hurley, P. M. 1973. Evaluation of Rb-Sr dating method applied to the Matachewan, Abitibi, Mackenzie, and Sudbury dike swarms in Canada. Canadian Journal of Earth Sciences, **10**: 900-919.

Gibb, R. A. 1978. A gravity survey of James Bay and its bearing on the Kapuskasing Gneiss Belt, Ontario. Tectonophysics, **45**: T7-T13.

Gibb, R.A. 1983. Model for suturing of Superior and Churchill plates: an example of double indentation tectonics. Geology, **11**: 413-417.

Gies, W. T., Cook, F. A., Green, A. G., Milkereit, B., Percival, J. A., and West, G. F. 1990. Thin thrust sheet forming Kapuskasing structural zone revealed by Lithoprobe reflection data. Geology, **18**: 513-516.

Goodings, C. R. and Brookfield, M. E. 1992. Proterozoic transcurrent movements along the Kapuskasing lineament (Superior Province, Canada) and their relation to surrounding structures. Earth Science Reviews, **32**: 147-185.

Grant, F. S. 1985. Aeromagnetics, geology, and ore environment, I. Magnetite in igneous, sedimentary and metamorphic rocks: an overview. Geoexploration, **23**: 303-333.

Grout, F.F. 1933. Contact metamorphism of the slates of Minnesota by granite and by gabbro magmas. BGSA **44**: 989-1040.

Groves, A.W., 1935. The charnockite series of Uganda, British East Africa. Geol. Soc. London, Quarl. Jour., **91**: 150-207.

Grunsky, E. 1981. Geology of the Grey Owl Lake area, District of Algoma. Ontario Geological Survey Report **205**: 76.

Gupta, V. K. 1991a. Total magnetic field of Ontario, east-central sheet. Ontario Geological Survey, Map 2586.

Gupta, V. K. 1991b. Bouguer gravity of Ontario, east-sheet. Ontario Geological Survey, Map 2594.

Halls, H. C. 1986. Paleomagnetism, structure, and longitudinal correlation of middle Precambrian dykes from northwestern Ontario and Minnesota. Canadian Journal of Earth Sciences, **23**: 142-157.

Halls, H. C. 1991. The Matachewan dyke swarm, Canada: an early Proterozoic magnetic field reversal. Earth and planetary Science Letters, **105**: 279-292.

Hall, H. C. and Bates, M. P. 1990. The evolution of the 2.45 Ga Matachewan dyke swarm, Canada. *In*: Mafic dykes and emplacement mechanisms. *Edited* by A. J. parker, P. C. Rickwood, and D. H. Tucker. A.A. Balkema, Rotterdam, The Netherlands, pp. 237-250.

Halls, H. C. and Mound, J. 1998. The McEwan Lake fault: gravity evidence for a new structural element of the Kapuskasing Zone. Canadian Journal of Earth Science, **35**: 696-701.

Halls, H. C. and Palmer, H. C. 1990. The tectonic relationship of two early Proterozoic dyke swarms to the Kapuskasing Structural Zone: a paleomagnetic study. Canadian Journal of Earth Sciences, **27**: 78-103.

Halls, H. C. and Shaw, E. G. 1988. Paleomagnetism and orientation of Precambrian dykes, eastern Lake Superior region, and their use in estimates of crustal tilting. Canadian Journal of Earth Sciences, **25**: 732-743.

Halls, H. C., Palmer, H. C., Bates, M. P., and Phenney, W. C. 1994. Constraints on the nature of the Kapuskasing Structural Zone from the study of Proterozoic dyke swarms. Canadian Journal of Earth Sciences, **31**: 1182-1196.

Halls, H. C. and Zhang, B. 1995a. Magnetic polarity domains in the early Proterozoic Matachewan dyke swarm, Canada: A novel method for mapping major faults. *In* Physics and Chemistry of Dykes. *Edited by* Baer, G. And A. Heimann, A.A. Balkema Publishers, Netherlands, pp. 165-170.

Halls, H. C. and Zhang, B. 1995b. Tectonic implications of clouded feldspar in Proterozoic mafic dyke swarms. Memoir Geological Society of India, No.33, pp. 65-80.

Halls, H. C. and Zhang, B. 1998. Uplift structure of the southern Kapuskasing Zone from 2.45 Ga dike swarm displacement. Geology, **26**: 67-73

Hanes, J. A., Archibald, D. A., Queen, M., and Lee, J. K. W. 1988a. $^{40}Ar/^{39}Ar$ geochronology of diabase dykes: implications for the tectonothermal evolution of the Kapuskasing uplift. Proceedings, Project Lithoprobe Kapuskasing Structural Zone Workshop I, Toronto, Ont., pp. 7-16.

Hanes, J. A., Archibald, D. A., Queen, M., and Lee, J. K. W. 1991. Summary of the $^{40}Ar/^{39}Ar$ geochronology in the Kapuskasing uplift and Abitibi greenstone belt. *In* Proceedings, Project Lithoprobe Kapuskasing Structural Zone, Workshop III, Toronto, Ont., pp.9-14.

Hanes, J. A., Archibald, D. A., Queen, M., and Farrar, E. 1994. Constrains from $^{40}Ar/^{39}Ar$ geochronology on the tectonothermal history of the Kapuskasing uplift in the Canadian Superior Province. Canadian Journal of Earth Sciences, **31**: 1146-1171.

Hanes, J. A., Queen, M., and Archibald, D. A. 1988b. $^{40}Ar/^{39}Ar$ geochronology of dykes of their contact aureoles in the Kapuskasing uplift. Proceedings, Project Lithoprobe Kapuskasing Structural Zone Workshop II, Toronto, Ont., pp. 165-172.

Hargraves, R.B. & W.M. Young 1969. Source of the stable remanent magnetization in the Lambertville diabase. Am. J. Sci. **267**: 1161-1177.

Heaman, L. M. 1988. A precise U-Pb zircon aga for a Hearst dyke [abstract]. Geological Association of Canada, Program with Abstracts, **13**: A53.

Heaman, L. M. 1989. U-Pb dating of mafic dyke swarms: what are the options? International Association of Volcanology and Chemistry of the Earth's Interior General Assembly, Program with Abstracts, *In* New Mexico Bureau of Mines and Mineral Resources, Bulletin 131, p. 125.

Heaman, L. M. 1995. U-Pb dating of mafic rocks: past, present and future. Abstract, Geological Association of Canada Annual Meeting, Victoria, Canada.

Heaman, L.M. 1997. Global mafic magmatism at 2.45 Ga: Remnants of an ancient large igneous province? Geology, **25**: 299-302.

Hoffman, P. F. 1989, Precambrian geology and tectonic history of North America. *In* The Geology of North America-an overview. *Edited* by Bally, A. W. and Palmer, A. R., Boulder, Colorado, Geological Society of America. Pp. 447-512.

Innes, M. J. S. 1960. Gravity and isostasy in northern Ontario and Manitoba. Publication of the Dominion Observatory (Ottawa), **21**: 261-338.

Innes, M. J. S., Goodacre, A. K., Weber, J. R., and McConnell, R. K. 1967. Structural implications of the gravity field in Hudson Bay and vicinity. Canadian Journal of Earth Sciences, **4**: 977-993.

Irving, E. and Naldrett, A. J. 1977. Paleomagnetism in Abitibi Greenstone belt and Matachewan diabase dikes: evidence of the Archean geomagnetic field. Journal of Geology, **85**: 157-176.

Johansson, L. 1992. Plagioclase clouding in mafic intrusions along the Protogine zone in southern Sweden. Geologiska Foreningensi Stockholm Forhandlingar, **144**: pp.353-358.

Judd, J.W., 1885, On the Tertiary and Older Peridotites of Scotland. Quart. Journ. Geol. Sco. London, **41**: pp. 354-418.

Keefer, C.M. and Shive, P.N. 1981. Curie temperature and lattice constant reference contours for synthetic titanomaghemites. Journal of Geophysics Research, **86**: 987-998.

Kirschvink, J. L. 1980. The least squares line and plane and the analysis of paleomagnetic data. Golophysical Journal of the Royal Astronomical Society, **62**: 699-718.

Knopf, E. B. and Jonas, A.I., 1929, The geology of the crystalline rocks of Baltimore Country. Maryland Geol. Survey. Pp. 97-199.

Krogh, T. E. and Moser, D. E. 1994. U-Pb zircon and monazite age from the Kapuskasing uplift: age constraints on deformation within the Ivanhoe Lake fault zone. Canadian Journal of Earth Sciences, **31**: 1096-1103.

Kuipers, A.J.M., and V.A.M. Brabers, 1976. Thermoelectric properties of magnetite at the Verwey transition, Phys Rev., **14**: 1401-140

Kynaston, H., 1901. In summary of progress for 1900. Mem. Geol. Survey. Great Britain, pp. 82-83.

Kynaston, H., 1905. Notes on contact metamorphism round the Cheviot granite. Trans. Edinburgh Geol. Soc., **8**: pp. 18-6.

Launeau, P., Cruden, A.R. & Bouchez, J.-L., 1994, Mineral recognition in digital images of rocks: a new approach using multichannel classification. Canadian Mineralogist, **32**: 919-933.

Leavitt, F. and Slemmons, D.,1962. Observations on order-disorder relations of natural plagioclase, IV. Order-disorder relations in plagioclase of the White Mountain and New Hampshire magma series. Norsk Geologisk Tidsskrift, **42:** 578-585.

Leclair, A.D. 1989. The third dimension of the central Kapuskasing uplift interpreted from geological data. Geological Association of Canada, Program with Abstracts, **14**: A102.

Leclair, A. D. 1990. Puskuta Lake shear zone and Archean crustal structure in the central Kapuskasing uplift. *In* Current Research, Part C, Geological Survey of Canada, paper 90-1C, pp. 197-206.

Leclair, A. D. 1992. Geology of the Kapuskasing - Groundhog River - Missinaibi River area, Foleyet (48B, north half) and Kapuskasing (42G, south half) map-areas, northern Ontario. Geological Survey of Canada, Open file 2515.

Leclair, A. D., Percival, J. A., Green, A. G., Wu, J., West, G. F., and Wang, W. 1994. Seismic reflection profiles across the central Kapuskasing uplift. Canadian Journal of Earth Sciences, **31**: 1016-1026.

Leclair, A. D. and Nagerl, P. 1988. Geology of the Chapleau, Groundhog River and Val Rita blocks, Kapuskasing area, Ontario. *In* Current research, Part C. Geological Survey of Canada, Paper 88-1C, pp. 83-91.

Leclair, A. D. and Poirier, G. G. 1989. The Kapuskasing Uplift in the Kapuskasing area, Ontario. *In* Current research, Part C. Geological Survey of Canada, Paper 89-1C, pp. 225-234.

Lowrie, W. and Fuller, M. 1971. On the alternating field demagnetization characteristics of multi-domain thermoremanent magnetization in magnetite. Journal of Geophysics Research, **76**: 6339-6349.

MacGregor, A. G. 1929. Metamorphism around the Lochnagar granite, Aberdeenshire. Rep. British Assoc. Glasgow, 1928, Sect. C, Geology, pp.553-554.

MacGregor, A. G. 1931. Clouded feldspars and thermal metamorphism. Mineralogical Magazine, **22**: pp.524-538.

Manson, M. L. 1996. Post Keweenawan compressive tectonism in the Midcontinent Rift of eastern Lake Superior. Ph.D. thesis. University of Toronto.

Manson, M.L and Halls, H. C. 1997. Proterozoic reactivation of the southern Superior Province and its role in the evolution of the Midcontinent rift. Canadian Journal of Earth Sciences. **34**: 562-575.

McElhinny, M. W. 1973. Paleomagnetism and plate tectonics. Cambridge University Press, Melbourne.

McFadden, P. L. and Jones, D. L. 1981. The fold test in paleomagnetism. Geophysical Journal of the Royal Astronomical Society, **67**: 53-58.

Molnar P. and Tapponnier, P. 1977. The collision between India and Eurasia. Scientific American, April,p.30-41.

Morgan, G.E. and Smith, P.P.K. 1981. Transmission electron microscope and rock magnetic investigations of remanence carries in a Precambrian metadolerite. Earth and Planetary Science Letters, **53**: 226-240.

Moser, D. 1988. Structure of the Wawa gneiss terrane near Chapleau, Ontario. Procceding Lithoprobe Workshop I: Kapuskasing Structural Zone Transect, pp. 89-96.

Moser, D. E. 1994. The geology and structure of the mid-crustal Wawa gneiss domain: a key to understanding tectonic variation with depth and time in the late Archean Abitibi-Wawa orogen. Canadian Journal of Earth Sciences, **31**: 1064-1080.

Nelson, D. O., Morrison, D. A., and Phinny, W. C. 1990. Open system evolution versus source control in basaltic magmas: Matachewan-Hearst dyke swarm, Superior Province, Canada. Canadian Journal of Earth Sciences, **27**: 767-783.

Ontario Geological Survey, 1991. Bedrock geology of Ontario, east-central sheet: Ontario Geological Survey, Map 2543. Scale: 1:1,000,000

O'Reilly, W. 1976, Magnetic minerals in the crust of the Earth. Rep. Prog., Phys., **39:** 857-908.

Osmani, I. A. 1991. Proterozoic mafic dyke swarms in the Superior Province of Ontario. *In* Geology of Ontario. *Edited* by P. C. Thurston, H. R. Williams, R. H. Sutcliffe, and G. M. Scott. Ontario Geological Survey, Special volume 4, Part I, pp. 661-682.

Özdmeir, Ö. and Dunlop. D.J. 1993. Magnetic domain structures on natural single crystal of magnetite. Geophys. Res. Lett., **20**: 1835-1838.

Özdmeir, Ö. and O'Reilly, W. 1981. High-temperature hysteresis and other magnetic properties of synthetic monodomain titanomaghemites. Phys. Earth Planet. Inter. **25**: 406-418.

Palmer, H. C. and Barnett, R. L. 1992. Amphibole and plagioclase chemistry in two Proterozoic dyke swarms and its relation to the uplift history of the Kapuskasing Structural Zone. Canadian Journal of Earth Sciences, **29**: 1791-1801.

Palmer, H.C., Merz, B.A., and Hayatsu,A. 1977. The Sudbury dykes of the Grenville Front region: Paleomagnetism and K-Ar age studies. Canadian Journal of Earth Sciences, **14**: pp. 1867-1877.

Percival, J. A. 1983. High-grade metamorphism in the Chapleau-Foleyet area, Ontario. American Mineralogist, **68**: 667-686.

Percival, J. A. 1985. The Kapuskasing structure in the Kapuskasing-Fraserdale area, Ontario. *In* Current research, part A, Geological Survey of Canada, Paper 85-1A, pp. 1-5.

Percival, J. A. and Card, K. D. 1983. Archean crust as revealed in the Kapuskasing uplift. Superior Province, Canada. Geology, **11**: 323-326.

Percival, J. A. and Coe, K. 1981. Parallel evolution of Archean low- and high-grade terranes: a view based on relationships between the Abitibi, Wawa and Kapuskasing belts. Precambrian Research, **14**: 315-331.

Percival, J. A. and McGrath, P. H. 1986. Deep crustal structure and tectonic history of the northern Kapuskasing Uplift of Ontario: an integrated petrological-geophysical study. Tectonics, 5: 553-572.

Percival, J. A., Palmer, H. C., and Barnett, R. L. 1994. Quantitative estimates of emplacement level of postmetamorphic mafic dykes and subsequent erosion magnitude in the southern Kapuskasing uplift. Canadian Journal of Earth Sciences, **31**: 1218-1226.

Percival, J. A. and Peterman, Z. E. 1994. Rb-Sr biotite and whole-rock data from the Kapuskasing uplift and their bearing on the cooling and exhumation history. Canadian Journal of Earth Sciences, **31**: 1172-1181.

Percival, J. A., Green, A. G., Milkereit, B., Cook, F. A., Geis, W., and West, G. F. 1989. Lithoprobe reflection profiles across deep continental crust exposed in the Kapuskasing uplift structure. Nature (London), **342**: 416-420.

Percival, J. A., Mortensen, J. K., Stern, R. A., Card, K. D., and Bégin, N. J. 1992. Giant granulite terranes of northeastern Superior Province: the Ashuanipi complex and Minto block. Canadian Journal of Earth Sciences, **29**: 2287-2308.

Percival, J. A., Parrish, R., Krogh, T. E., and Peterman, Z. 1988. When did the KSZ come up? Proceedings, Project Lithoprobe Kapuskasing Structural Zone Workshop I, Toronto, Ont., pp. 43-48.

Percival, J. A. and West, G. F. 1994. The Kapuskasing uplift: a geological and geophysical synthesis. Canadian Journal of Earth Sciences, **31**: 1256-1286.

Peterman, Z.E. and Day, W. 1989. Early Proterozoic activity on Archean faults in the western Superior Province-evidence from pseudotachylite. Geology, **17**: 1089-1092.

Philpotts, A. R., 1966, Origin of the anorthosite-magerite rocks in Southern Quebec. Journal of Petrology, **7**: 1-64.

Phinney, W. C. and Nelson, D. O., 1991, Sources and intrusion mechanisms of the Matachewan dike swarm, Ontario: implications for lateral intrusion and hot spots. Geological Association of Canada, Program with Abstracts, **16**: A99.

Pichamuthu, C.S.. 1959. The significance of clouded plagioclase in the basic dykes of Mysore state, India. Journal of the Geological Society of India, **1**: 68-79.

Poldervaart, A. and Gilkey, A.K. 1954, On clouded feldspars. The American Mineralogist, **39**: 75-91.

Pullaiah, G., Irving, E., Buchan, K. L., and Dunlop, D. J. 1975. Magnetization changes caused by burial and uplift. Earth and Planetary Science Letters, **28**: 133-143.

Ramsay, J. G. and Huber, M. I., 1983. The techniques of Modern Structural Geology.ACDEMIC PRESS INC. Volume I.

Riller, U., Schwerdner, W.M., Halls, H.C., and Card, K.D., 1999. Tranpressive tectonism in the Eastern Penokean Orogen, Canada: Consequences from Preterozoic kinematics and continental fragmentation. Tectonophysics (in press).

Robertson, I.D.M. and Van Breeman, O. 1970. The southern satellite dykes of the Great Dyke, Rhodesia. Geological Society of South Africa, Special Publication, Vol. 1, pp. 621-644.

Schutts, L. D. and Dunlop, D. J. 1981. Proterozoic magnetic overprinting of Archean rocks in the Canadian Superior Province. Nature (London), **291**: 642-645.

Schwarz, E. J. 1977. Depth of burial from remanent magnetization: the Sudbury irruptive at the time of diabase intrusion (1250 Ma). Canadian Journal of Earth Sciences, **14**: 82-88.

Shand, S.J. 1945. Coronas and coronites. BGSA 56: 247-266.

Sims, P.K., Van Schmus, W.R., Schulz, K.J., and Peterman, Z.E. 1989. Tectono-stratigraphic evolution of the Early Proterozoic Wisconsin magmatic terranes of the Penokean Orogen. Canadian Journal of Earth Sciences, **26**: 2145-2158.

Sims, P.K., Card, K.D., Morey, G.B., and Peterman, Z.E. 1980. The Great Lake tectonic zone – a major crustal structure in central North America. Geological Society of America Bulletin, **91**: 690-698.

Smith, J.V. 1974. Feldspar Minerals. I, II. Springer-Verlag: Heideberg.

Smith, P.P.K. 1979, The identification of single-domain titanomagnetite particles by means of transmission electron microscopy, Canadian Journal of Earth Sciences, **16**: 375-379.

Smith, P. E. and Farquhar, R. M. 1988. U-Th-Pb isotope studies of mafic dykes and gneisses in the KSZ. Procedings, Project Lithoprobe Kapuskasing Structural Zone Workshop II, Toronto, Ont., pp. 187-190.

Smith, P. E., Farquhar, R. M., and Halls, H. C. 1992. Pb isotope study of mafic dykes in the Superior Province, Ontario: uniformity of initial Pb isotope ratios of the Hearst dykes. Chemical Geology (Isotope Geoscience Section), **94**: 261-280.

Stacey, F. D. 1960. Magnetic anisotropy of igneous rocks. Journal of Geophysical Research, **65**: 2429-2442.

Strangway, D. W. 1961. Magnetic properties of diabase dykes. Journal of Geophysics Research, **66**: 3021-3032.

Strangway, D. W. 1964. Rock magnetism and dyke classification. Journal of Geophysical Research. **72**: 648-663.

Symons, D.T.A. and Vandall, T.A. 1990. Paleomagnetic evidence for Proterozoic tectonism in the Kapuskasing Structural Zone, Ontario. Journal of Geophysical Research, B, **95**: 19199-19211.

Symons, D.T.A., Lewchuk, M.T., Dunlop, D.J., Costanzo-Alvarez,V., Halls, H.C., Bates, M.P., Palmer, H.C., and Vandall, T.A. 1994. Synopsis of paleomagnetic studies in the Kapuskasing structural zone. Canadian Journal of Earth Sciences, **31**: 1206-1217.

Tarling, D. H. 1983. Paleomagnetism. Principles and applications in geology, geophysics and archaeology. Chapman and Hall, London.

Teall, J.J.H., 1899, In the Silurian rocks of Britain, Vol. I, Scotland. Mem. Geol. Survey, Great Britain.

Teall, J.J.H., 1918. Dynamic metamorphism. A review, mainly personal. Proc. Geol. Assoc. London, **29**: pp. 1-15.

Teall, J.J.H., 1907. In the geological structure of the north-west Highlands of Scotland. Mem. Geol. Survey, Great Britain.

Thurston, P. C., Siragusa, G. M., and Sage, R. P., 1977. Geology of the Chapleau area: districts of Algoma, Sudbury and Cochrane. Ontario Division of Mines, Geological report 157.

Tilley, C.E. 1921. The granite-gneisses of southern Eyre Peninsula (South Australia) and their associated amphibolites. Quart. Jour. Geol. Soc. (London) **77**: 75-131.

Topponnier, P., Peltzer, G., Le Dain, A.Y., Armijo, R. and Cobbold, P., 1982. Propagating extrusion tectonics in Asia: New insights from simple experiments with plasticine. Geology, **10**:611-616.

Törnebohm, A. E. 1877, Ueber die wichtigeren Diabase- und Gabbro-gesteine Schwedens. NJMG 379-393.

Verwey, E.J.W. 1939. Electronic conduction of magnetite (Fe_3O_4) and its transition point at low temperatures. Nature, **144**: 327-328.

Verwey, E.J., et.al. 1947. Physical properties and cation arrangement of oxides with spinel structures. J. Chem. Phys., **15**: 181-187.

Watson, J. 1980. The origin and history of the Kapuskasing structural zone, Ontario, Canada. Canadian Journal of Earth Sciences, **17:** 866-875.

West, G. F. and Ernst, R. E. 1991. Evidence from aeromagnetics on the configuration of Matachewan dykes and the tectonic evolution of the Kapuskasing structural zone, Ontario, Canada. Canadian Journal of Earth Sciences, **28**: 1797-1811.

Whitney, P.R. 1972. Spinel inclusions in plagioclase of metagabbros from the Adirondack Highlands. American Minerologist, **57**: pp. 1429-1436.

Williams, G.H., 1886. The gabbros and associated hornblende rocks occurring in the neighborhood of Baltimore, Md. Bull. U.S. Geol. Survey, No. 28.

Williams, H. R. 1992. Quetico Subprovince. *In* Geology of Ontario. *Edited* by P. C. Thurston, H. R. Williams, R. H. Sutcliffe, and G. M. Stott. Ontario Geological Survey, Special Volume 4, Part 1, pp. 383-403.

Williams, H. R., Stott, G. M., Thurston, P. C., Sutcliffe, R. H., Bennett, G., Easton, R. M., and Armstrong, D. K. 1992. Tectonic evolution of Ontario: summary and synthesis. *In* Geology of Ontario. *Edited* by P. C. Thurston, H. R. Williams, R. H. Sutcliffe, and G. M. Stott. Ontario Geological Survey, Special Volume 4, Part 2, pp. 1255-1332.

Williamson, W.O. 1936. Some minor intrusions of Glen Shee. Perthshire. GM **73**: 145-157.

Zhang, B. 1988. Preliminary study on Proterozoic dyke swarms in north Sanxin. M.Sc thesis, Peking University (in Chinese with English Abstract).

Zhang, B. and Halls, H. C. 1992. Does another thrust sheet lie above the Kapuskasing Zone? Eos, **73**: 92.

Zhang, B. and Halls, H.C.1994. Feldspar cloudiness in diabase dykes: its quantification and possible relation to crystallization depth in the vicinity of the Budd Lake fault zone, northern Ontario. Geological Association of Canada Annual Meeting, Waterloo, Program of Abstracts, p. A12.

Zhang, B. and Halls, H.C. 1995a. The origin and age of the feldspar clouding in the Matachewan dyke swarm. *In* Physics and Chemistry of Dykes, *Edited* by Baer, G. and Heimann, A., Balkema, Rotterdam, pp.171-176.

Zhang, B. & Halls, H.C. 1995b, Paleomagnetic polarity domains in the Matachewan dyke swarm reveal major faults in the Canadian Shield. Abstract, Geological Association of Canada Annual Meeting, Victoria, Canada.

Zhao, J. and McCulloch, M.T. 1993. Melting of a subduction-modified continental lithosphere mantle: evidence from late Proterozoic mafic dyke swarms in central Australia, Geology, **2**: pp. 463-466.

Zijderveld, J. D. A. 1967. A. C. demagnetization of rocks: analysis of results. *In* Methods in paleomagnetism. *Edited* by Collinson, D. W., Creer, K. M., and Runcorn, S. K.. Elsevier, Amsterdam, pp. 254-286.

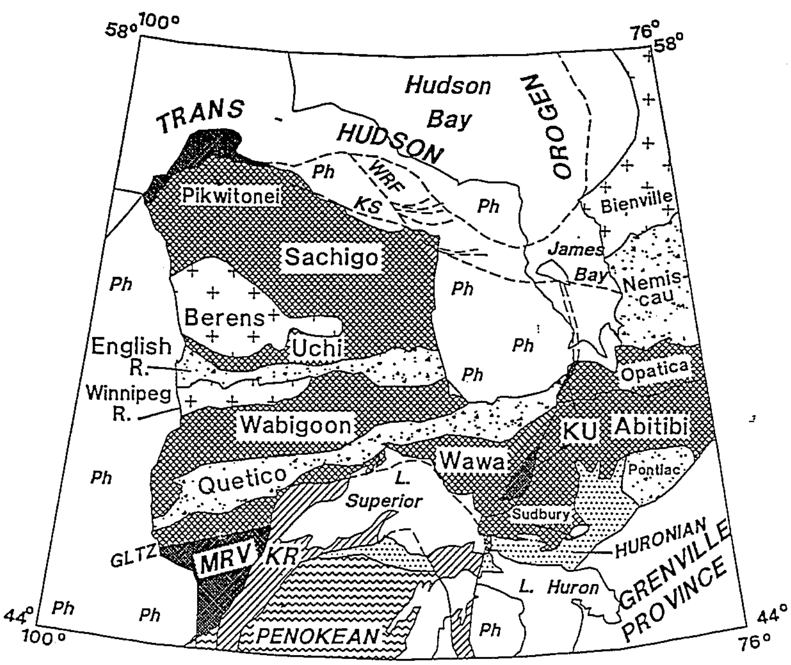

Fig. 1-1. Regional geology of southwestern Superior province and surrounding Proterozoic belts (after Percival and West 1994). GLTZ: Great Lakes Tectonic Zone; KR: Keweenawan Rift; KS: Kenyon Structure; KU: Kapuskasing Uplift; MRV: Minnesota River Valley; Ph: Phanerozoic cover; WRF: Winisk River fault.

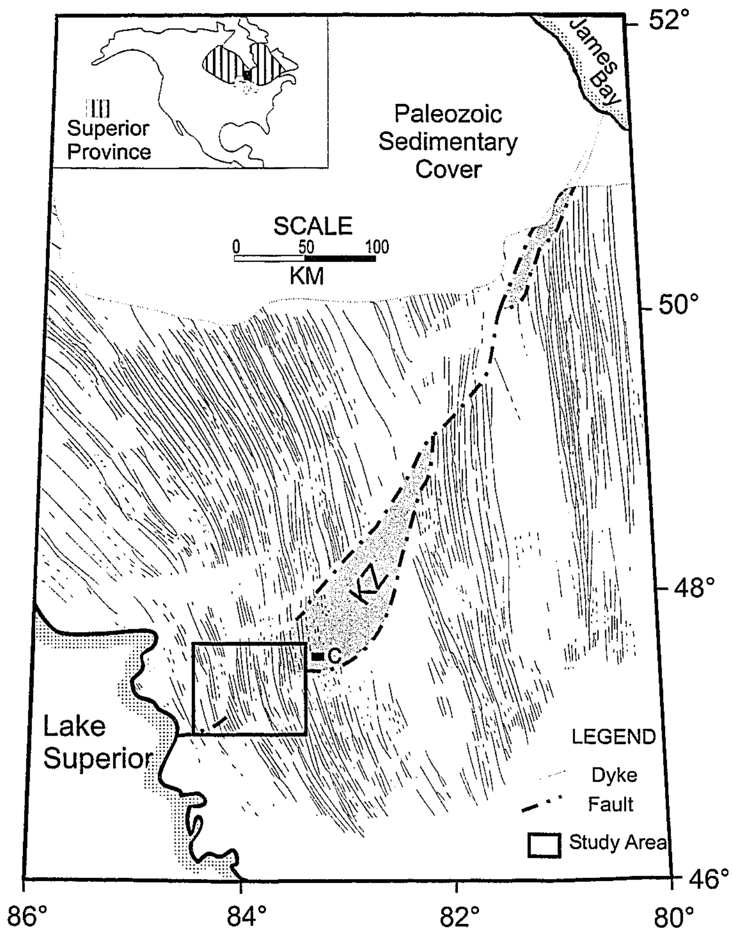

Fig. 1-2. Map of the Matachewan dyke swarm, the Kapuskasing Zone, and the area of study. Symbols: C: Chapleau; KZ: Kapuskasing Zone. The locations of dykes (thin black lines) are based mainly on aeromagnetic interpretation (West and Ernst 1991).

Fig. 1-3. Map of site locations.

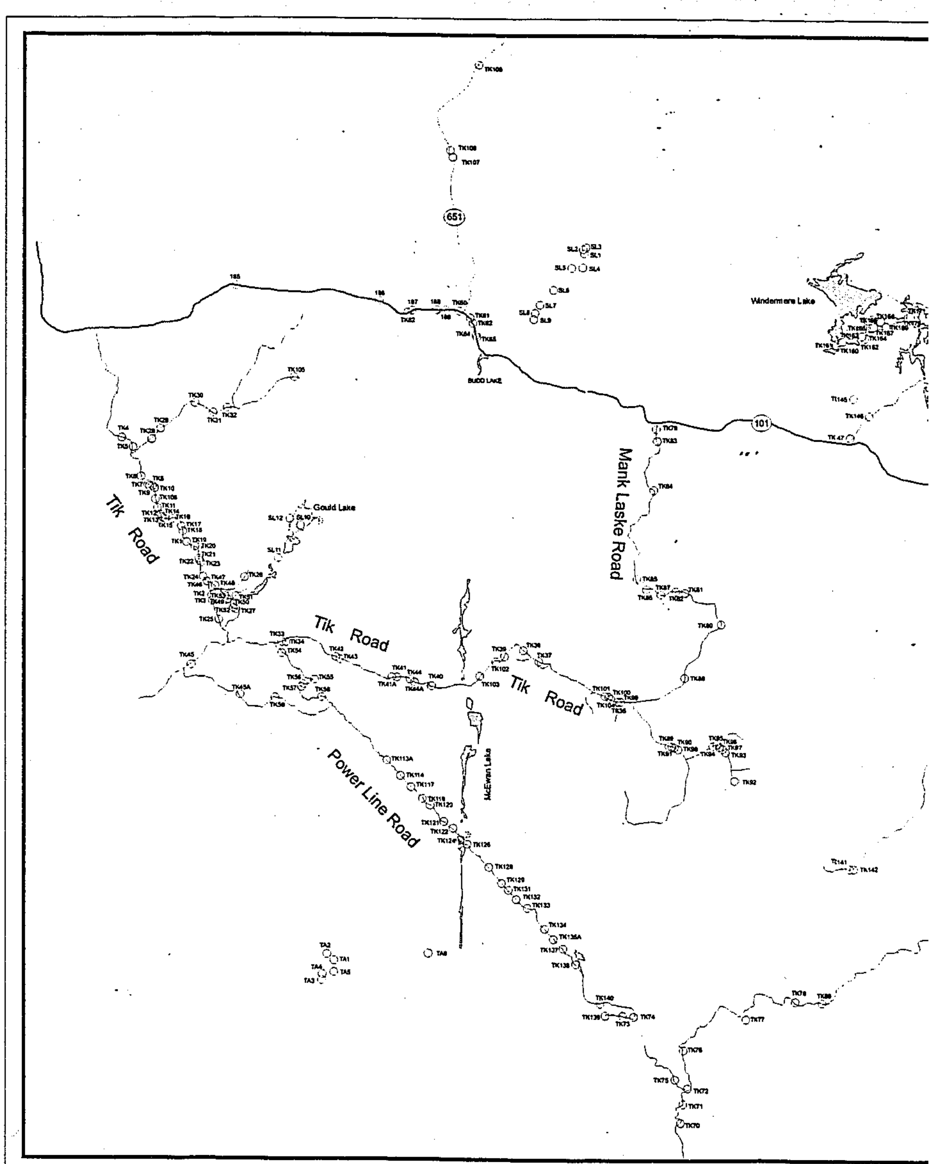
Tik Road
Tik Road
Tik Road
Power Line Road
Mank Laske Road
Gould Lake
McEwan Lake
Windermere Lake
BUDD LAKE
651
101

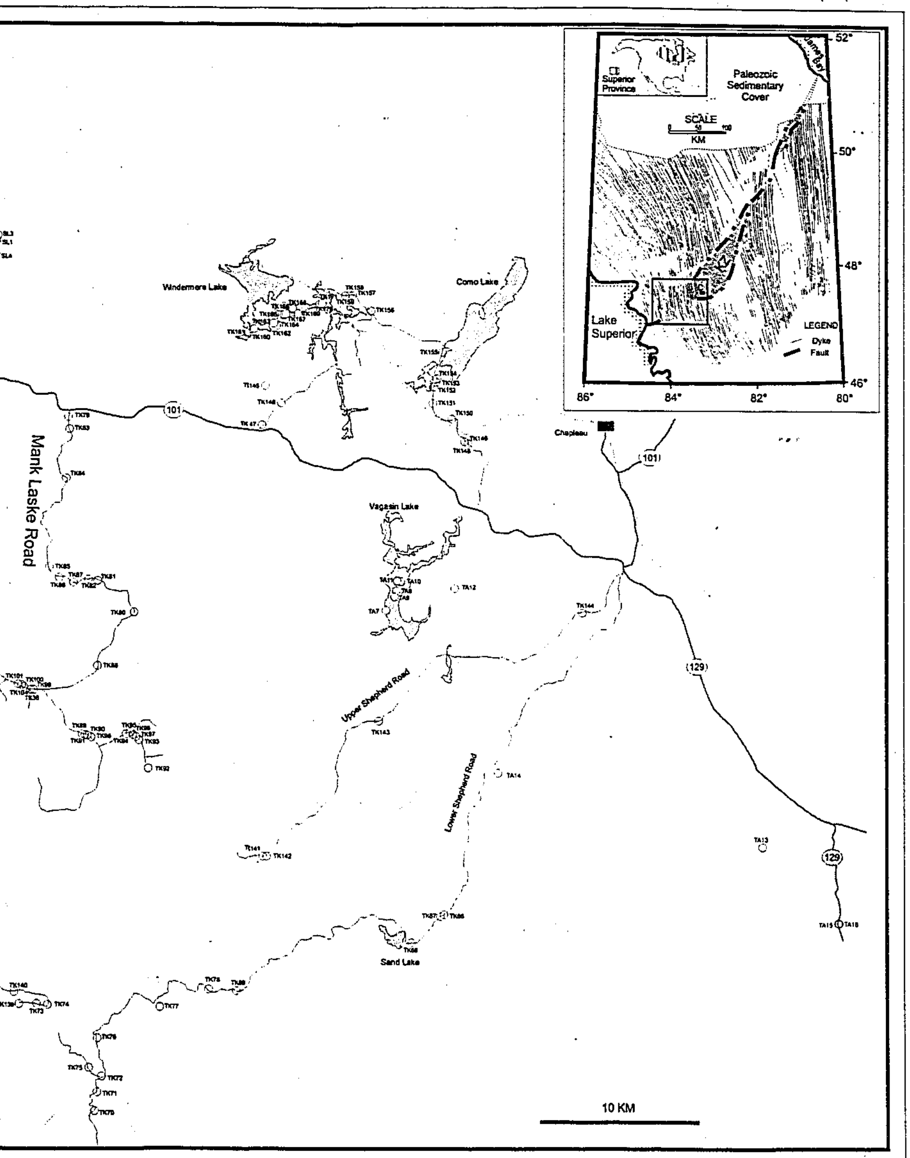
Paleozoic Sedimentary Cover
Superior Province
SCALE
KM
Lake Superior
LEGEND
Dyke
Fault
52°
50°
48°
46°
86°
84°
82°
80°
Windermere Lake
Como Lake
Chapleau
Mank Laske Road
Vagasin Lake
Upper Shepherd Road
Lower Shepherd Road
Sand Lake
101
129
10 KM

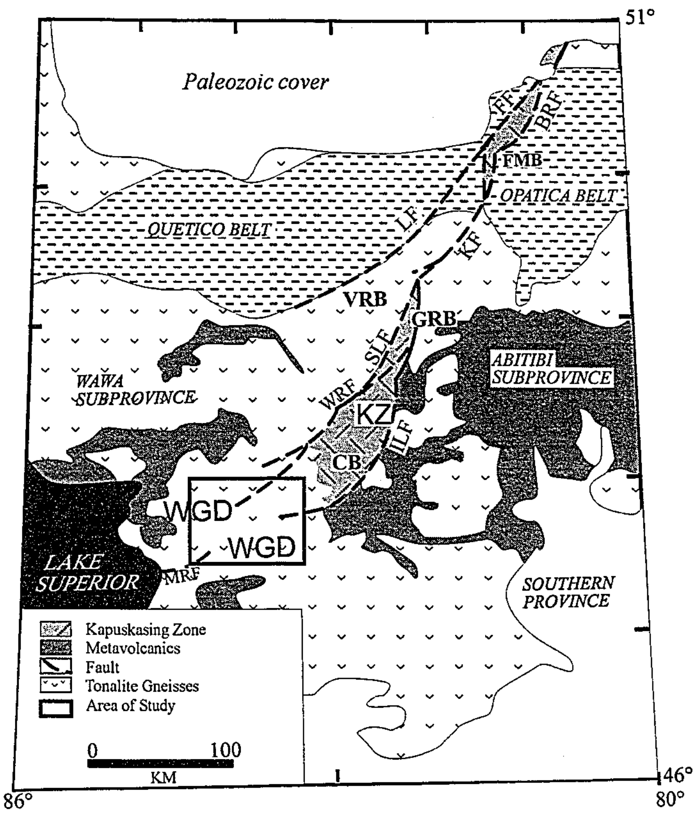

Fig. 1-4. A simplified geological map of the Kapuskasing Zone showing important blocks and bounding faults (map modified after West and Ernst 1991).

Faults:

- FF: Foxville fault,
- LF: Lepage fault,
- BRF: Bad River fault,
- KF: Kineras fault,
- WRF: Wakusimi River fault,
- ILF: Ivanhoe Lake fault,
- MRF: Montreal River fault,
- SLF: Saganash Lake fault,

Blocks:

- VRB: Val Rita block,
- CB: Chapleau block,
- FMB: Fraserdale-Moosonee block,
- GRB: Groundhog River block,
- WGD: Wawa Gneiss Domain,
- KZ: Kapuskasing Zone.

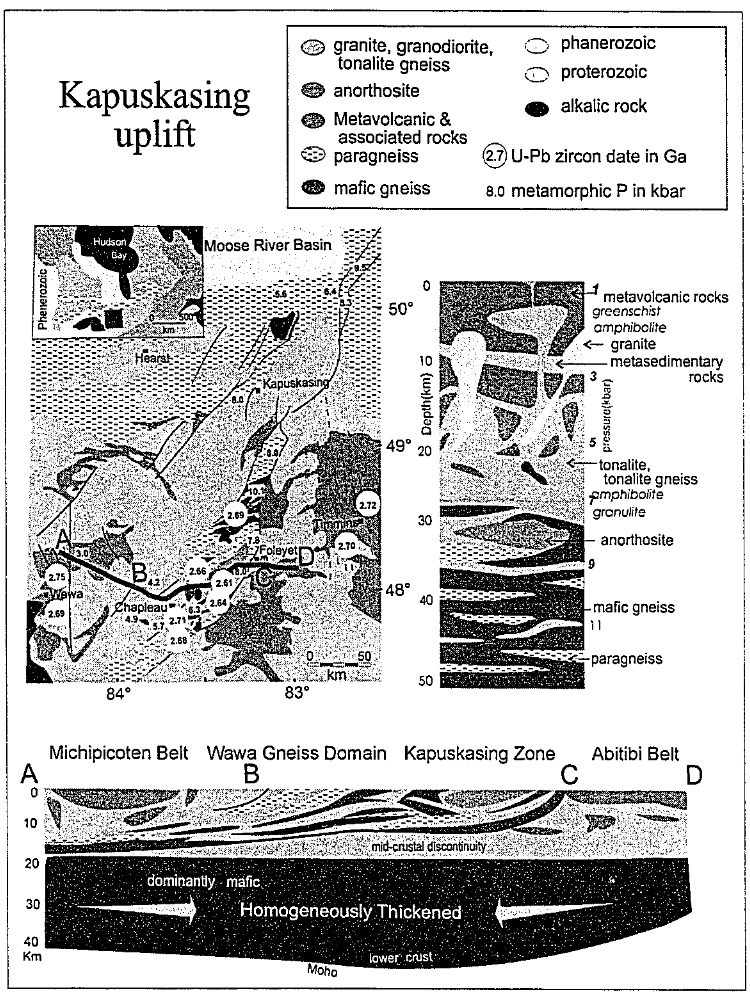

Fig. 1- 5. Geology of the Kapuskasing uplift, south central Superior province (After Percival 1989). Upper right: Crustal column is referred from oblique cross-section exposed at surface. Below: Crustal cross-section consistent with metamorphic geobarometry based on Lithoprobe seismic refraction profiling.

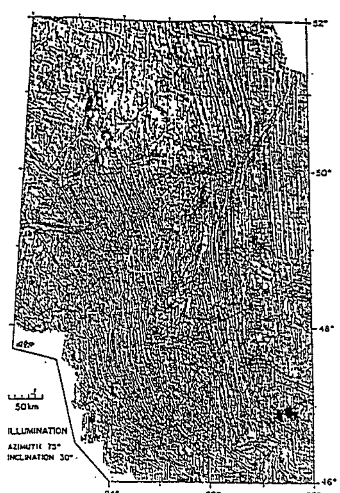

b

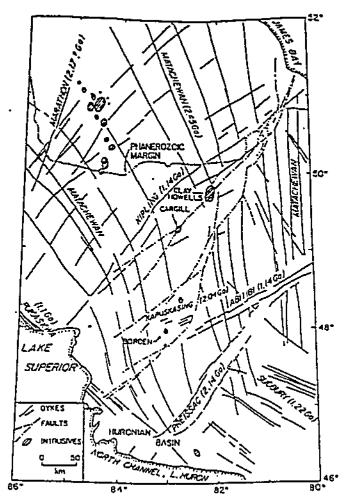

a

c

Fig. 1-6
a: Locations and ages of Proterozoic mafic dyke swarms in the vicinity of the Kapuskasing Zone.

b: A shaded relief aeromagnetic map designed to show the Matachewan dyke swarm prominently.

c: Distribution of the Matachewan dyke swarm near the Kapuskasing Zone, M_1, M_2, and M_3 are three main subswarms. Note that M_2 and M_3 are obviously affected by the KZ (Modified after West and Ernst 1991).

Fig. 2-1. Appearances of cloudy feldspars under plane polarized light. The grey patches are caused by submicroscopic particles. Cloudiness varies in individual feldspar crystals and different grains. Cloudiness tends to occur in the centre of the feldspar crystals. PL: Plagioclase; PX: Pyroxene.

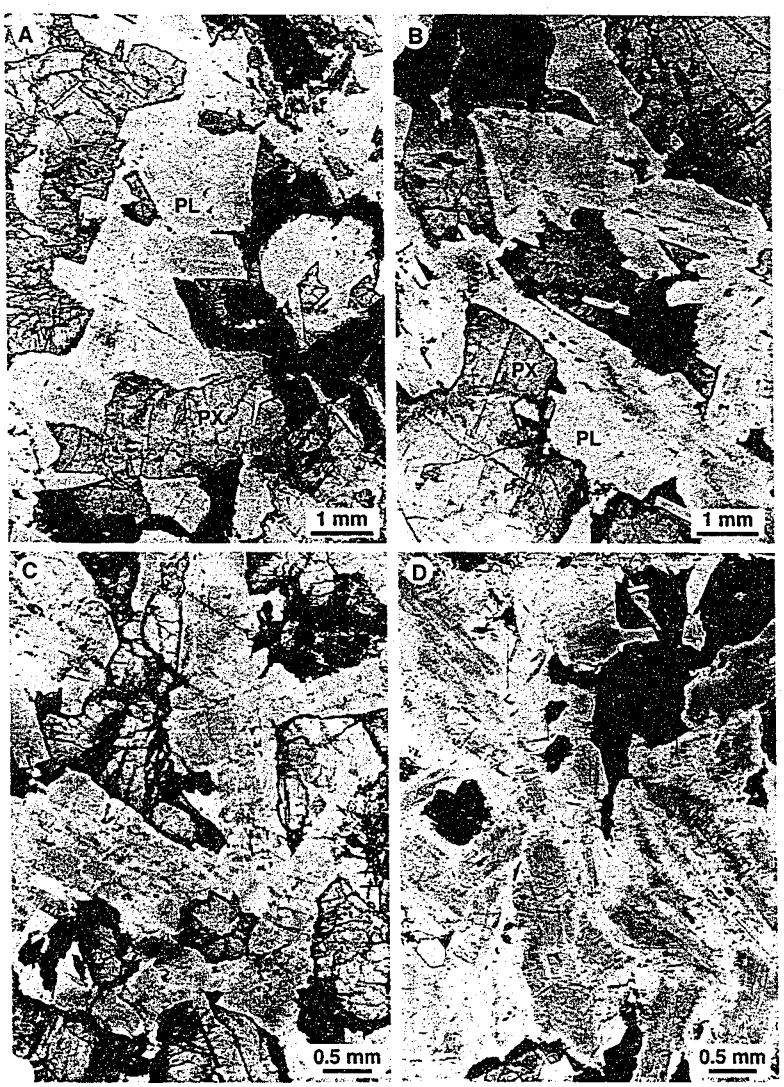
A
PL
PX
1 mm
B
PX
PL
1 mm
C
0.5 mm
D
0.5 mm

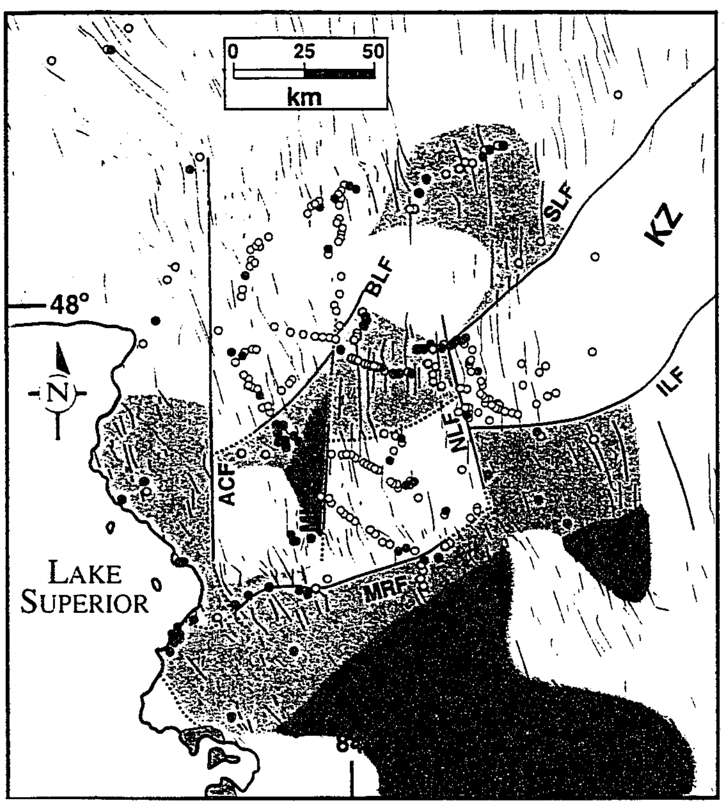

Fig. 2-2. Map showing variations in the degree of feldspar saussuritization determined from thin sections taken from coarse-grained dyke interiors. The hydrous alteration tends to be higher at interpreted shallower crustal levels (Halls, unpublished data)

. Blue, red, and yellow dots correspond to a high, moderate, and low degree of feldspar saussuritization.

Red, orange, and yellow shading corresponds to those regions containing dykes that have an overall high, moderate, and low level of saussuritization.

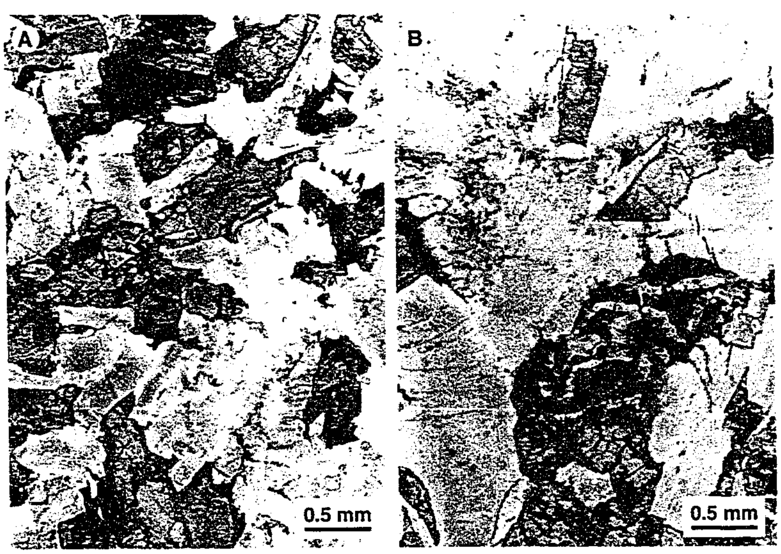

Fig. 2-3. (a),(b), variation of cloudiness. Cloudiness varies within a crystal and between grains. In uniformly clouded grains, cloudiness tends to leave a relatively clear mantle.

Fig. 2-4. (a), (b), A close look at cloudy feldspars (x300). Small clouding patches and bigger grains tend to line up along feldspar albite twin lamellae. (c), (d), SEM image of a cloudy feldspar. The clouding particles appear as short rods or long needles with sizes of a few micrometers.

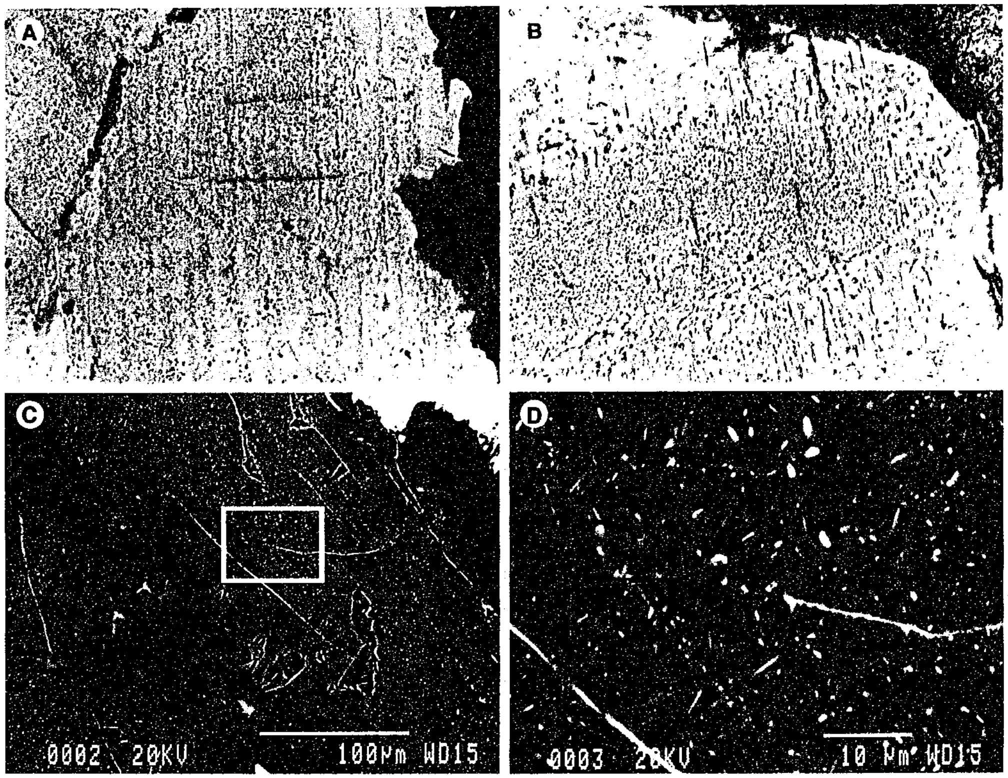
A
B
C
D
0002 20KV 100µm WD15
0003 20KV 10 µm WD15

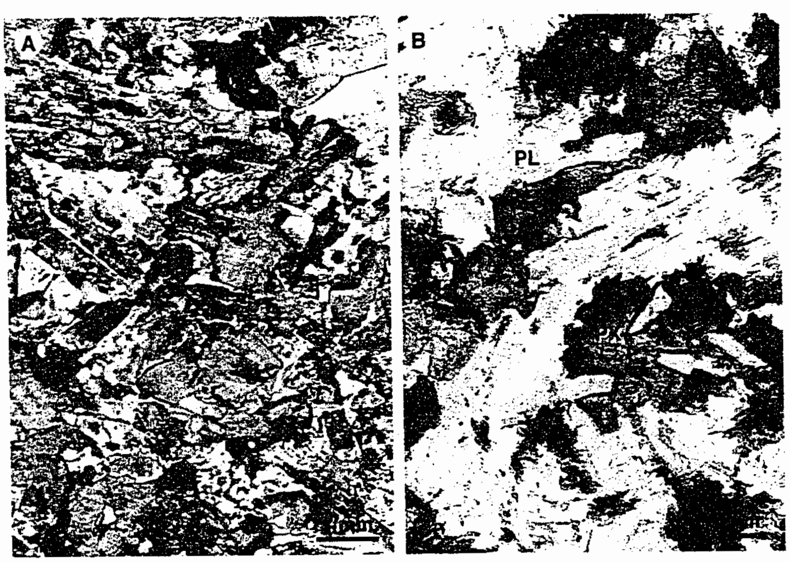

Fig. 2-5. Different appearances of saussuritization (a) and cloudiness of feldspars (b) under plane polarized light.

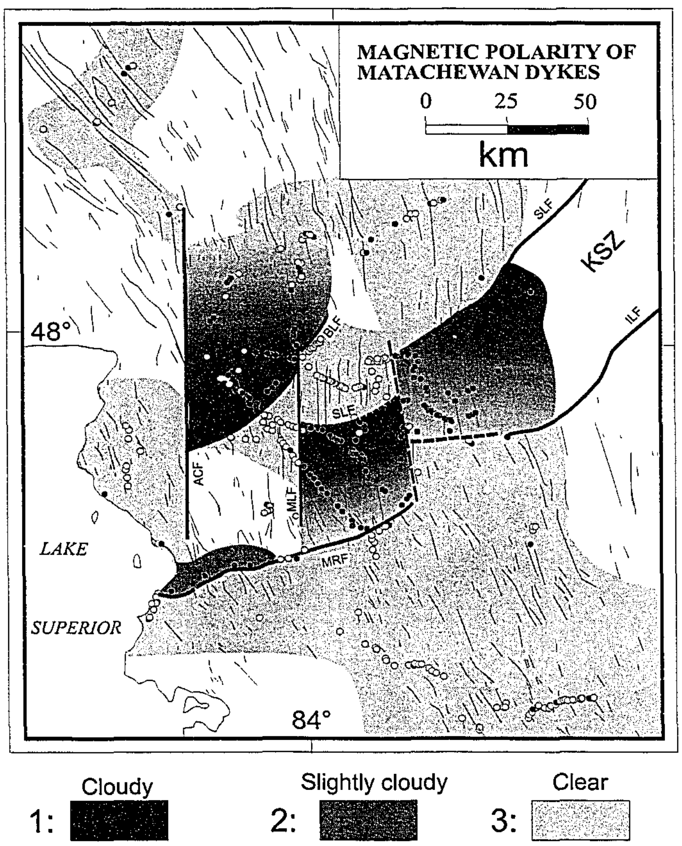

Fig. 2-6. Map showing location of sampling sites in Matachewan dykes at the southwestern end of the Kapuskasing Zone (KZ). Sites are grey-coded according to their degree of feldspar clouding: black -- cloudy; grey -- slightly cloudy; white -- clear. Shading refers to overall clouding level in different regions (light grey through dark grey to black indicates increasing average cloudiness). Symbols: KZ- Kapuskasing Zone; CB - Chapleau block; PB - Pineal Lake block; GB - Gould Lake block; ILF - Ivanhoe Lake fault; SLF - Saganash Lake fault; NLF - Nagasin Lake fault; MRF - Montreal River fault; MLF - McEwen Lake faultl; ACF - Agawa Canyon fault; BLF - Budd Lake fault. Some data is from H.C. Halls' previous work around the region. (From Halls and Zhang 1998).

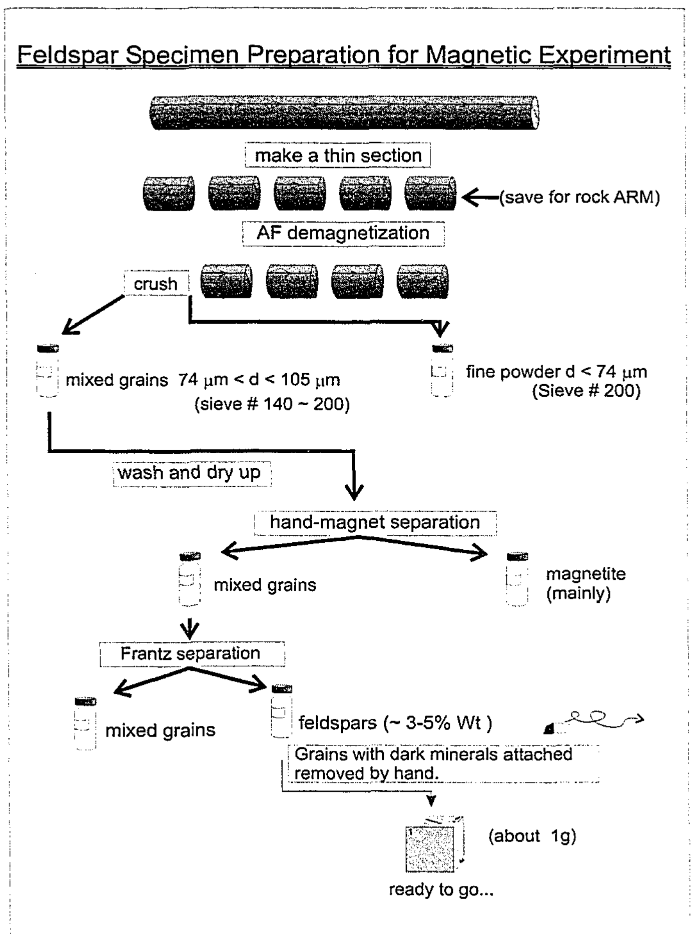

Fig. 2-7 Diagram showing method of preparing feldspar separates for magnetic experiments.

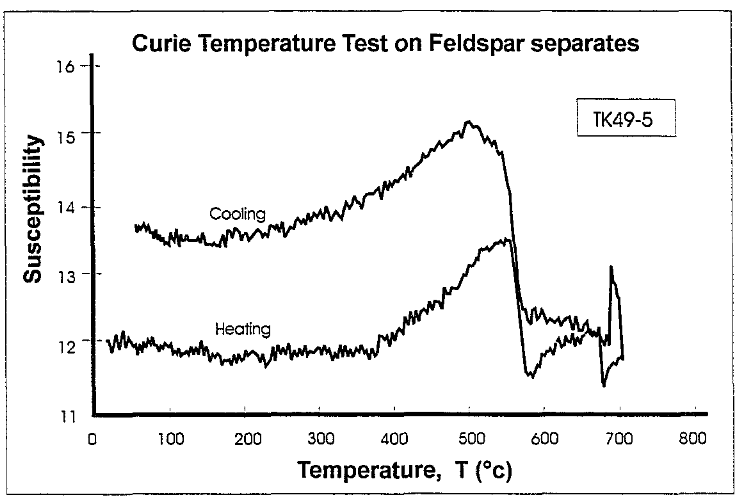

Fig. 2-8. Susceptibility test on medium clouded feldspar samples showing a clear magnetite Curie point (580~585°C) and an obvious Hopkinson effect (see text for detail).

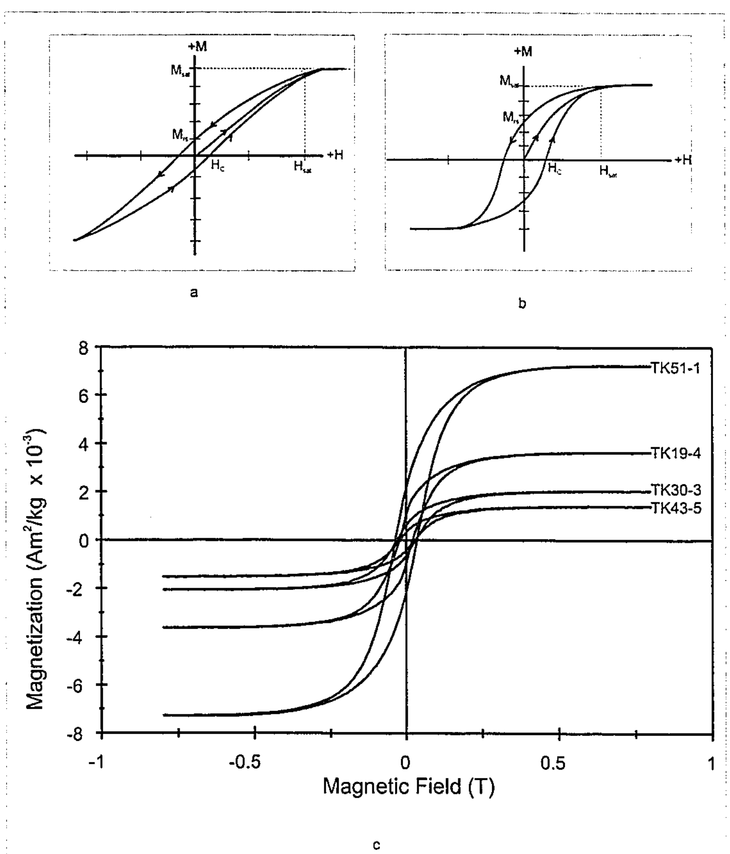

Fig.2-9.
a: Idealized hysteresis loop for a multi-domain grain size magnetite.
b: Idealized hysteresis loop for a single domain grain size magnetite.
c: Examples of hysteresis loops for feldspars separated from four Matachewan dykes,TK51, TK19, TK30 and TK43, that have progressively lower clouding intensities.

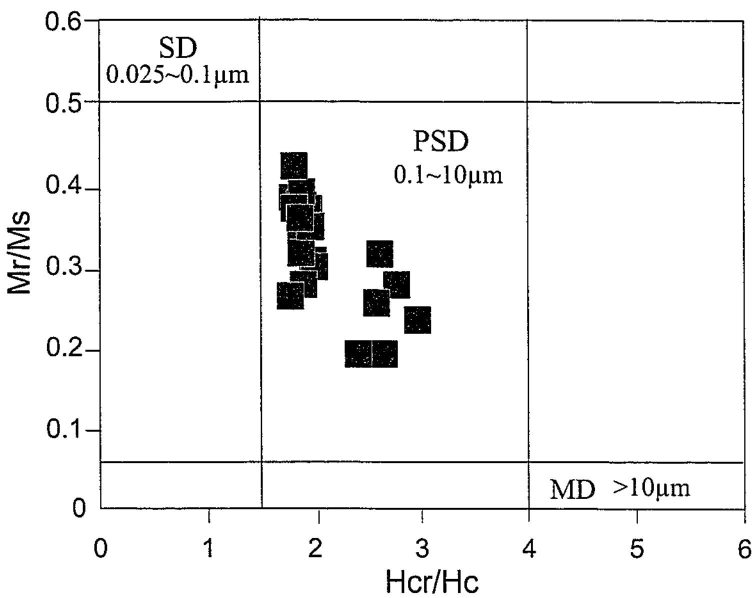

Fig.2-10. Determination of the grain size of magnetite in cloudy feldspars using hysteresis properties of the feldspar (Day et al. 1977). Mr: remanent magnetization; Ms: saturation magnetization; Hc: coercive force; Hcr: remanence coercive force.
SD: single domain; PSD: pseudo single domain; MD: multi-domain.

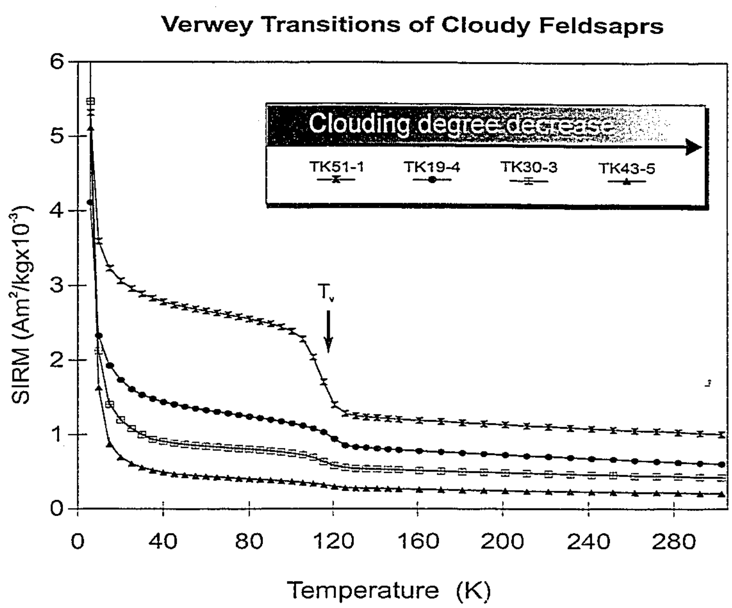

Fig.2-11. Plot of saturation isothermal remanent magnetization (SIRM) against temperature, showing examples of the Verwey transition (T_v) in feldspar separates. The amplitude of the transition has a positive correlation with the clouding degree of the feldspar samples.

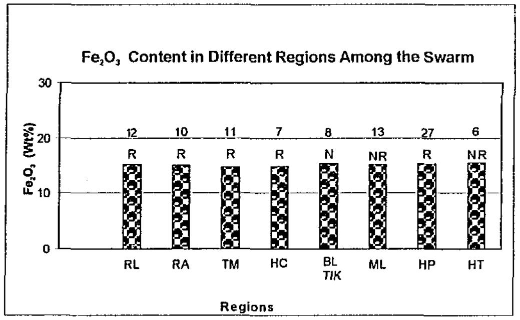

a

a. Average Fe_2O_3 content of Matachewan dykes in different areas around the KZ showing that regardless of magnetic polarity, Matachewan dykes have similar Fe content across the swarm. Signs above the bars are number of dykes used in the analysis and their polarity. (Except Budd Lake and Tik Road, data are from W.C.

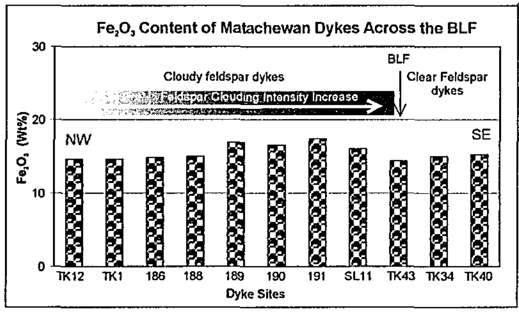

b

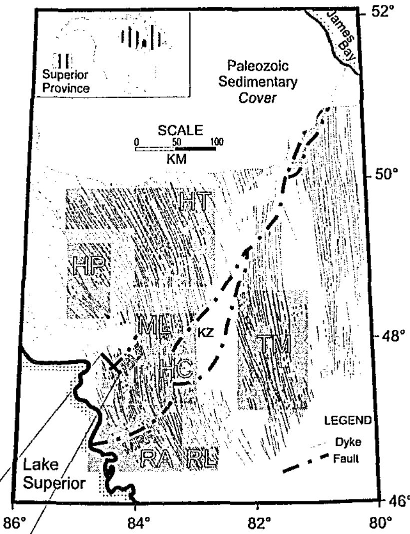

Fig.2-12. Studied areas among the Matachewan dyke swarm. Symbols: RL: Rocky Island Lake; RA: Ranger Lake; TM: Timmins; HC: Chapleau & Hwy10; ML: Missinaibi Lake; HP: Hornepayne; HT: Hearst; BL& TIK: Budd Lake and Tik road. (Map modified from Bates & Halls 1991)

b. Average Fe_2O_3 content of Matachewan dykes across the BLF showing that although feldspars in the dykes have different clouding intensity, the dykes have similar Fe content.

Fig. 2-13. Example of SEM results from single feldspar crystals with varying cloudiness.

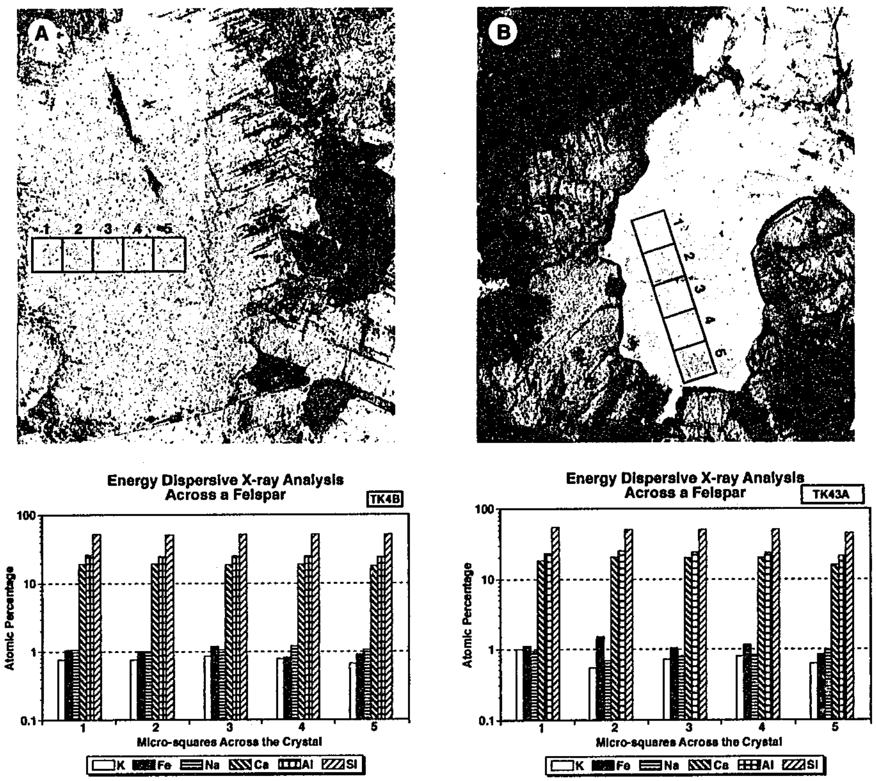
A
1
2
3
4
5
B
1
2
3
4
5
Energy Dispersive X-ray Analysis Across a Felspar
TK4B
Atomic Percentage
100
10
1
0.1
Micro-squares Across the Crystal
K
Fe
Na
Ca
Al
Si
Energy Dispersive X-ray Analysis Across a Felspar
TK43A
Atomic Percentage
100
10
1
0.1
Micro-squares Across the Crystal
K
Fe
Na
Ca
Al
Si

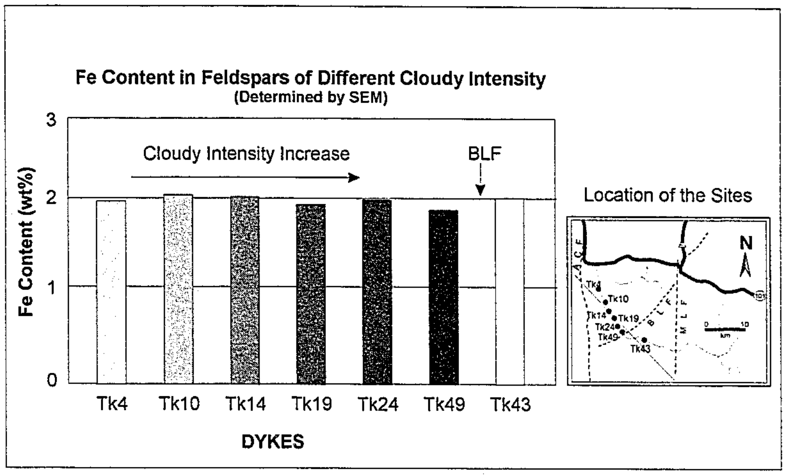

Fig. 2-14. SEM results on feldspars from different dykes in a traverse across the BLF. Note that despite the variation in cloudiness, the total Fe content from the feldspars is similar.

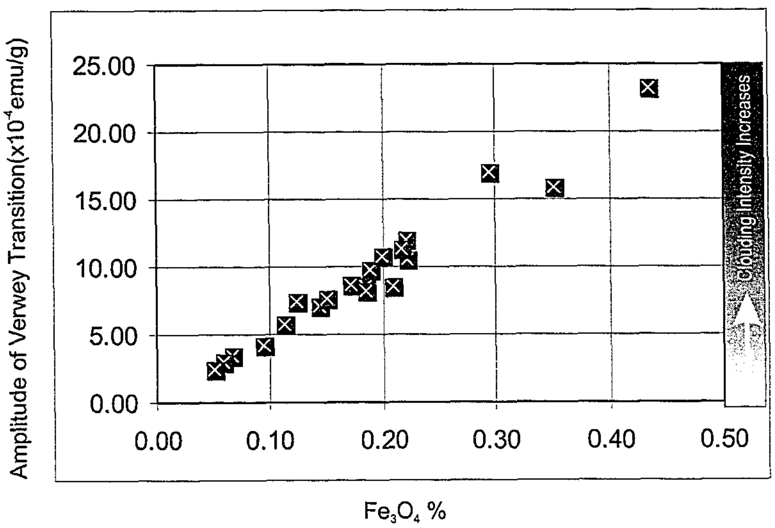

Fig.2-15. Plot of amplitude of Verwey transition against magnetite concentration of feldspars from different Matachewan dykes. The magnetite content is calculated from saturation magnetization of the samples at a temperature of 6 K. The linear relation indicates that the amplitude of Verwey transition is a good measure of magnetite concentration and clouding intensity of the feldspars.

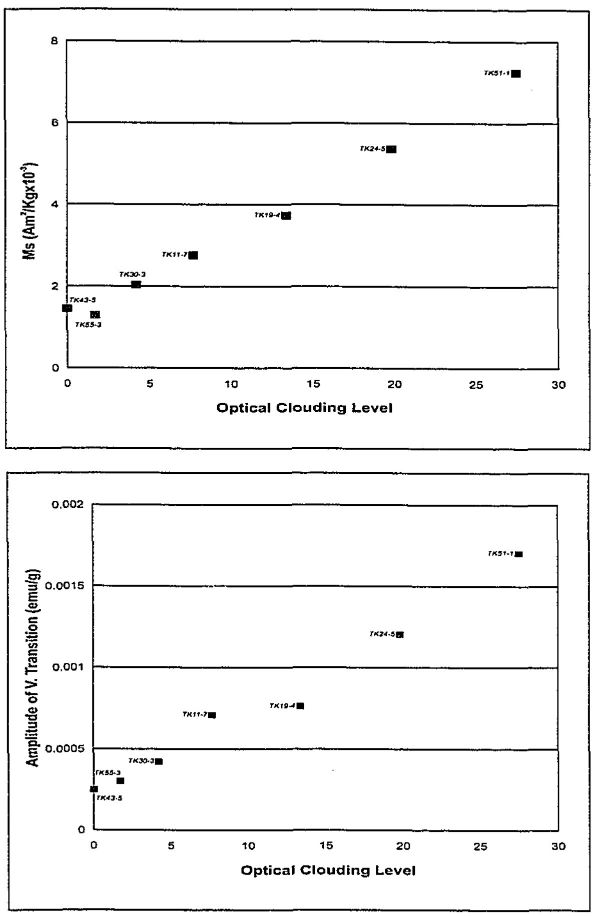

Fig.2-16. Plots of feldspar clouding intensity against the saturation magnetization (M_s) and amplitude of the Verwey transition of the feldspars. Clouding intensity values, determined by image analysis, are relative to the lowest one which has been set at zero.

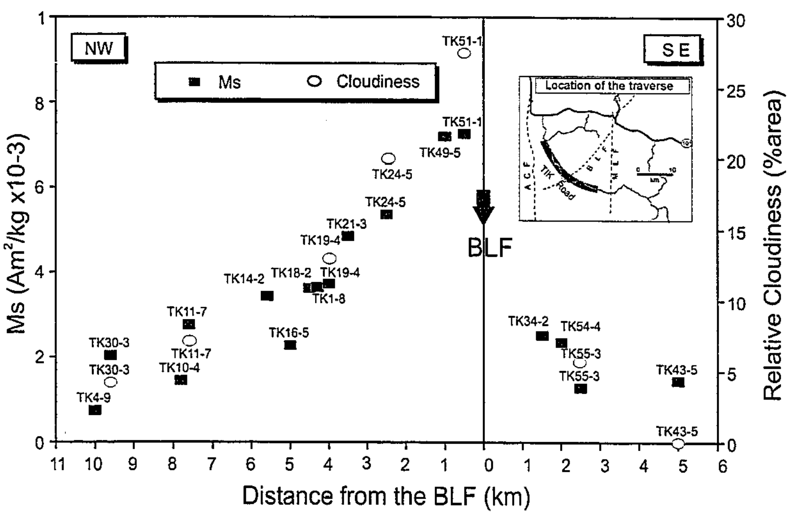

Fig.2-17. Saturation magnetization and feldspar clouding intensity plotted across the Budd Lake fault (BLF) along Tik road. The cloudiness intensities have been normalized according to that of site Tk43. (See Fig.1-3 for location of sites)

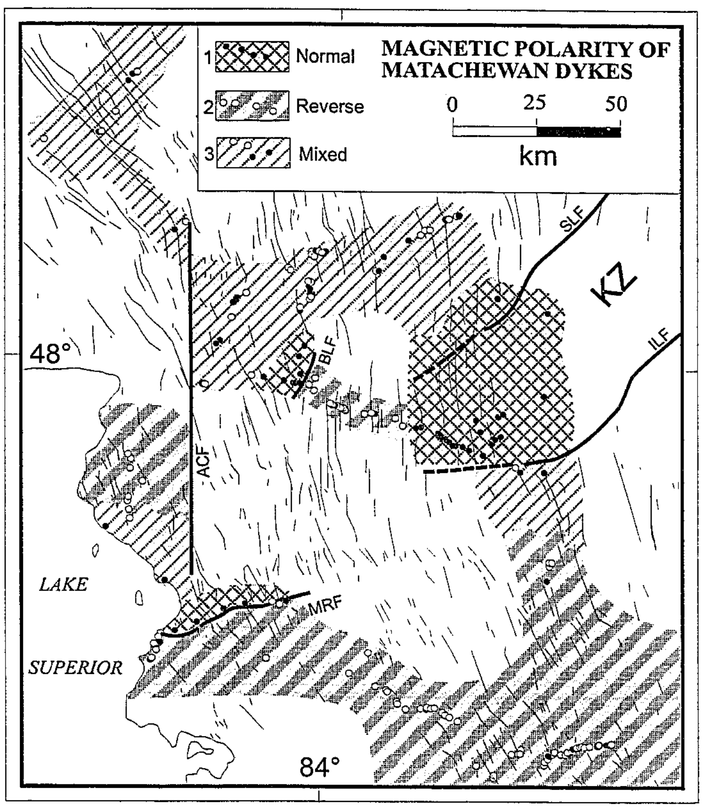

Fig. 3-1. Map showing the distribution of normal (N) and reversed (R) magnetized Matachewan dykes in the vicinity of the Kapuskasing zone, based on paleomagnetic data obtained before 1992 when the thesis started. Black, white dots: N, R dykes. The shading emphasizes regions or domains of contrasting polarity characteristics: 1- all N dykes; 2- ratio of R to N dykes greater than 4:1; 3- R and N dykes in about equal proportions. The boundaries between these regions are necessarily diffuse except where sharp contrasts occur across major faults. Faults are shown as solid/dashed lines where they are relatively well defined/more speculative. Abbreviations for faults as in Fig.2-6.

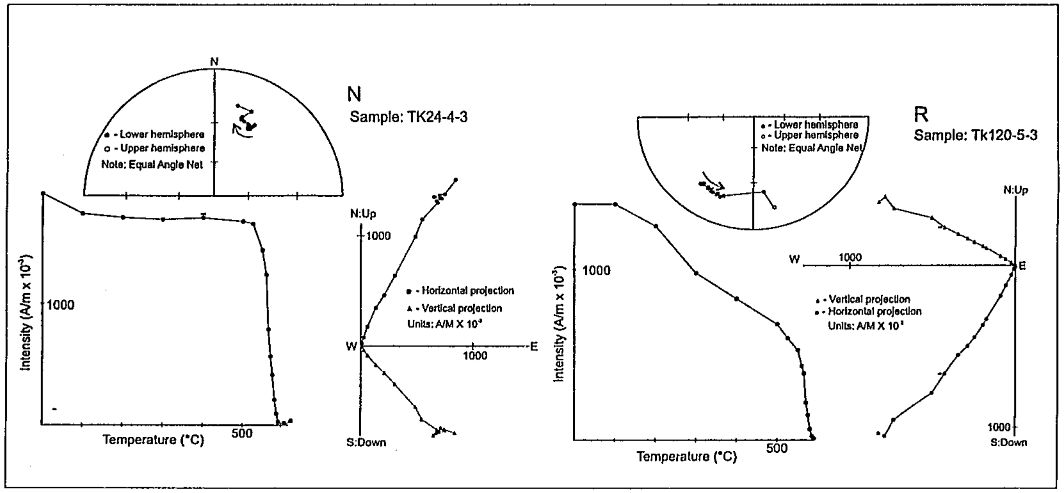

Fig.3-2. Examples of thermal demagnetization for **N** and **R** dykes. Note that for both dykes, the Curie temperature is about 580°C indicating that the magnetization is carried by magnetite. However, the **R** dyke has much wider unblocking temperature spectrum than that of the **N** dyke, which demonstrates that the **R** remanence is carried by larger grain size magnetite than that for the **N** remanence. For locations of the sites see Fig.1-3 or Fig.3-6.

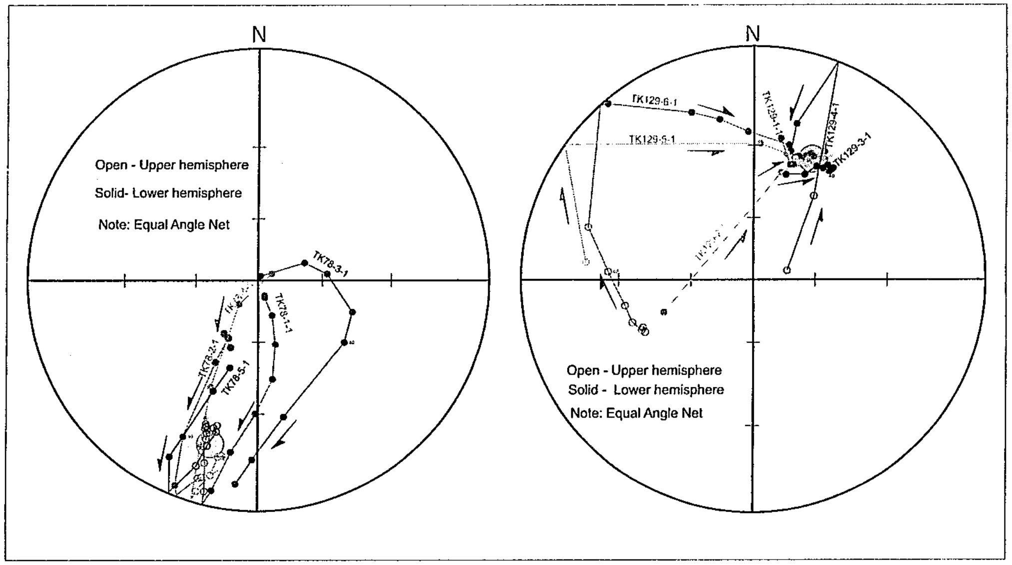

Fig. 3-3. Examples of alternating field (AF) demagnetization for **N** and **R** dykes. Note that stepwise removal of low coercivity components defines great circles on a Wulff net, and the intersection (or possible intersection) defines the direction of primary, high coercivity components.

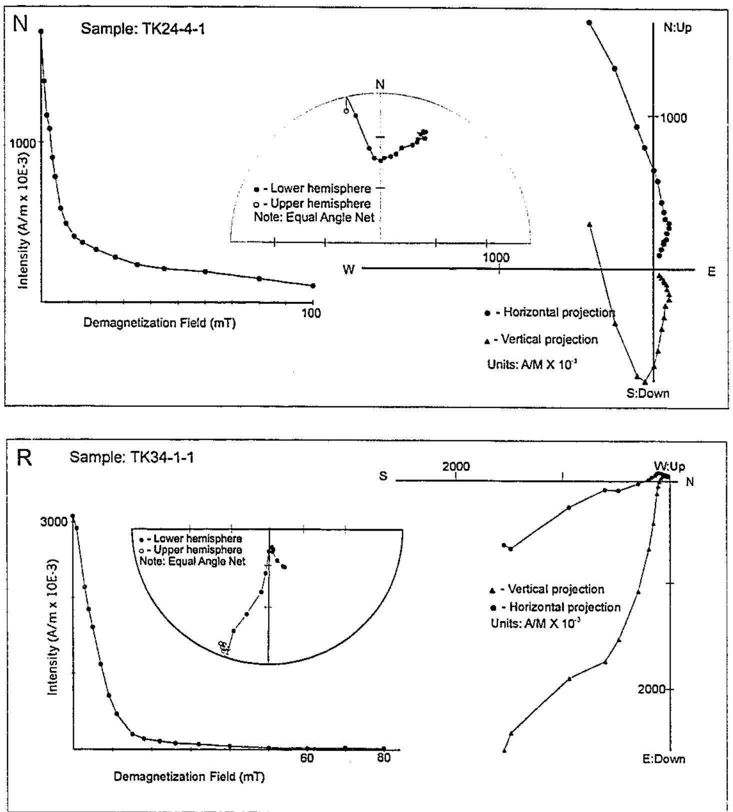

Fig.3-4. Example of AF demagnetization on N and R dykes. Three components are revealed on both dykes. The first components has a weak and unstable direction. The ow-coercivity components have steep inclinations; The stable components are isolated after removal of about 90% of the NRM. Note that compared with the R dyke, N dyke has a stable high coercivity component that can survive over 100 mT demagnetization field.

Polarity Distribution of Matachewan Trending Sites

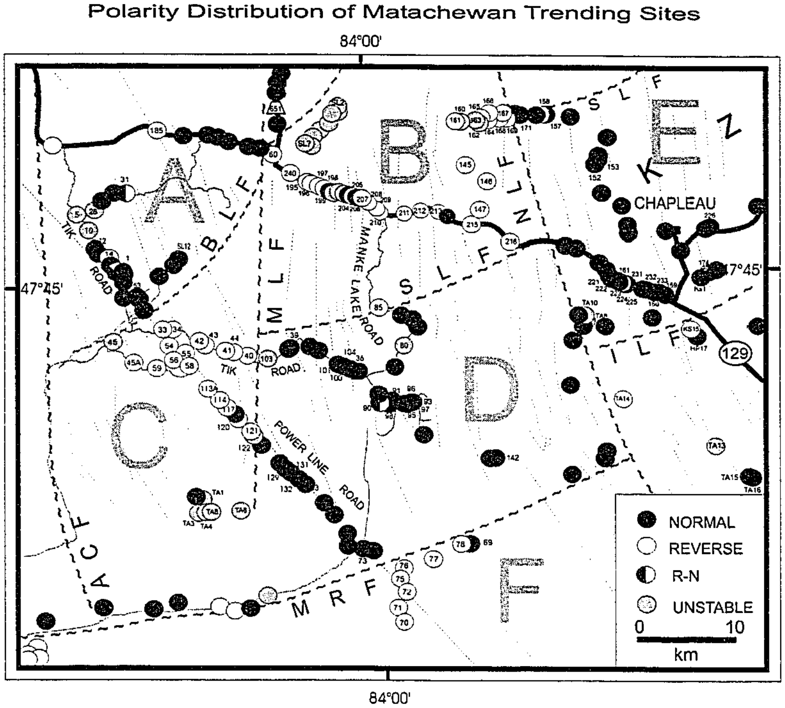

Fig. 3-5. Map shows detailed polarity distribution of the Matachewan dykes in study area. Sites with numbers higher than 171 are from Halls and Palmer (1990). Polarity change defines major faults, which separate the study area into five polarity domains or blocks. ILF: Ivanhoe Lake fault; SLF Saganash Lake fault; NLF: Nagasin Lake fault; MRF: Montreal River Fault; MLF: McEwan Lake fault; BLF: Budd Lake fault; ACF: Agawa Canyon fault; KZ: Kapuskasing Zone.

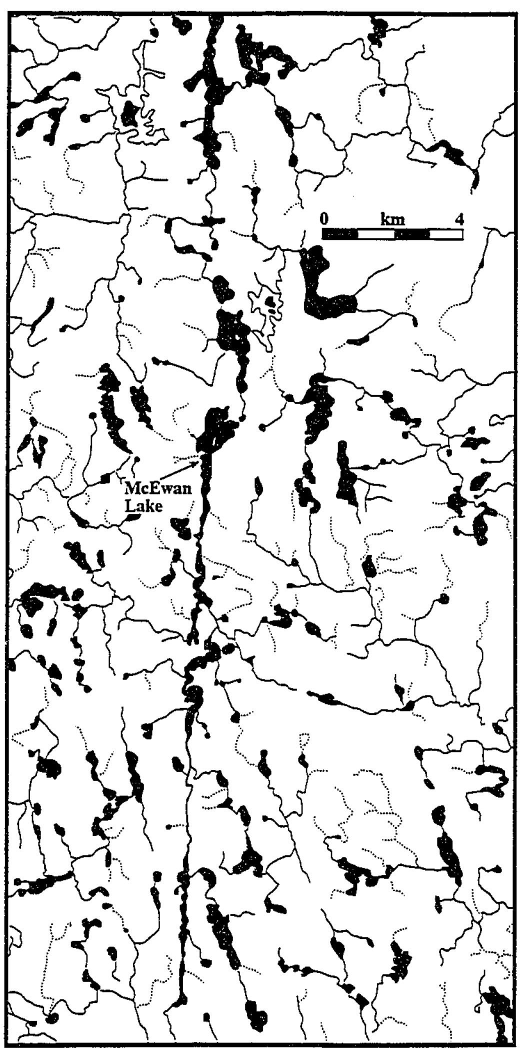

Fig.3-6. Change of topographic features across McEwan Lake fault showing that NNW trending chains of lakes on the eastern side do not go through the McEwan Lake chain.

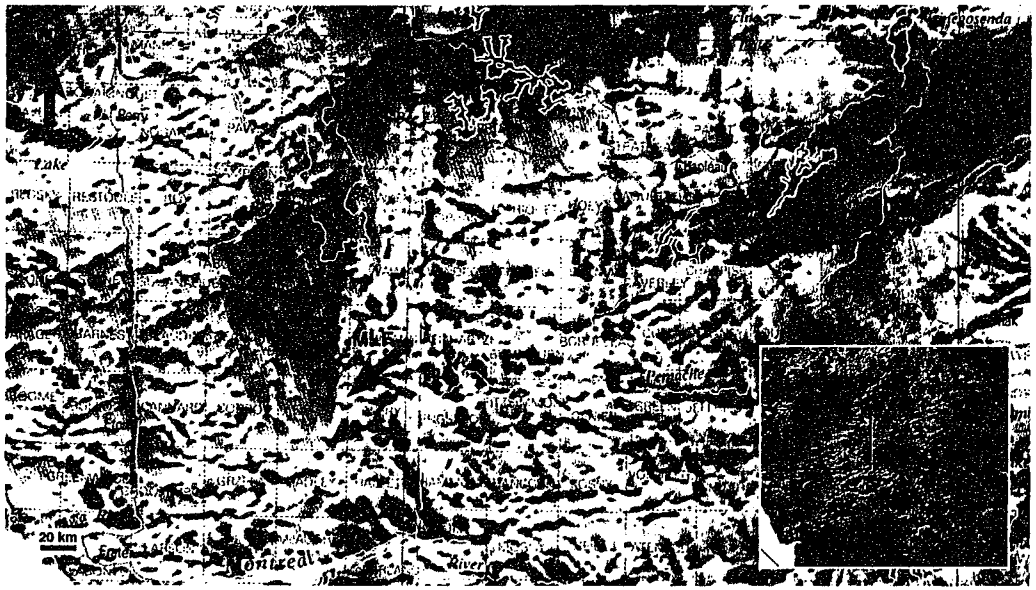

Fig.3-7. Aeromagnetic map in the vicinity of southwestern extension of KZ showing obvious anomaly of McEwan Lake fault.

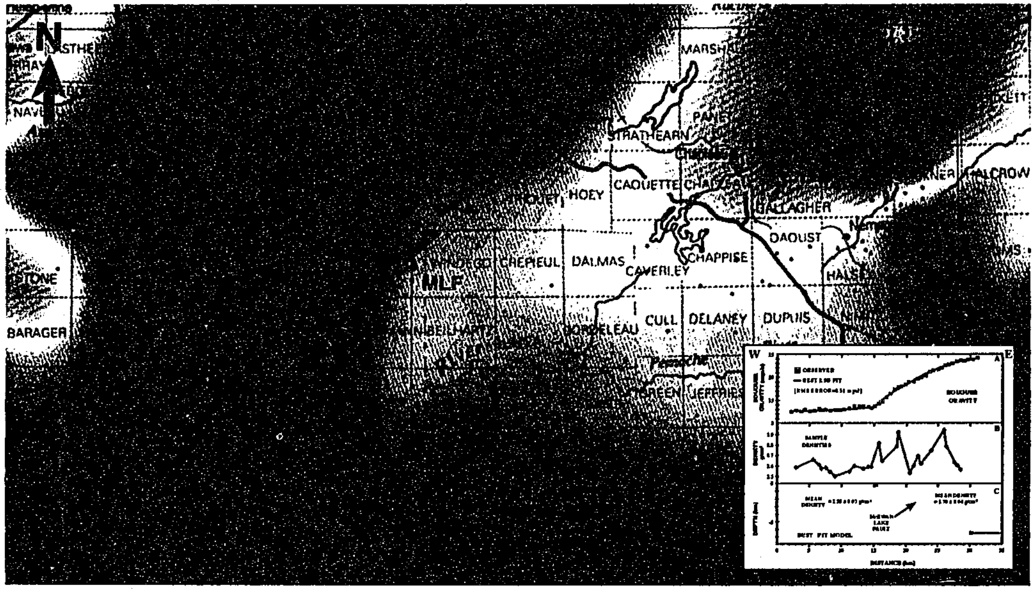

Fig.3-8. Gravity anomaly of the McEwan Lake fault. Bottom right corner is gravity survey results along the traverse A-B.

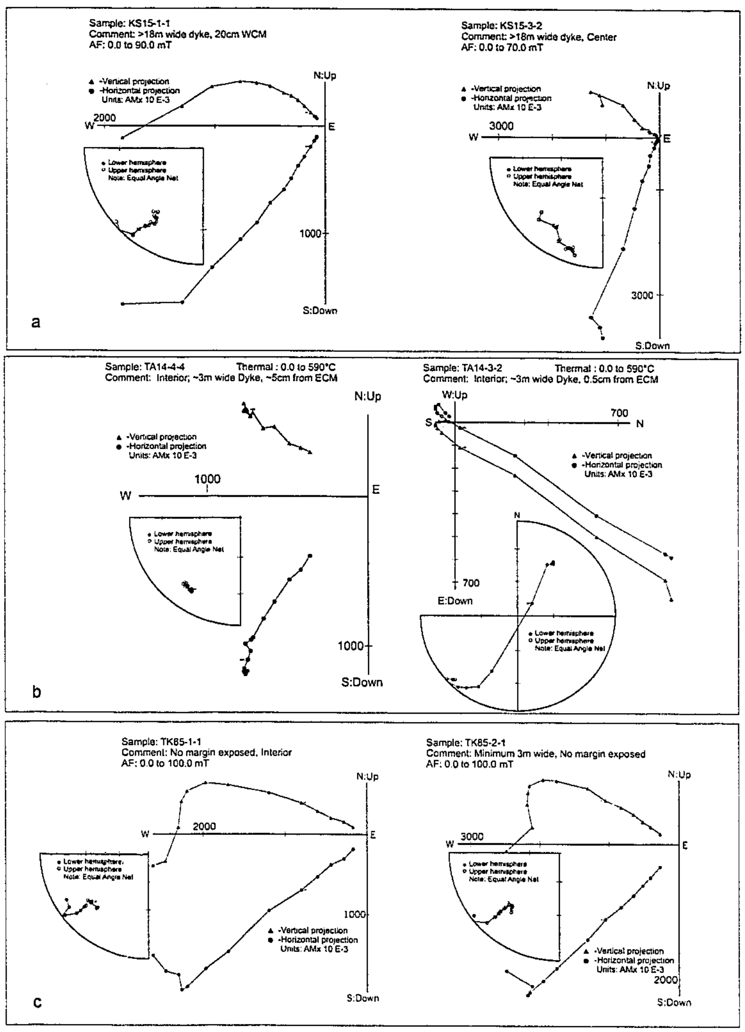

Fig. 3-9. AF demagnetization of site KS15 (a), TA14 (b), and TK86 (c). Their definite R signatures help to identify the major faults and to constrain their position. Site locations see Fig.3-5.

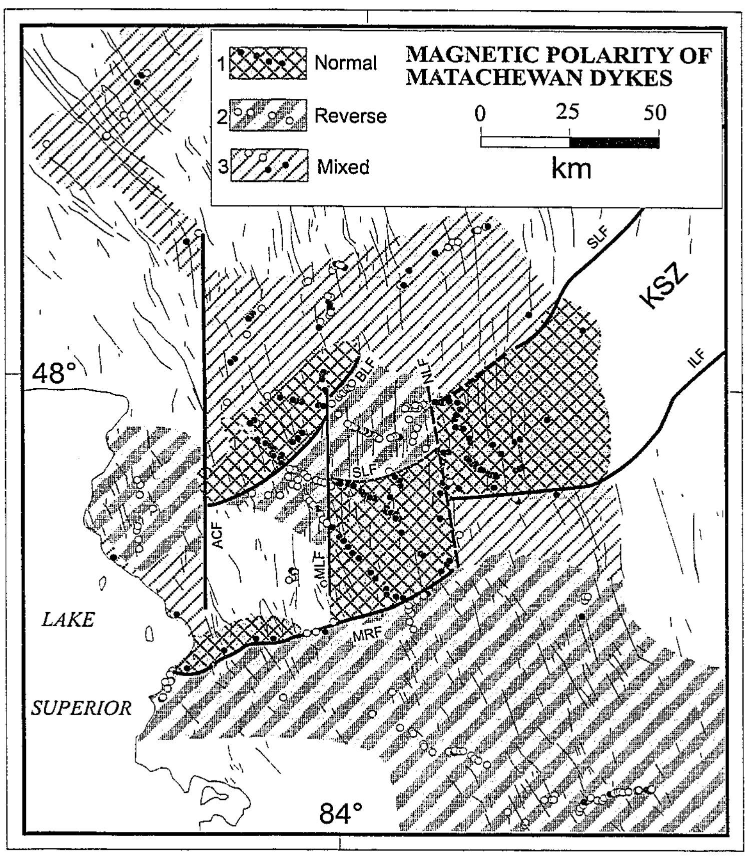

Fig. 3-10. An updated version of Fig.3-1, incorporating results from the latest paleomagnetic data. Note that the McEwan Lake fault (MLF) and Nagasin Lake fault (NLF) are now more firmly established, the Budd Lake fault (BLF) can be extended farther to the southwest, and the Montreal River fault (MRF) extended towards the east. A possible western extension of the Saganash Lake fault (SLF) has also been discovered. Symbols are defined as in Fig. 3-1.

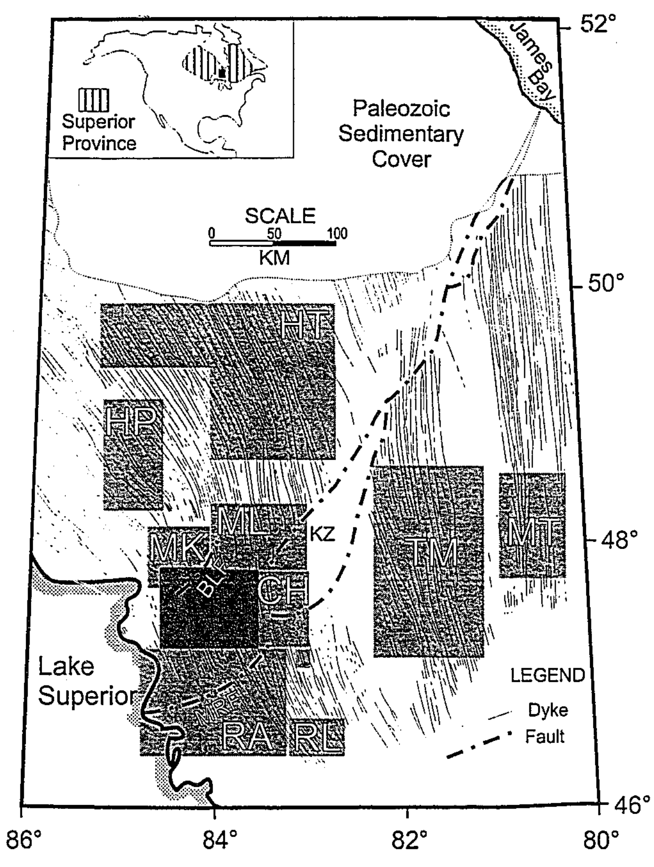

Fig.3-11. Name and location of paleomagnetic data sets from previous study (Bates & Halls 1991). The darker shaded square is the area of study for the thesis.

HP: Homepayne
HT: Hearst
MK: Manitowik Lake
TM: Timmins
ML: Missinaibi Lake
CH: Chapleau & Hwy101
WL: Wenebegon Lake
RL: Rocky Island Lake
RA: Ranger Lake & Montreal River
MT: Matachewan and Otto stock.

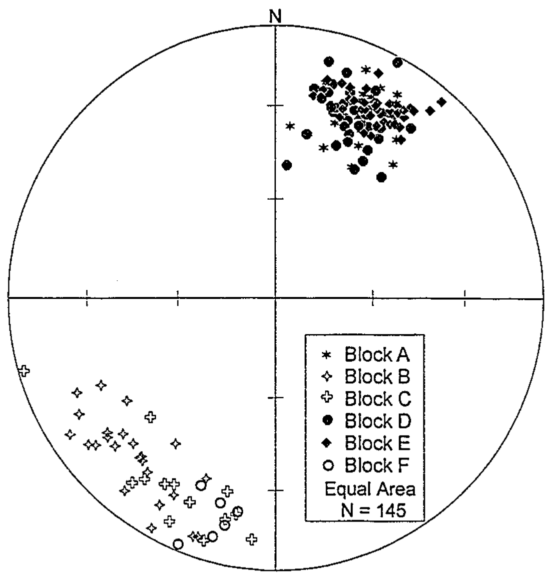

Fig.3-12. Stereonet plot of site-mean paleomagnetic stable end points from all the blocks.

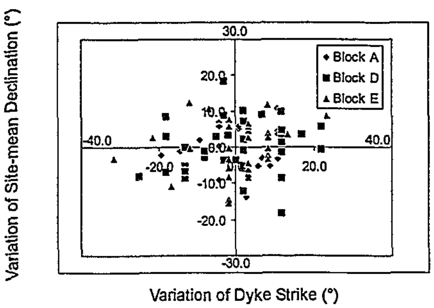

a

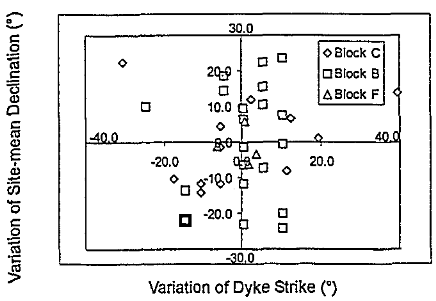

b

Fig. 3-13. Plot of variation of site-mean declination against that of dyke strike in all polarity blocks. (a: N blocks; b: R blocks). Note that lack of obvious correlation indicates that variation of paleomagnetic declination is not due to shape anisotropy of the dykes.

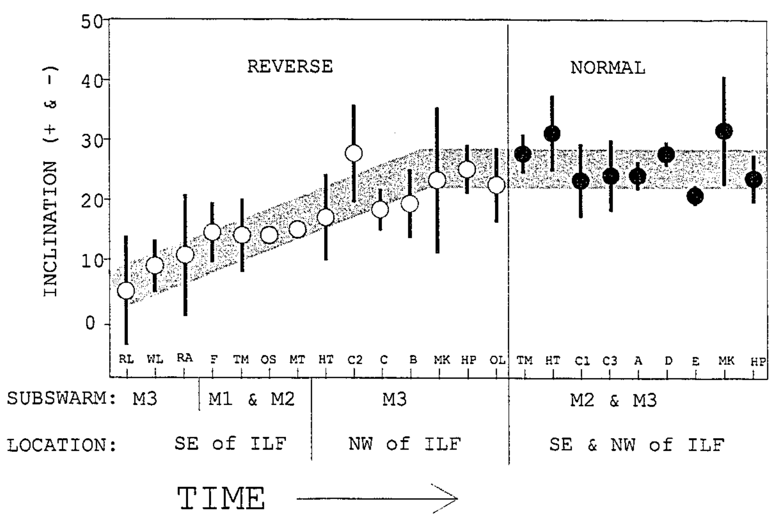

Fig.3-14. Schematic diagram showing the observed change of magnetization inclination for the Matachewan swarm in space and possibly in time. It shows that towards the northwest the dykes acquired younger magnetizations either as a consequence of younger emplacement ages or because of uplift following delayed cooling at greater crustal depths. The model assumes a progressive change in inclination during the R period and a single reversal of the Earth's magnetic field during igneous activity (Halls 1991). Within the four subswarm groups no specific time sequence of the paleomagnetic data is implied. Bars are one standard deviation for inclination. Data sets except A, B, C, D, E, F are from Bates and Halls (1991). Location of the data sets see Fig.3-12.

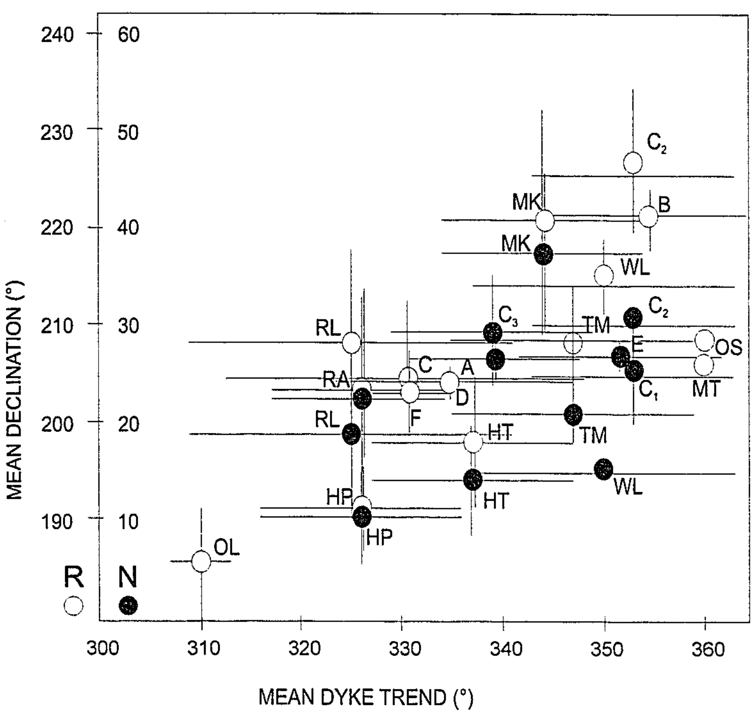

Fig.3-15. Plot of block mean paleomagnetic declination via block mean dyke trend. All data sets (A, B, C, D, E, F) are from M_3. The other sites are from Bates and Halls (1991). The general positive correlation indicates that the blocks have undergone relative rotation after dyke intrusion. Bars are one standard deviation for both declination and dyke strike. Location of data sets see Fig.3-12.

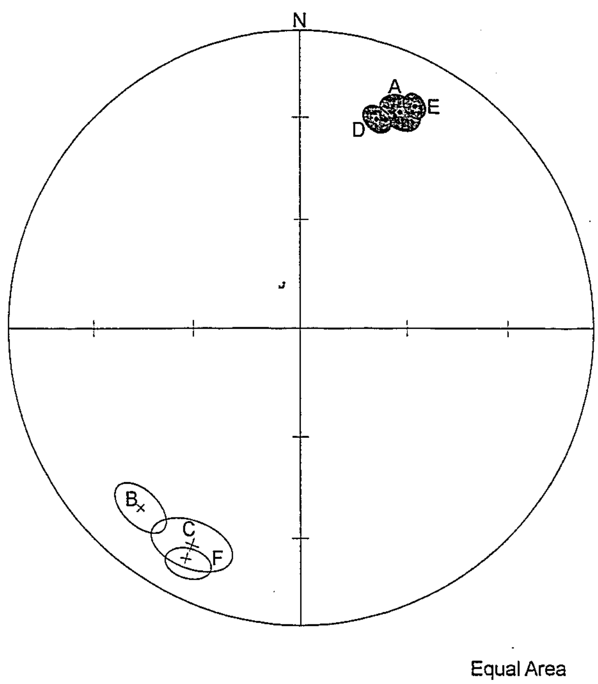

Fig. 3-16. Stereonet plot of block-mean paleomagnetic directions. Note that R blocks have similar inclination but larger declination range indicating mainly horizontal rotation about steeply dipping axes (Regional direction of RA 204.1°, -11.6° α_{95}=5.4° is used for Block F plot). N blocks have almost identical directions, except that compared to E, block D is tilted about 10° eastward around a N-S horizontal axis.

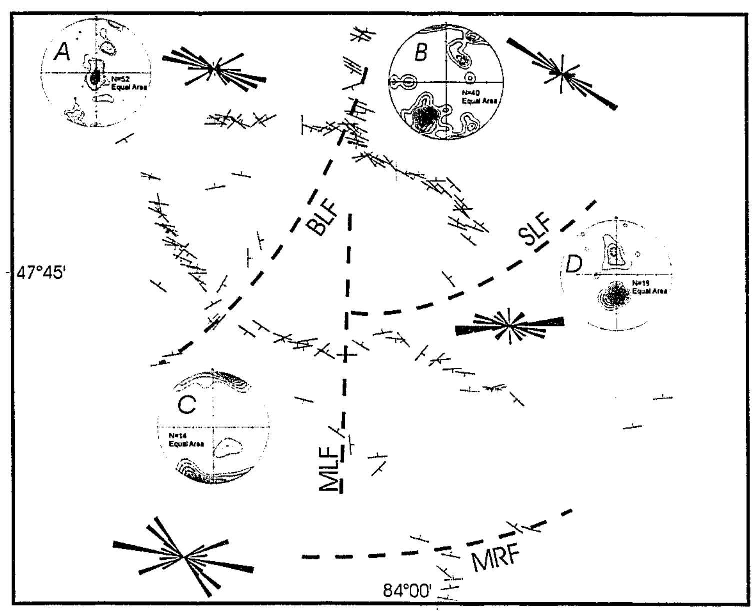

Fig.3-17. Map of country rock foliation along main traverses in study area. Stereonets show the density distribution of normals to foliation planes. Circular histogram (Rose-diagram) shows the average strike direction of foliation in block A, B, C and D.

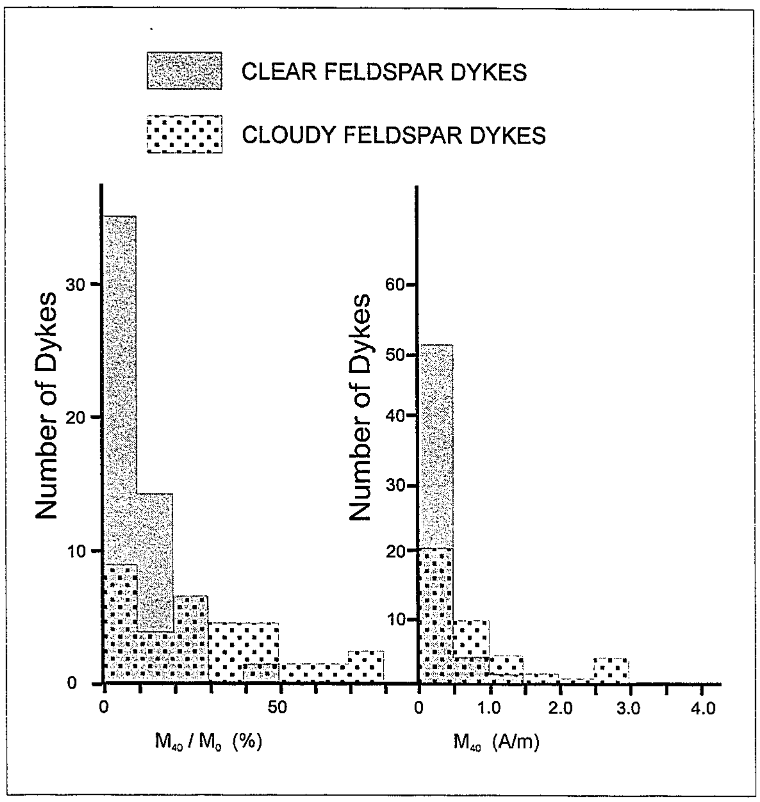

Fig. 4-1. Histogram for normal polarity Matachewan dykes with clear or cloudy feldspars according to visual inspection of thin sections. M_0: initial magnetization intensity, M_{40}: intensity remaining after a demagnetization step of 40 mT. Note that more cloudy dykes have high coercivity components than clear dykes, indicating that cloudy feldspars enhance the strength of the magnetization. In most cases the values used are averages of 2~6 samples per dyke. The analyses include data from about 100 dykes, representing more than 250 individually demagnetized samples. (Zhang and Halls, 1995).

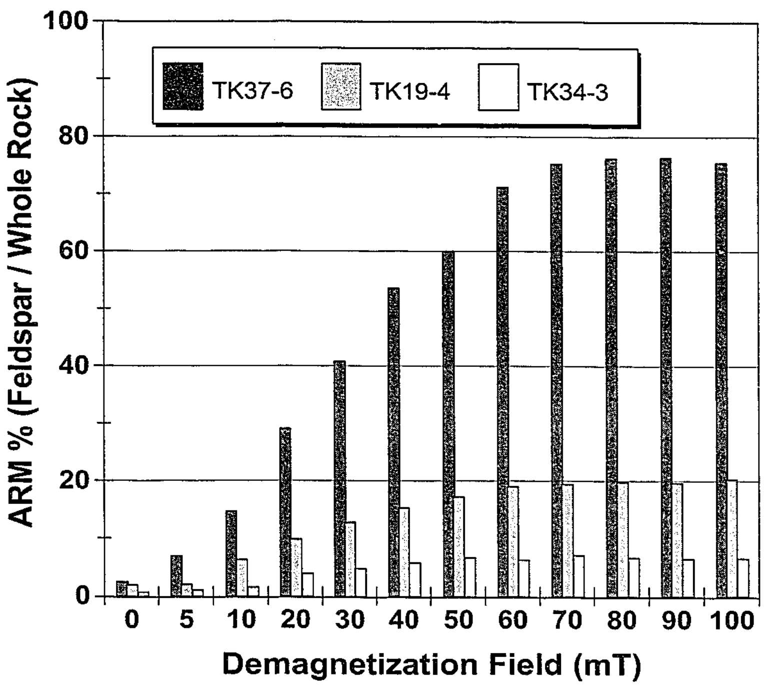

Fig.4-2. ARM experiment result showing the percentage of ARM carried by feldspars over the whole rock ARM. TK37 and TK19 are "cloudy dykes" with TK37 is cloudier than TK19, and TK34 is a "clear dyke". The result shows that (1) cloudy feldspars are responsible for higher coercivity magnetization; (2) feldspar ARM percentage in the rocks has a positive co-orelation with clouding intensity.

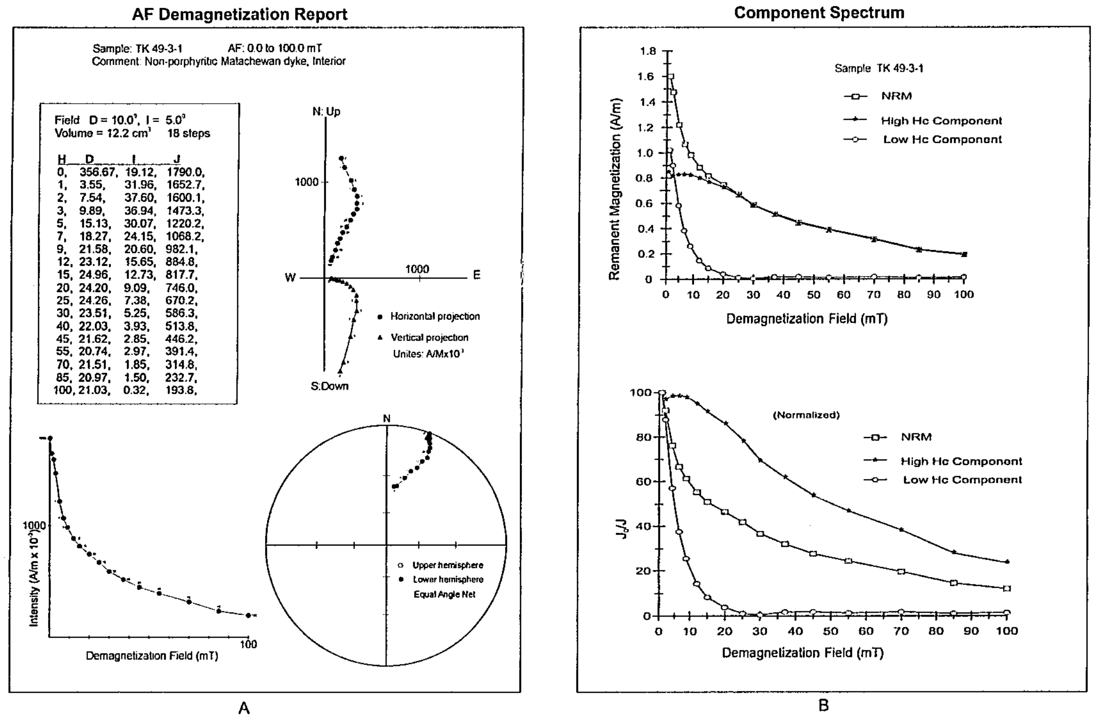

Fig.4-3. An example of intensity separation of NRM components.
A: AF demagnetization result of a medium cloudy feldspar dyke (TK49, see Fig.1-3 or Fig.3-5 for field location).
B: Intensity spectrum of the two components, with high and low coercivities, separated by AF demagnetization.

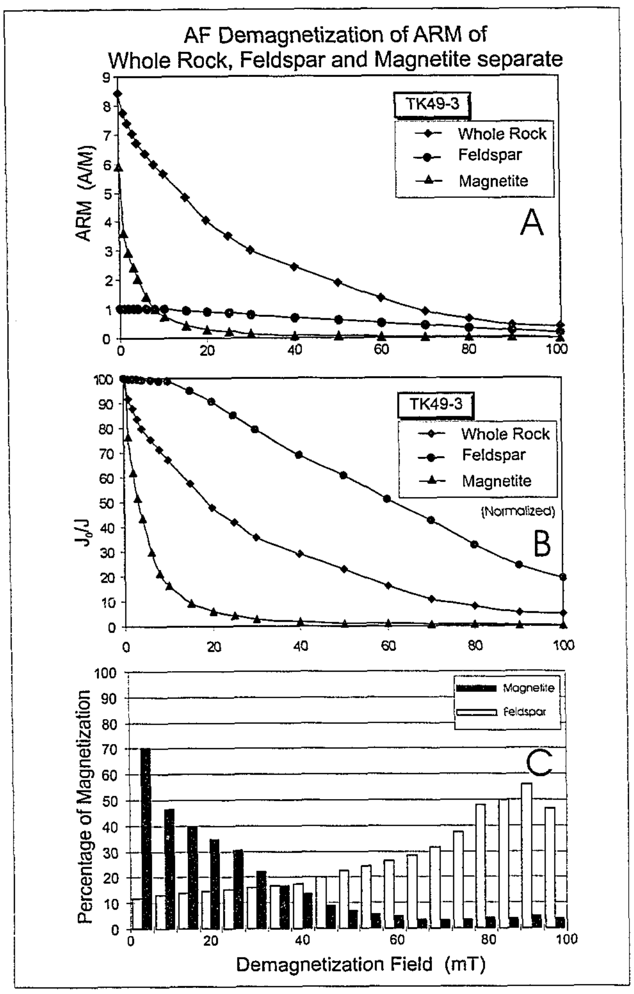

Fig. 4-4. AF demagnetization of ARM in whole rock, feldspar and magnetite separates. A: ARM spectrum with demagnetization field, B: normalized data, C: percentage of the ARM carried by feldspars and coarse magnetite in the rock at different demagnetization stages.

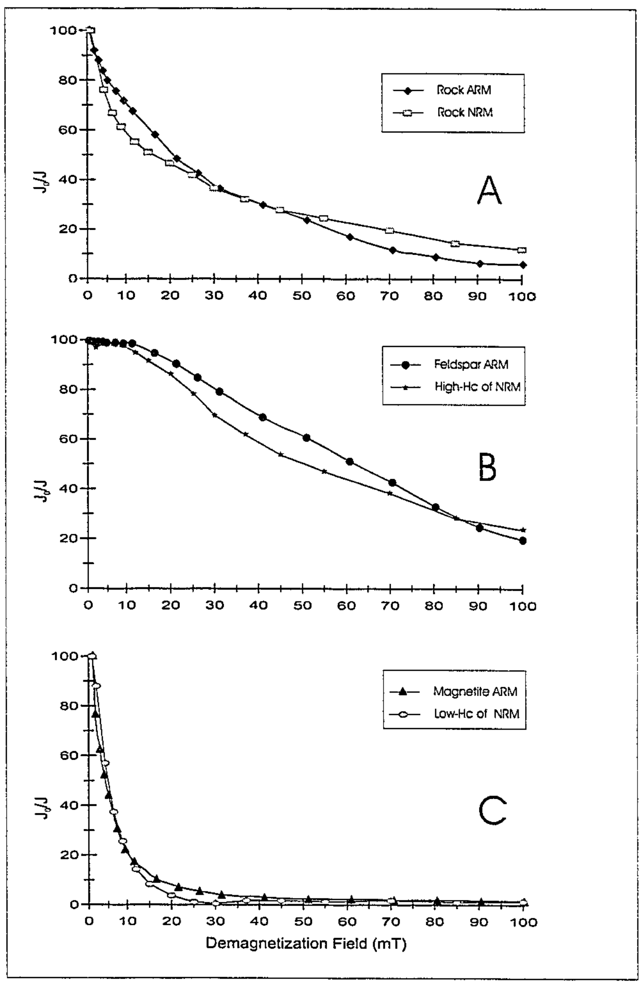

Fig.4-5. Comparison of ARM with NRM components.
A: whole ARM - rock NRM,
B: feldspar ARM - high coercivity component of NRM,
C: magnetite ARM - low coercivity component of NRM

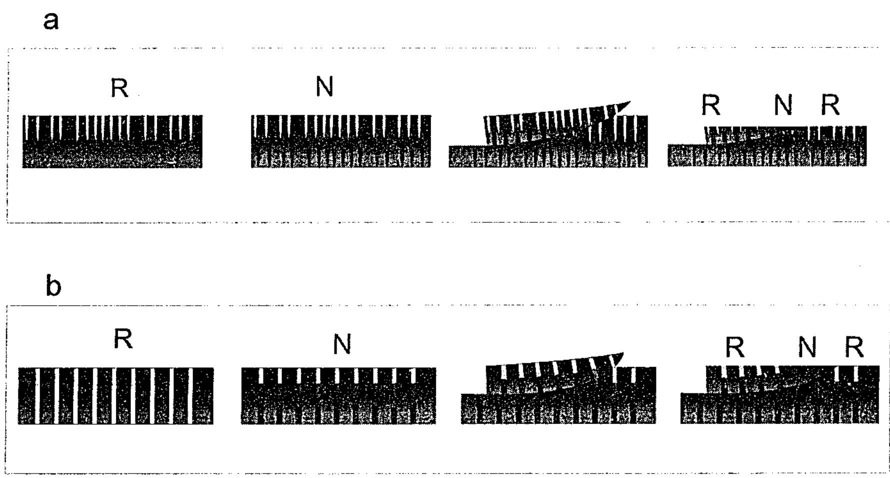

Fig. 4-6. Two possible models for formation of the N-R distribution pattern of Matachewan dyke swarm across the Kapuskasing Zone.

a: multi-phase injection model: dykes intruded in R epoch confined to shallow levels while dykes intruded after the Earth's magnetic field reversal were mostly confined to deeper crustal levels.

b: delayed cooling model: Dykes intruded during R epoch. Due to high ambient temperature in deeper crustal levels, the lower sections of the dykes did not acquire magnetization until the Earth's magnetic field reversed to N.

In both cases, subsequent thrusting and erosion brought the deeper, N dykes up.

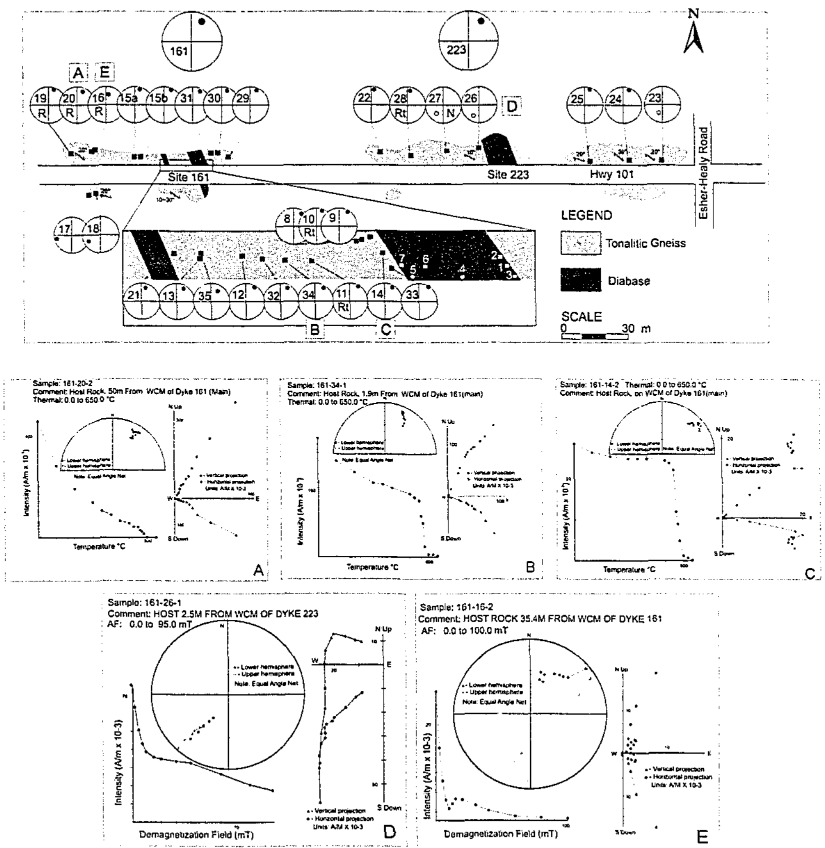

Fig. 4-7. Schematic map of roadcuts along Hwy 101, about 10 km southwest of Chapleau, showing the distribution of samples used in a baked contact test for **N** Matachewan dyke sites 161 and 223 of Halls and Palmer (1990). A,B,C are examples of thermal demagnetized N polarity tonalitic country rocks. Note that farther from the main dyke 161, the component has lower unblocking temperature. The symbols **R** and **Rt** in some equal-area plots signify that despite the dominant **N** magnetization, a small **R** component was present at the highest coercivity or unblocking temperatures, respectively (D). Example (E) shows a strong R component carried by fine grained magnetite surviving after AF removal of the N overprint.

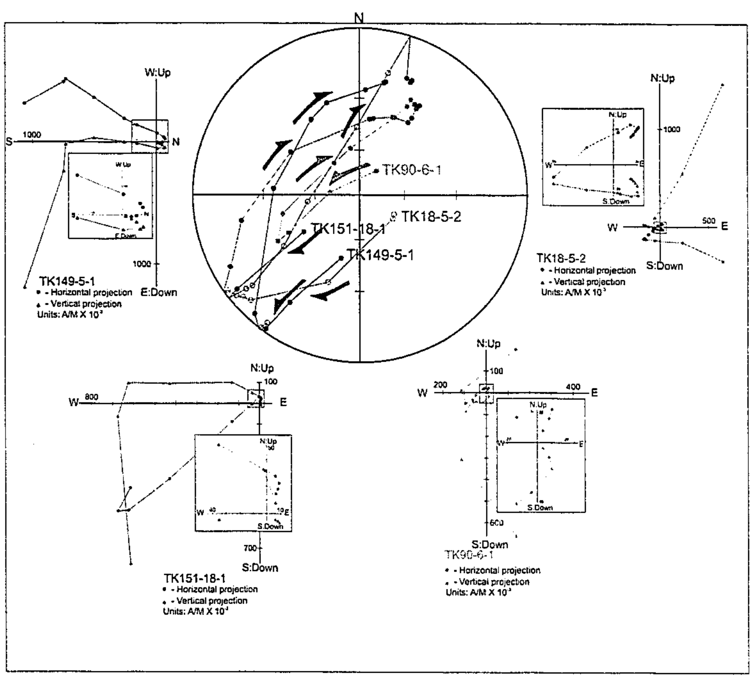

Fig. 4-8. Examples of AF demagnetization on samples that carry both R and N remanences. Three components can be isolated in these cases. The first is an approximately SE steep down overprint, the second is the Matachewan R component, and the last is the Matachewan N component. This relationship demonstrates that the N component is carried by finer grained magnetite than that for R component (see Fig.3-5 for locations of the sites).

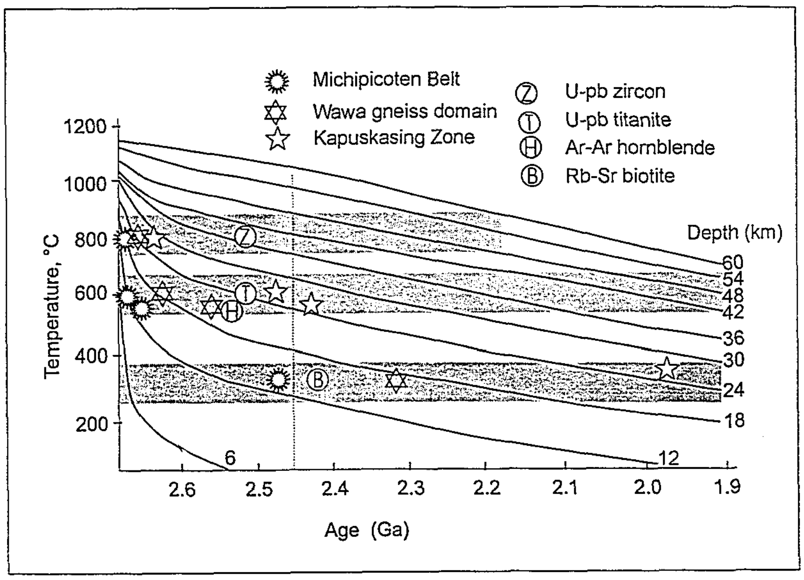

Fig.5-1 Thermal evolution model of Kapuskasing Zone. Depth (km) is before erosion. Temperature - time data are from the geochronological compilation of the KZ area. (From Percival and West, 1994).
Note that when the Matachewan dykes were emplaced at about 2.45 Ga, the Wawa gneiss domain was at about 500°C at 20 km depth. The cooling rate was about 1~1.5°C/Ma

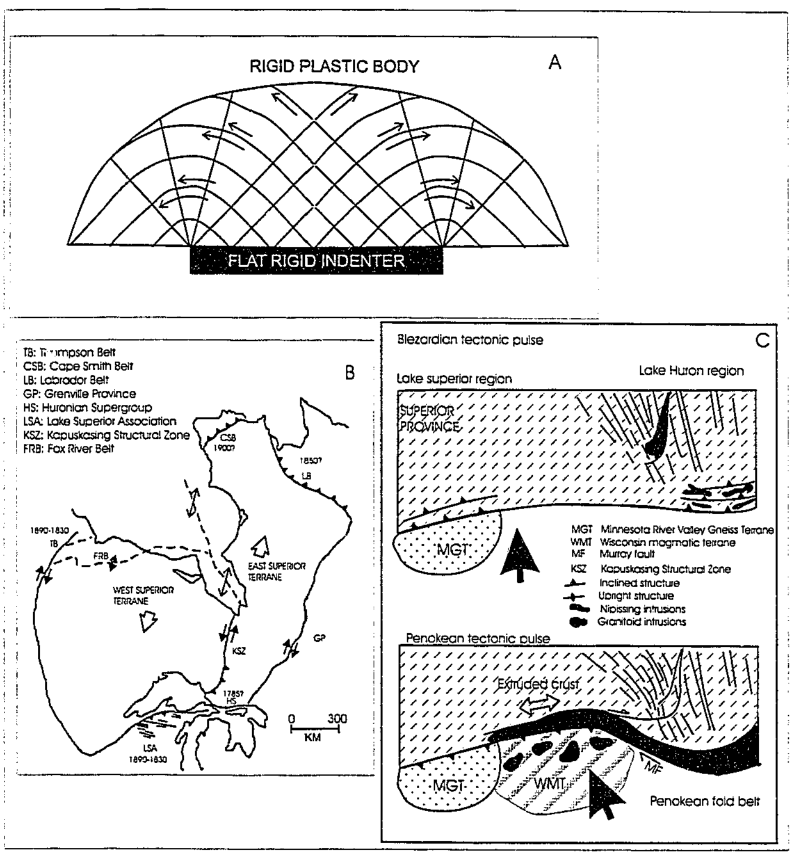

Fig. 5-2 Penokean indentor

A. Geometry of indenting model showing mass escape directions (Monlar and Tapponnier, 1977)

B. The Superior Province and bordering Proterozoic belts showing possible relationship between the KSZ and the Penokean indentor (Goodings and Brookfield,1992)

C. Formation of the Penokean indentor (Riller et al., 1999)

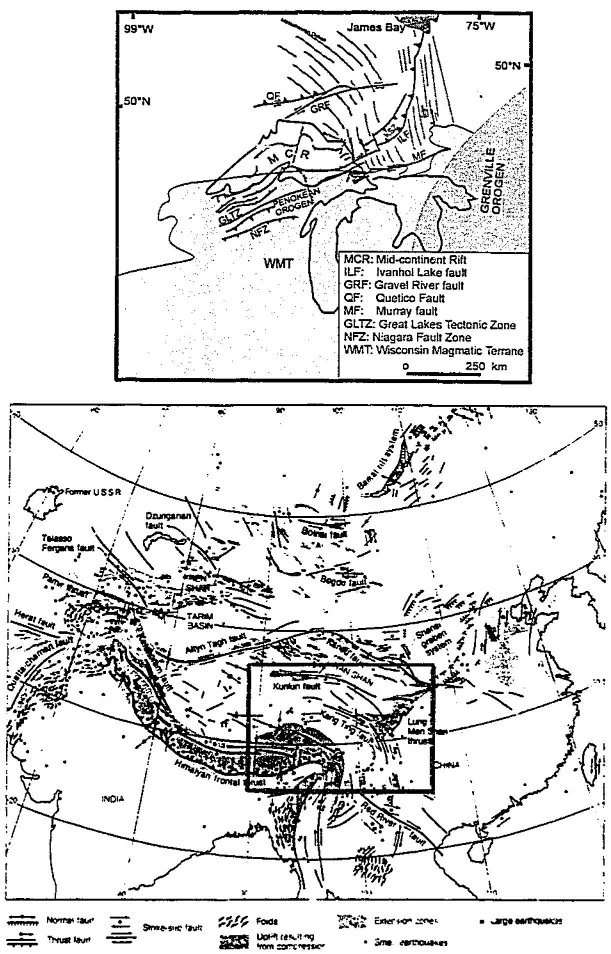

Fig.5-3 Comparison of Penokean-Kapuskasing structure with Himalayan collision.
Top: Schematic map modified from Manson and Halls (1997), Williams (1991), Riller et al. (1999).
Bottom: Geological map of Himalayan indentor (Molnar and Tapponnier 1977). The red square is correspondent both in scale and structural location to the top map.

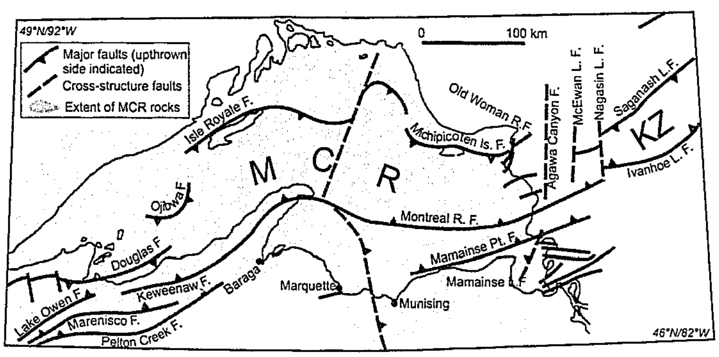

Fig.5-4 Major crustal faults in the Midcontinent rift (MCF) - Kapuskasing Structural Zone (KSZ) tectonic linkage. Note the similar characteristics between KSZ faults and MCR faults (From Manson and Halls 1997).

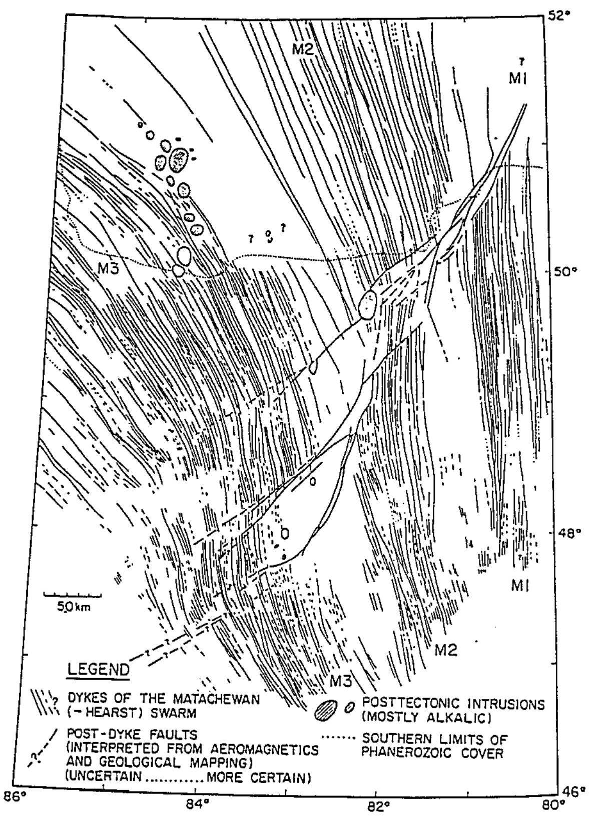

Fig.A-1. Overall image of the Matachewan dyke swarm in the vicinity of the Kapuskasing Zone. Note that subswarms M_2 and M_3 were disturbed by deformation of the KZ. M_2 was truncated by faults that bound KZ in the north whereas M_3 was dextrally sheared to form an open Z shape pattern. (From West and Ernst 1991)

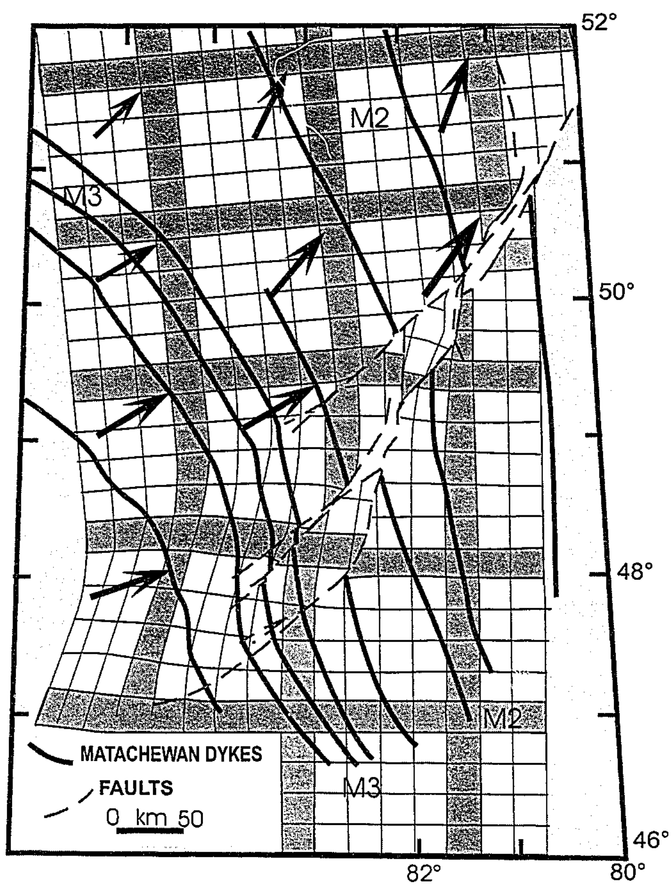

Fig.A-2. Grid map shows regional horizontal strain field in the vicinity of the KZ indicated by the Matachewan dyke configuration derived from aeromagnetic data (West and Ernst 1991). The arrows are displacement vectors related to the Southeast region of the KZ (assumed fixed). The motion is one of solid body rotation about 4° counterclockwise around vertical axis at about (50°N,82.5°W). Note that in the area of study, SW end of the KZ, main strain was basically SE-NW shortening and NE-SW extension.

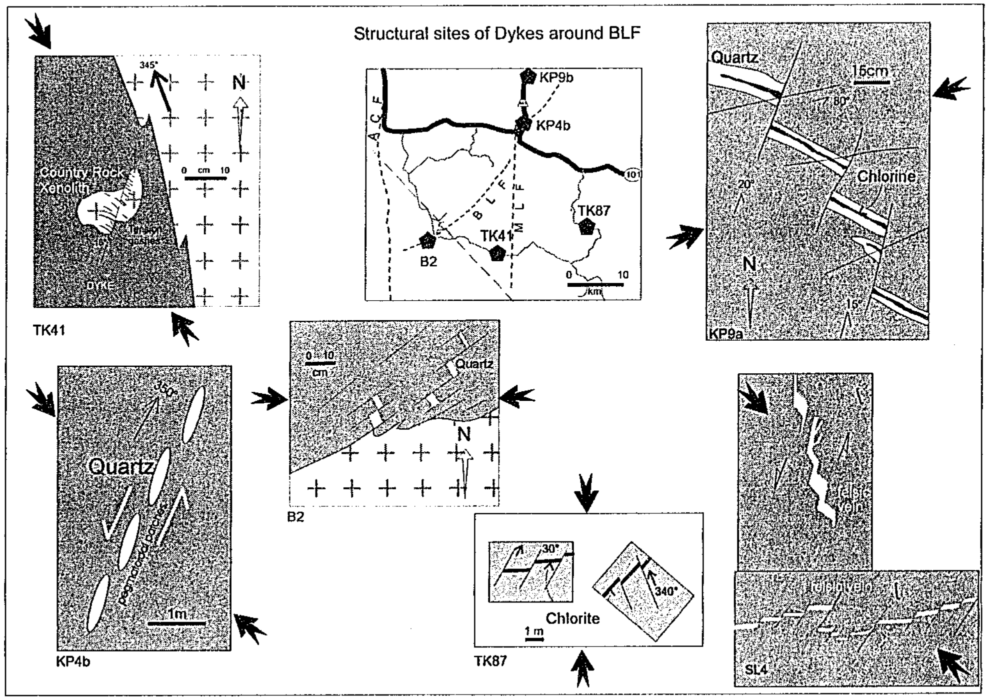

Fig.A-3(1) Structural criteria preserved in dykes: en-echelon veins and sheared veins. All sites are flat outcrops. Black arrows are directions of estimated horizontal maximum compression.

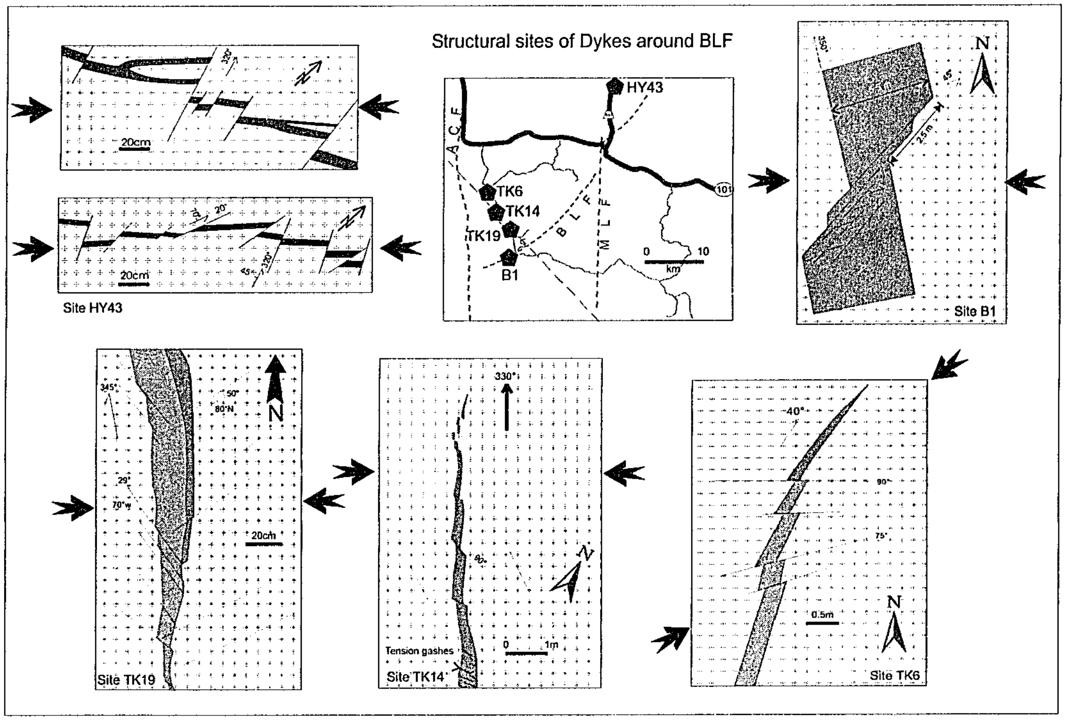

Fig.A-3(2) Structural criteria preserved in dykes: sheared dyke and dykelets. All sits are flat outcrops.
Black arrows are directions of estimated horizontal maximum compression.

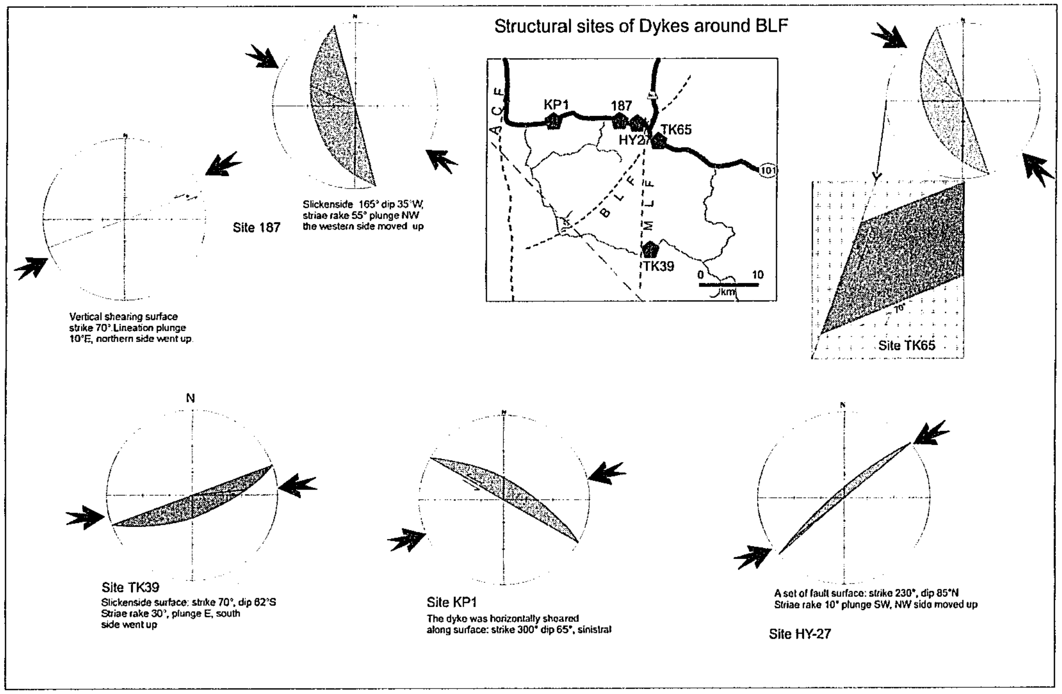

Fig.A-3(3) Structural criteria preserved in dykes: slickenside lineations. All sites are flat outcrops.
Black arrows are directions of estimated horizontal maximum compression.

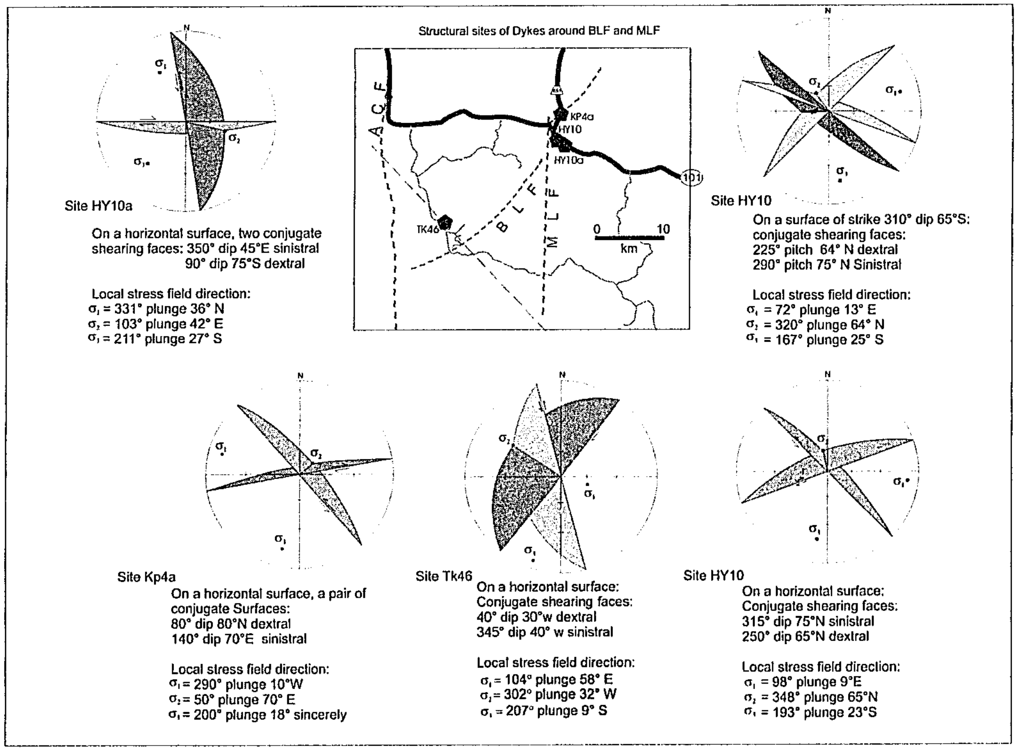

Fig.A-4. Stereographic net projection of local stress field direction at four sites near the BLF. σ_1, σ_2, and σ_3 are the maximum, intermediate, and least compressions. See text for the method of stereo net projection.

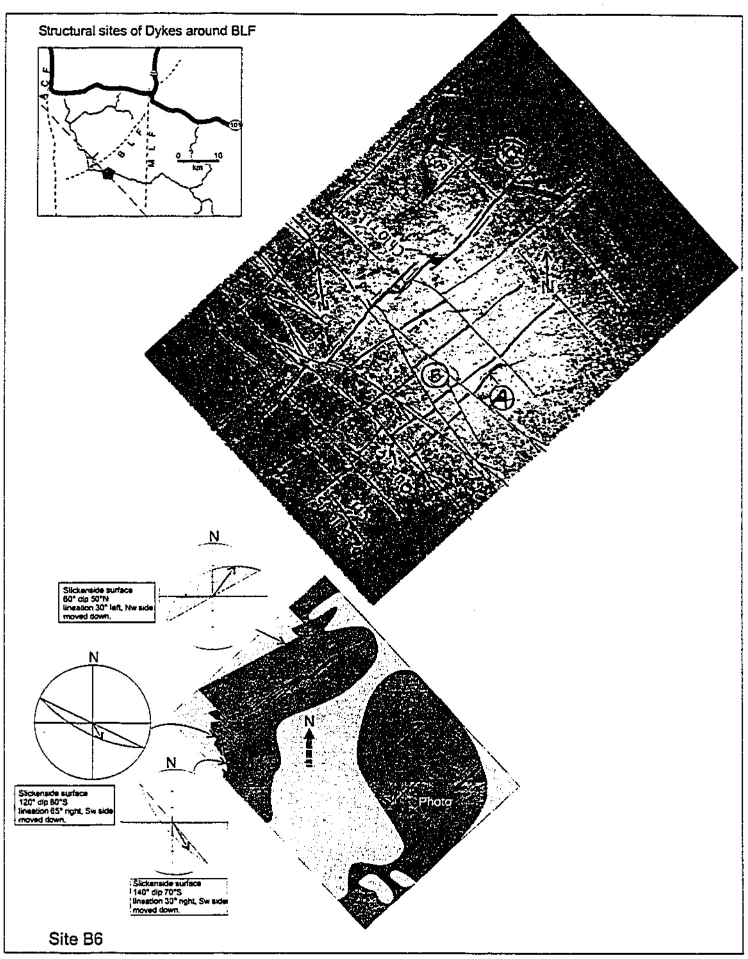

Fig.A-5. An example of structural sites (B6). Three phases of compression were revealed by the pattern of micro-faults and joints: (1). NE-SW compression to form joints A; (2). NW-SE compression to form conjugate micro-faults B that offset A and which are filled by quartz afterwards; (3). E-W compression causing some A joints to open and to be filled by chlorite. Slickenside lineation on the microfault surface was formed during the last E-W compression.

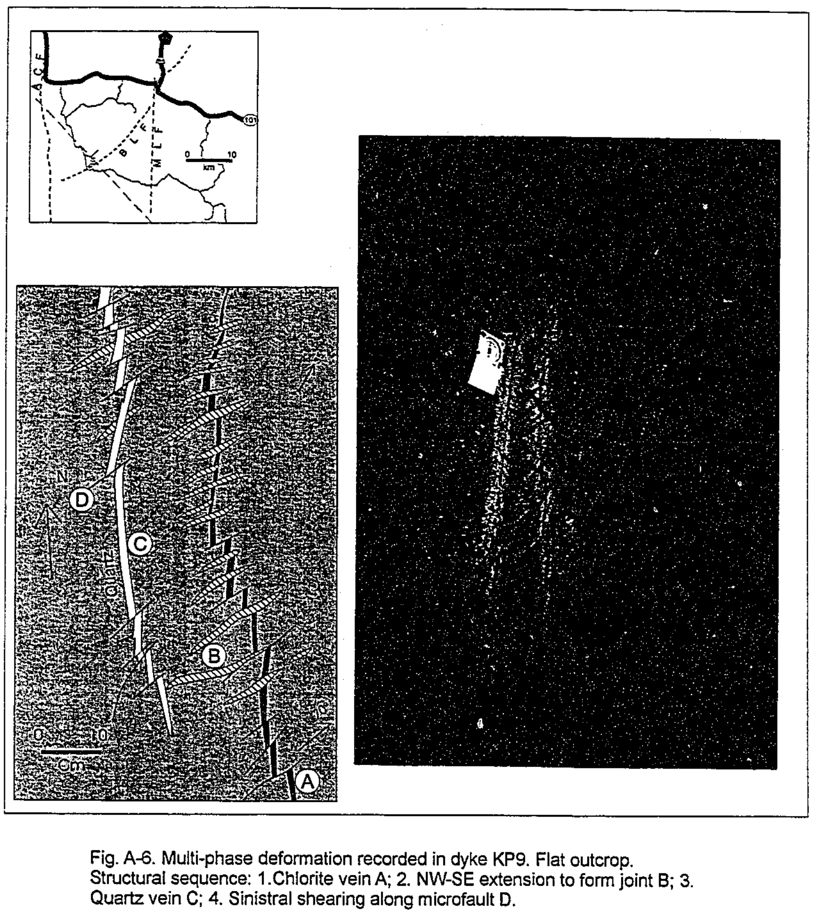

Fig. A-6. Multi-phase deformation recorded in dyke KP9. Flat outcrop.
Structural sequence: 1.Chlorite vein A; 2. NW-SE extension to form joint B; 3. Quartz vein C; 4. Sinistral shearing along microfault D.

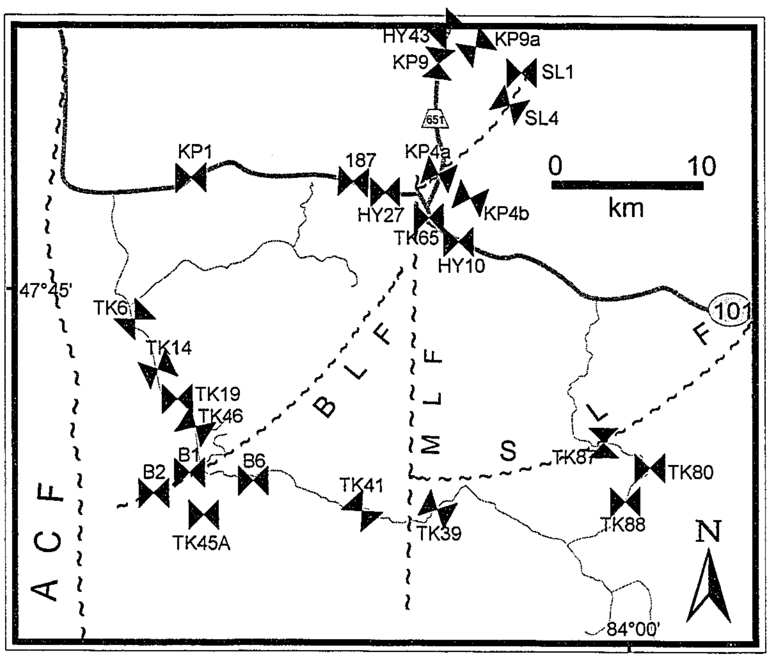

Fig.A-7. Distribution of the structural sites around MLF and BLF.
The black arrows indicate horizontal maximum compression directions.